

MARTIN MARIETTA ENERGY SYSTEMS LIBRARIES



3 4456 0278214 8

ORNL/TM-10499

ornl

**OAK RIDGE
NATIONAL
LABORATORY**

MARTIN MARIETTA

Shale: Measurement of Thermal Properties

T. M. Gilliam
I. L. Morgan

OAK RIDGE NATIONAL LABORATORY
CENTRAL RESEARCH LIBRARY
CIRCULATION SECTION
ROOM RD007175
LIBRARY LOAN COPY
DO NOT TRANSFER TO ANOTHER PERSON
If you wish someone else to see this
report, send it to room with report and
the library will arrange a loan.

OPERATED BY
MARTIN MARIETTA ENERGY SYSTEMS, INC.
FOR THE UNITED STATES
DEPARTMENT OF ENERGY

Printed in the United States of America. Available from
National Technical Information Service
U.S. Department of Commerce
5285 Port Royal Road, Springfield, Virginia 22161
NTIS price codes---Printed Copy: A08 Microfiche A01

This report was prepared as an account of work sponsored by an agency of the United States Government. Neither the United States Government nor any agency thereof, nor any of their employees, makes any warranty, express or implied, or assumes any legal liability or responsibility for the accuracy, completeness, or usefulness of any information, apparatus, product, or process disclosed, or represents that its use would not infringe privately owned rights. Reference herein to any specific commercial product, process, or service by trade name, trademark, manufacturer, or otherwise, does not necessarily constitute or imply its endorsement, recommendation, or favoring by the United States Government or any agency thereof. The views and opinions of authors expressed herein do not necessarily state or reflect those of the United States Government or any agency thereof.

Chemical Technology Division

SHALE: MEASUREMENT OF THERMAL PROPERTIES

T. M. Gilliam
I. L. Morgan

NOTICE This document contains information of a preliminary nature.
It is subject to revision or correction and therefore does not represent a
final report.

Date of Issue: July 1987

Prepared by the
OAK RIDGE NATIONAL LABORATORY
Oak Ridge, Tennessee 37831
operated by
MARTIN MARIETTA ENERGY SYSTEMS, INC.
for the
U.S. DEPARTMENT OF ENERGY
under contract DE-AC05-84OR21400

MARTIN MARIETTA ENERGY SYSTEMS LIBRARIES



3 4456 0278214 8

CONTENTS

	<u>Page</u>
LIST OF FIGURES	v
LIST OF TABLES	vii
ABSTRACT	1
1. INTRODUCTION	1
2. REPORTED THERMAL CHARACTERIZATION STUDIES OF SHALE	2
2.1 Effects of Composition	2
2.2 Effects of Temperature	4
2.3 Effects of Porosity	4
2.4 Effects of Pressure	5
2.5 Effects of Anisotropy	5
2.6 Heat Capacity	6
2.7 Guidance for Present Study	6
3. DESCRIPTION OF SHALES TESTED	7
3.1 Devonian Shale Samples	7
3.2 Pierre Shale Samples	9
3.3 Green River Formation Shale Samples	9
4. EXPERIMENTAL PROCEDURE	10
4.1 Thermal Conductivity	10
4.2 Heat Capacity	15
4.3 Linear Thermal Expansion	18
5. EXPERIMENTAL RESULTS	18
5.1 Thermal Conductivity	20
5.2 Heat Capacity	22
5.3 Thermal Expansion	24
6. SUMMARY	30
7. REFERENCES	32
APPENDIX A: TECHNIQUES FOR THE MEASUREMENT OF THERMAL PROPERTIES	35
APPENDIX B: THERMAL CONDUCTIVITY DATA FOR SHALE SAMPLES	53

APPENDIX C: HEAT CAPACITY DATA FOR SHALE SAMPLES 87

APPENDIX D: THERMAL EXPANSION DATA FOR SAMPLES OF DEVONIAN
SHALE 131

LIST OF FIGURES

<u>Fig. No.</u>		<u>Page</u>
1	Thermal conductivity analyzer	11
2	Thermal conductivity sample configuration	12
3	Schematic of thermal conductivity analyzer	13
4	Typical calibration verification curve using Pyrex 7740 sample	16
5	Typical plot of dH/dt vs dT/dt obtained from the DSC	17
6	Typical plot of thermal expansion vs temperature obtained from push-rod dilatometer	19
7	Thermal conductivity as a function of temperature for shale from 176.8 m (EGSP Kentucky No. 5 Well)	21
8	Heat capacity as a function of temperature for shale from 187.8 m (EGSP Kentucky No. 5 Well)	25
9	Thermal expansion data for shale from 157 m (EGSP Kentucky No. 5 Well)	26
10	Thermal expansion data for shale from 157.1 m (EGSP Kentucky No. 5 Well)	27
11	Thermal expansion data for shale from 157.4 m (EGSP Kentucky No. 5 Well)	28
12	Thermal expansion data for shale from 191.6 m (EGSP Kentucky No. 5 Well)	29

SHALE: MEASUREMENT OF THERMAL PROPERTIES

T. M. Gilliam
I. L. Morgan

ABSTRACT

Thermal conductivity and heat capacity measurements were made on samples of Devonian shale, Pierre shale, and oil shale from the Green River Formation. In addition, thermal expansion measurements were made on selected samples of Devonian shale. Measurements were obtained over the temperature range of ambient to 473 K. Average values for thermal conductivity and heat capacity for the samples studied were within two standard deviations of all data over this temperature range.

1. INTRODUCTION

The Sedimentary Rock Program (SERP) at Oak Ridge National Laboratory (ORNL) is characterizing a series of argillaceous rocks to assess the potential for using such rocks as a geologic repository for radioactive waste disposal. One of the parameters being studied involves thermal properties, and this report represents an initial review of the methods used in making thermal measurements and the data that have been obtained on a series of representative samples of shale-rich strata.

In an effort to obtain data that represent the broad spectrum of rocks that can be termed "shale," the SERP has selected a variety of shale-rich rocks that are representative of the different compositional extremes found for shales. These include Devonian shale, Pierre shale, oil shale from the Green River Formation, and Lower Paleozoic shale (Conasauga Group shale). Samples used in this study were from Devonian shale, Pierre shale, and oil shale from the Green River Formation.

In assessing the suitability of a site for long-term disposal of waste, such as in a repository, stability is a major issue. For high-level waste, one of the characteristics that may affect stability is heat generation since the resulting thermal stresses have the potential of opening migration pathways or altering existing pathways. For an assessment of this potential, data on three thermal characteristics are needed: thermal conductivity, heat capacity (or thermal diffusivity), and thermal expansion. This report addresses these characteristics over the temperature range of ambient to 473 K.

2. REPORTED THERMAL CHARACTERIZATION STUDIES OF SHALE

Published data on the thermal properties of shale are limited in number. Most of the identified studies¹⁻¹⁴ have been focused on thermal conductivity. The reported data¹⁻¹⁴ indicate that the thermal conductivity of most shales at ambient conditions is within the range of 0.5 to 2.2 W/m·K. Individual researchers have concluded that variables that affect thermal conductivity are dependent on the particular shale samples studied. No systematic study has been found which addresses variables affecting the thermal characteristics of several shale types. However, a review of all studies¹⁻¹⁴ gives guidance for this study by providing a list of variables of potential interest. These include composition, temperature, porosity, pressure, and anisotropy.

2.1 EFFECTS OF COMPOSITION

Thermal conductivity data on a variety of geologic media indicate a dependence on composition.¹³⁻¹⁵ Research on shale has demonstrated a dependence of thermal conductivity on water content,¹⁴ clay content,¹² Fisher assay of the shale (in gallons per ton),^{2,3} and inorganic mineral content.⁸ However, the heterogeneity of natural material makes prediction of thermal conductivity difficult. As reported by Birch and Clark¹⁶ and summarized as follows by Dell'Amico, Captain, and Chansky:¹

1. The conductivities of many of the constituent minerals are not accurately known.

2. In geologic media, these constituents usually do not occur as discrete, unflawed crystals.
3. The resistances are not always exclusively in series or in parallel but very often are in some combination of these or in a completely random pattern.

The impact of this heterogeneity is illustrated by Birch and Clark,¹⁶ who have reported differences in thermal conductivities as high as 50% between adjacent samples of coarse-ground rock cut 1 cm apart. It should be noted that, although the authors presumed that the differences were due to variations in composition, supporting evidence was not given.¹⁶ Correlations between thermal conductivity and composition have historically been empirical and need to be based on a large number of data.

Diment and Robertson⁸ reported a relationship between thermal conductivity and composition of shale from the Conasauga Group as

$$\lambda = 2761 - 15 R , \quad (1)$$

where λ is thermal conductivity (in watts per meter kelvin) and R is the weight percent of shale that is insoluble in dilute hydrochloric acid.

Tihen, Carpenter, and Sohn³ have reported the relationship between thermal conductivity and composition of oil shales from the Green River Formation which assay between 0.04 and 0.24 L/kg as

$$\lambda = C_1 + C_2F + C_3T + C_4F^2 + C_5T^2 + C_6FT , \quad (2)$$

where

λ = thermal conductivity, W/m·K;

C_1 – C_6 = constants;

F = Fisher assay of the shale, L/kg;

T = temperature, K.

Significantly, this equation indicates that the effects of composition and temperature are interrelated for some shales.

2.2 EFFECTS OF TEMPERATURE

Thermal conductivity measurements on geologic media have indicated a dependence on temperature.^{10,16,17} As indicated previously,³ thermal conductivity of oil shales from the Green River Formation is reported to be a function of T^2 . In some cases, this dependence resulted in a 50% decrease in thermal conductivity at 653 K compared with that at 353 K. On the other hand, Dell'Amico, Captain, and Chansky¹ have reported that, for shales from the Conasauga Group at temperatures below 373 K, thermal conductivity is independent of temperature, as shown in Table 1.

The differences in the strength of the relationship between thermal conductivity and temperature for the two shale types may be due to compositional differences, as indicated by the empirical equation presented by Tihen, Carpenter, and Sohn.³ However, differences in the porosities of the samples may also have contributed to the differences.

Table 1. Thermal conductivity of shale from the Conasauga Group as a function of temperature below 373 K^a

Temperature (K)	Thermal conductivity (W/m·K)
301.3	1.33
302.7	1.32
339.9	1.39
360.7	1.31

^aData reported by Dell'Amico, Captain, and Chansky.¹

2.3 EFFECTS OF POROSITY

For porous media, thermal conductivity is a strong function of porosity and the fluid contained in the voids. Numerous empirical models have been developed which relate thermal conductivity and porosity.¹⁸ Porosity may be a significant variable affecting thermal conductivity, with some shales having porosities as high as 50%.¹⁹

Dell'Amico, Captain, and Chansky¹ and Robertson¹⁴ have shown, respectively, that thermal conductivities of water-saturated shale samples (at ambient temperature) were 3% and 50% higher than vacuum-dried samples. Shale samples from the Conasauga Group which were studied by Dell'Amico, Captain, and Chansky¹ had an average porosity of 1.45% (as determined by water uptake of vacuum-dried samples). Presumably, this low porosity, and hence the small amount of fluid contained in the samples, accounted for the negligible change in thermal conductivity for water-saturated vs vacuum-dried samples and may have contributed to the lack of sensitivity to temperature (Sect. 2.2).

2.4 EFFECTS OF PRESSURE

The thermal conductivity of geologic media may vary as a function of confining pressure.²⁰ The effects of pressure may range from relatively insignificant changes in thermal conductivity of <3% to 25% at pressures of 100 MPa, depending on the type of material being studied.^{20,21} The change in thermal conductivity is attributed to closer intragranular contact due to compression of the sample. However, the magnitude of this effect should depend somewhat on the composition and compressibility of the fluid contained in the voids.

Evidence that pressure has little effect on thermal conductivity of shales with low porosity is given by Dell'Amico, Captain, and Chansky.¹ For a shale from the Conasauga Group with an average porosity of 1.45%, thermal conductivity at ambient temperature increased 2.1% at 10 MPa over that obtained at 2.5 MPa.

2.5 EFFECTS OF ANISOTROPY

All researchers have reported significant differences between thermal conductivity corresponding to heat flow in a direction perpendicular to the shale bedding plane and that corresponding to heat flow in a direction parallel to the stratigraphic planes.¹⁻¹⁴ In general, thermal conductivities parallel to the bedding planes are higher than those obtained perpendicular to the bedding planes. For shale from the Conasauga Group, Dell'Amico, Captain, and Chansky¹ reported that thermal

conductivity values parallel to the bedding plane were 30% higher than those obtained perpendicular to the bedding plane; while Nottenburg et al.² reported that the increase exhibited by oil shales from the Green River Formation was ~50%.

2.6 HEAT CAPACITY

The literature search did not reveal an independent determination of shale heat capacity. However, Tihen, Carpenter, and Sohn³ reported thermal diffusivity values for oil shales from the Green River Formation and found that the data can be represented by

$$\ln(a) = \frac{4\pi\theta\lambda}{Q} + \gamma + \ln \frac{R^2}{4t} \quad , \quad (3)$$

where

- a = thermal diffusivity,
- θ = temperature rise,
- λ = thermal conductivity,
- Q = heat input,
- γ = Euler's constant,
- R = distance from line heat source,
- t = time.

Note that thermal diffusivity is equal to

$$a = \frac{\lambda}{\rho C_p} \quad , \quad (4)$$

where ρ is density and C_p is specific heat. Although not explicitly stated, presumably the presence of thermal conductivity on the right-hand side of Eq. (3) indicates a relationship with Fisher assay as well [as in Eq.(2)]. Furthermore, it provides evidence that variables that affect conductivity may affect heat capacity as well.

2.7 GUIDANCE FOR PRESENT STUDY

Previously reported data have indicated that composition, temperature, porosity, pressure, and anisotropy should be considered in a

shale thermal characterization study (Sects. 2.1 to 2.6). No study has been found which addresses all of these variables for several shale types. Consequently, comparisons and explanations of differences in thermal characteristics are somewhat speculative. For this reason, little comparison will be made between data generated in the study presented here and the previously reported values, except in a general sense (e.g., order-of-magnitude comparison).

A systematic study that addressed all of these identified variables would require an extensive effort. Significantly, the data discussed in Sects. 2.1 to 2.6 give some indication that if porosity, water content, and pressure are major variables of concern, then this will be reflected in a pronounced relationship between thermal conductivity and temperature. Consequently, the study presented here was concentrated on obtaining thermal conductivity data as a function of temperature.

3. DESCRIPTION OF SHALES TESTED

Experiments were performed on samples of Devonian shale from Kentucky, Pierre shale from Nebraska, and oil shale from the Green River Formation in Colorado. Measurements of thermal conductivity and heat capacity were made over the temperature range of ambient to 473 K for all samples. In addition, thermal expansion measurements were made on selected Devonian shale samples over the same temperature range.

3.1 DEVONIAN SHALE SAMPLES

Samples were obtained under the Eastern Gas Shale Program (EGSP) and supplied by the Morgantown Energy Technology Center, Morgantown, West Virginia. The samples originated from a drill site in Rowan County, Kentucky, referred to as the EGSP Kentucky No. 5 Well (hereafter the samples will be referred to in the same manner). The shale is Devonian in age and consists of the following formations: Cleveland, Chagrin, Upper Huron, Middle Huron, and Lower Huron. The samples came from six depth intervals and are described by Cliff Minerals, Inc.,²² as follows:

<u>Interval</u>	<u>Description</u>
450.0'-460.0' (10.0')	Mudstone and silty mudstone, gray grading downward to grayish black and then back to gray again (N3, N2, N3), thinly laminated to thickly bedded. A band of pyrite about 0.1 feet thick occurs at 450.0'. Just below that at 450.1', 2 small brown lenses (5YR 4/1) are present. Pyrite nodules occur throughout the interval. At 451.4' a nodule of brown sandstone with a center of pyrite is present. A 1/2 inch thick lamina of pyrite occurs at 453.3', a 1 cm thick lens of pyrite at 455.2'. The interval is noncalcareous. The interval was sampled at 453'7 1/3" and 456'11".
507.0'-515.0' (8.0')	Mudstone and silty mudstone, dark gray (N3), thinly laminated to thickly bedded. Tiny laminae (<1 mm thick) of calcareous material occur around 508'. Pyrite blebs are present at 509' and 509.3'. Carbonaceous fossils occur at 509.2'. Carbonaceous fossils and pyrite nodules occur at 512' with more pyrite nodules at 513.6'. A thin lamina, about 5 mm thick, of light gray (N7) calcareous sandstone is present at 513.9'. The interval was sampled at 512'5".
515.0'-533.0' (18.0')	Mudstone and silty mudstone, dark gray (N3) to grayish black (N2), thickly laminated. The entire interval of core has the scribe marks shaved off. It is also contaminated with foreign oil products. Much of the lithology is obscured by the oiliness. The interval was sampled at 517' 1 1/2", 521' 3/4", 527' 4 3/4" and 532' 4 1/2". A 0.1 feet thick lamina of calcareous sandstone is present at 418.6' and a 0.15 foot thick bed of it at 525.5'. Three small laminae of pyrite 5 mm, 3 mm and 1 mm, respectively, occur at 523.9'. The lighter gray (N3) becomes more predominant toward the lower part of the interval. Pyrite nodules are present throughout.
534.0'-543.0' (9.0')	Mudstone and silty mudstone, olive gray (5Y 3/2), dark greenish gray (5GY 3/2) and olive black (5Y 2/1), thinly laminated to thin bedded. Pyrite nodules are present throughout the interval. One thin lamina of calcite cemented calcareous sand is present

at 532.7'. A carbonaceous fragment occurs at 537'. Resinous spore bodies at 538.6'. The interval was sampled at 535'4".

574.0'-581.0'
(7.0')

Mudstone and silty mudstone, dark gray (N3), olive black (5Y 2/1) and greenish gray (5GY 6/1), thinly laminated to thick bedded. The greenish gray mudstone is present as 2 thick beds at 580' and 581.1'. The gamma ray log shows a drop in gamma ray count from 570' to 590'. Pyrite is present as disseminated grains and as nodules throughout the interval. The interval was sampled at 575'4" and 580'6 1/4".

610.0'-620.0'
(10.0')

Mudstone and silty mudstone, grayish black (N2), dark gray (N3), dark greenish gray (5GY 4/1), and olive black (5Y 2/1), thinly laminated to thick bedded. A 3-foot long vertical fracture occurs at 611'. The solid gray black of the preceding intervals changes to greenish gray with dark bands at 613.1'. The interval is strongly bioturbated and the color banding varies from <1 mm to 6". Pyrite occurs as disseminations, nodules and lenses. The interval is noncalcareous and contains few fossils.

3.2 PIERRE SHALE SAMPLES

The samples supplied by the U.S. Army Corps of Engineers were taken from the Moberge Formation, drill hole 84-20 (sample U-6) at a depth of 45.1 to 49.1 m (148 to 161 ft).²³ The samples are described as "claystone, thick-bedded to medium-bedded, nonfissile, slightly to moderately calcareous, moist, medium gray with slight olive tinge, soft to medium hard, dense, solid, slakes very slowly on exposure, nonweathered, with many fine white calcareous particles RQD: 90%."²³

3.3 GREEN RIVER FORMATION SHALE SAMPLES

The samples taken from the Colony Mine near Parachute, Colorado, were suitable for two thermal conductivity determinations and one heat capacity measurement. The samples are described as "highly indurated, brittle, and contain less than 1% water by weight. Contain ~50% carbonate (calcite,

dolomite, and siderite), ~31% quartz, plagioclase feldspar and ~4% illitic clay."²⁴

4. EXPERIMENTAL PROCEDURE

The equipment used for this study included a differential scanning calorimeter, a push-rod dilatometer, and comparative thermal conductivity equipment. This equipment represents well-established, accepted thermal measurement techniques, with accuracy comparable to that of more expensive "high-precision" techniques (Appendix A).

4.1 THERMAL CONDUCTIVITY

The thermal conductivity of a shale sample was determined using a Dynatech Corporation Model TCFM-N20 comparative thermal conductivity analyzer in conjunction with a Hewlett-Packard Model 3052A automatic data acquisition and control system (Fig. 1) to facilitate consecutive measurements over an extended time period (>8 h).

The shale samples were cut and machined from a 0.05-m-diam core (Fig. 2). After cutting to rough dimensions, the samples were ground until the top and bottom surfaces were flat and parallel to within 0.005 cm. A small groove was then cut in both sides of the sample to allow the installation of a 38-gage, type-K thermocouple, which was cemented in place just below the surface of the sample using Saureisen Insa-lute Hi-Temp Cement paste. After placement of the thermocouple, the surface was again machined to remove any excess cement paste.

The shale sample was then sandwiched between two materials of known thermal conductivity (in this case, Pyrex 7740), as illustrated in Fig. 3. This stack was placed between a top (main) and bottom (auxiliary) heating element. Contact between the components of the resulting stack was maintained using a screw-tightened pressure pad located at the top of the stack. The entire stack was then enclosed in an annular guard heater, with the free space remaining in the annulus filled with loose vermiculite to minimize thermal shunting from radial heat flow.

The main and auxiliary heaters provided a temperature gradient across the stack, while the guard heaters maintained temperatures similar to

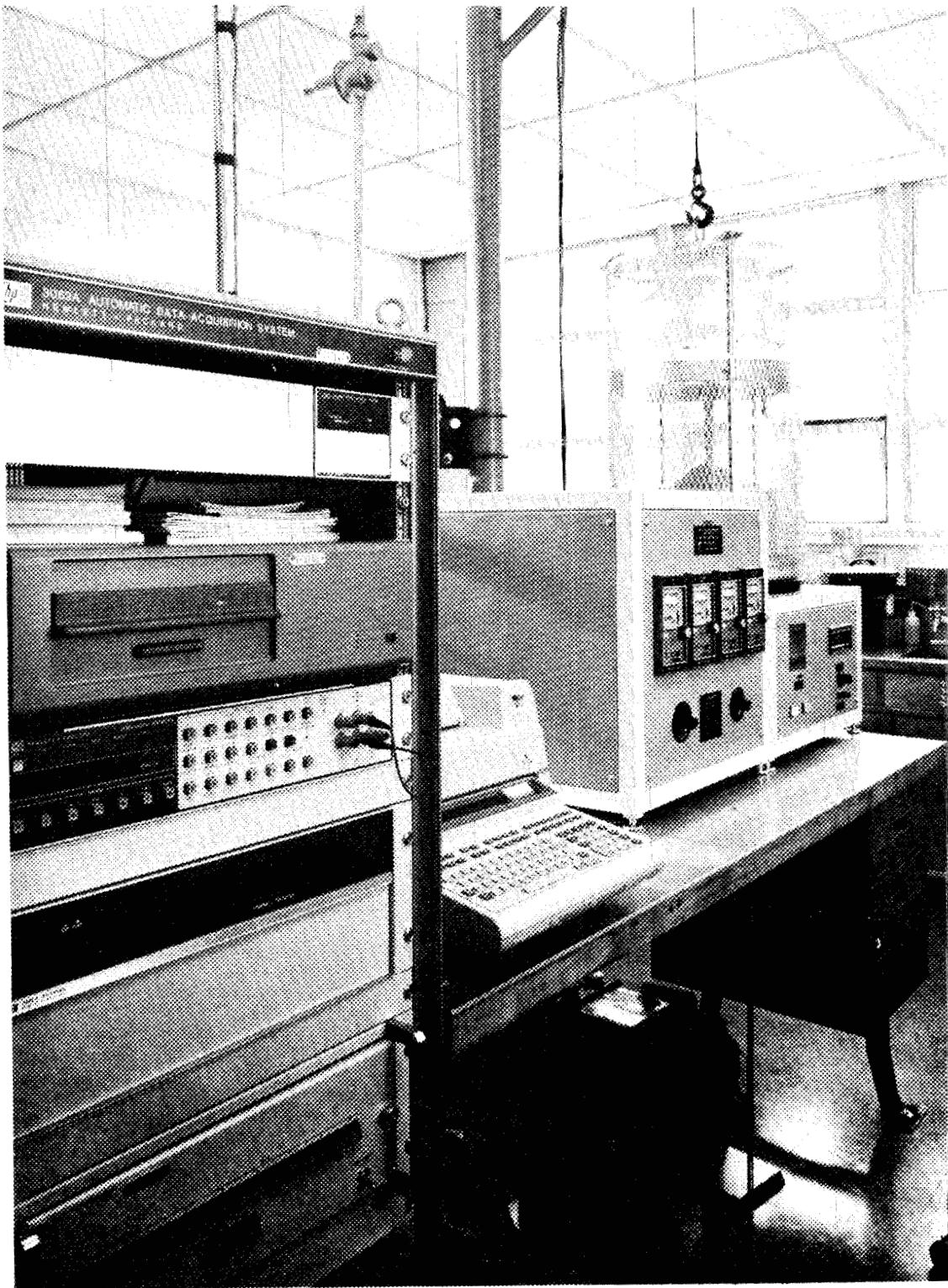


Fig. 1. Thermal conductivity analyzer.

ORNL DWG 86-19882

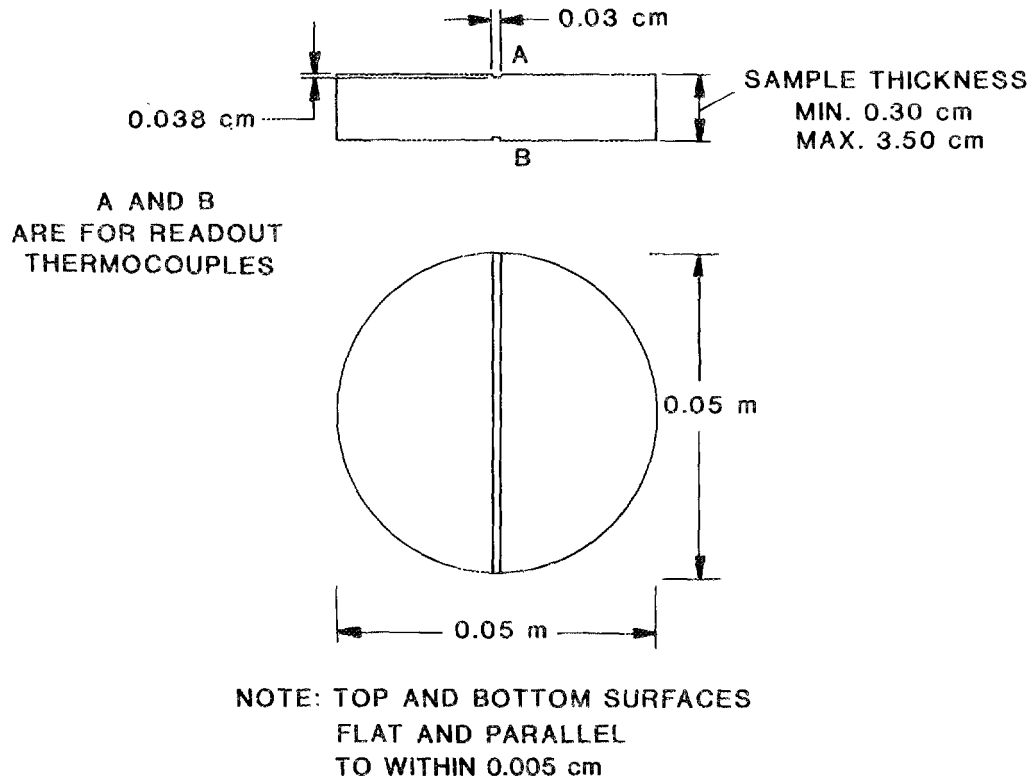


Fig. 2. Thermal conductivity sample configuration.

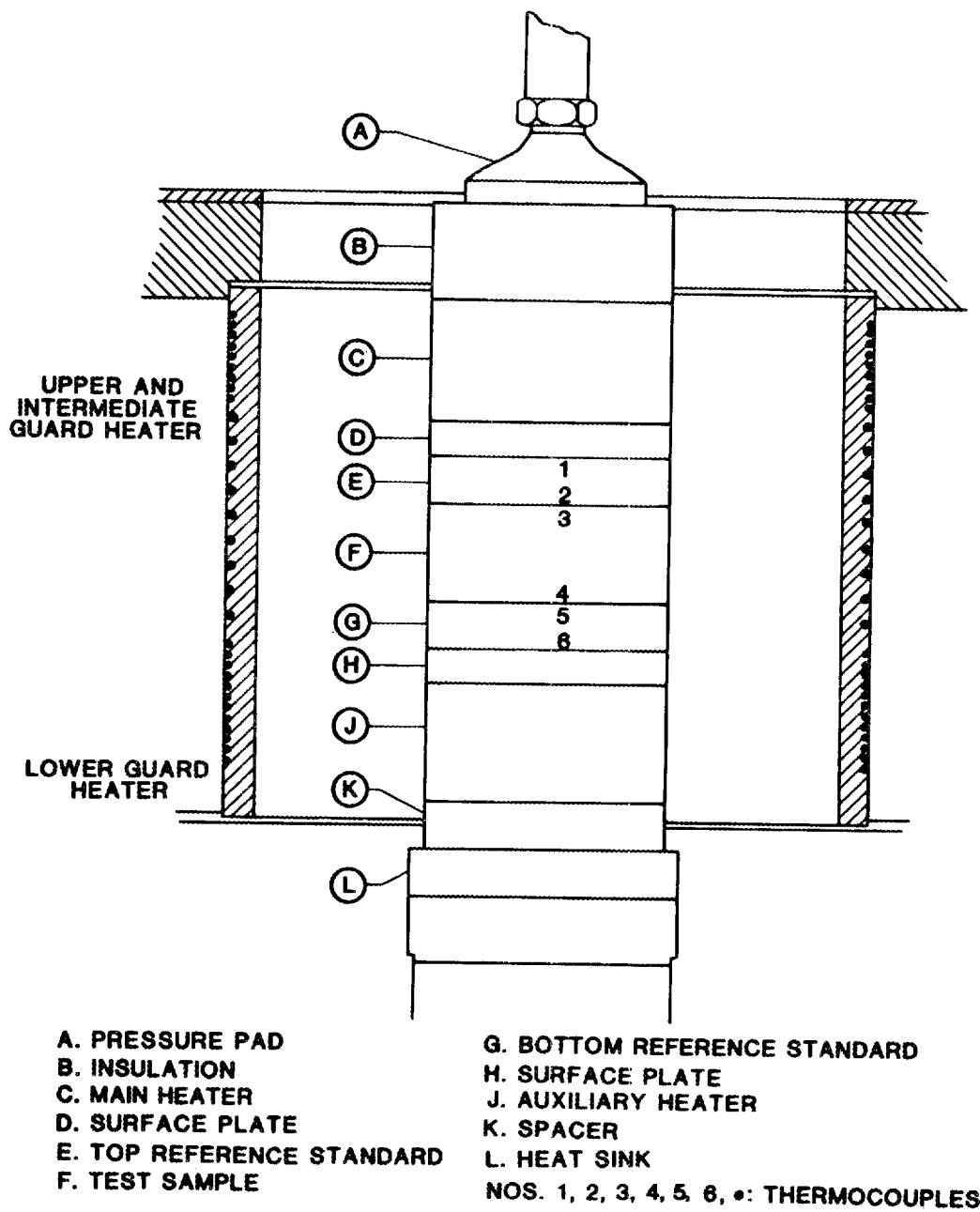


Fig. 3. Schematic of thermal conductivity analyzer.

those of the stack. This arrangement minimized radial heat losses to ensure uniaxial heat flow through the stack.

During operation, temperature readings at thermocouple locations 1 through 6 (Fig. 3) were taken approximately every 3 min. Each temperature reading was compared with the previous two measurements. When three successive readings were within three-tenths of a degree at each of the six thermocouples, the system was assumed to be in equilibrium, and the thermal conductivity of the shale sample was calculated by

$$\lambda_{\text{shale}} = \frac{1}{2} \left(\frac{\Delta X}{\Delta T} \right)_{\text{shale}} \left[\left(\frac{\lambda \Delta T}{\Delta X} \right)_{\text{top reference}} + \left(\frac{\lambda \Delta T}{\Delta X} \right)_{\text{bottom reference}} \right], \quad (5)$$

where

λ = thermal conductivity, W/m·K;

ΔX = thickness of material, m;

ΔT = temperature drop, K, through axial length ΔX .

Also in Eq. (5),

$$\Delta T_{\text{shale}} = T_3 - T_4 \text{ (Fig. 3),}$$

$$\Delta T_{\text{top reference}} = T_1 - T_2 \text{ (Fig. 3),}$$

$$\Delta T_{\text{bottom reference}} = T_5 - T_6 \text{ (Fig. 3),}$$

$$\lambda_{\text{top reference}} = \text{thermal conductivity of reference material at } (T_1 + T_2)/2,$$

$$\lambda_{\text{bottom reference}} = \text{thermal conductivity of reference material at } (T_5 + T_6)/2,$$

$$\lambda_{\text{shale}} = \text{thermal conductivity of the shale at } (T_3 + T_4)/2.$$

This technique, in effect, uses the known thermal conductivity of the reference material to calculate heat flux. From the heat flux, the thermal conductivity of the shale was then calculated.

Equipment calibration was performed monthly by running the equipment with Pyrex 7740 instead of the shale sample. Measured values were then compared with true values as determined by the National Bureau of Standards. A typical calibration curve is shown in Fig. 4.

4.2 HEAT CAPACITY

Heat capacity values of shale were determined with a DuPont Model 1090 differential scanning calorimeter (DSC). A DSC compares the amount of energy required to raise the temperature of a known weight of a standard reference material (in this case, sapphire) at a predetermined heatup rate to a predetermined temperature with the amount of energy required to raise the temperature of the shale under identical conditions. The procedure used involved establishing a baseline correction factor for the DSC by using a standard reference material (sapphire). The sapphire was placed in a sample pan of known mass and heat capacity, which was then placed in the DSC. The DSC then heated the sample at a constant rate to the temperature of interest. The heat capacity of the reference was then calculated by using the equation

$$\frac{dH}{dt} = MC_p \frac{dT}{dt}, \quad (6)$$

where

dH/dt = rate of energy input to the system, J/h;

M = mass of the sapphire, kg;

C_p = calculated heat capacity of the sapphire, J/kg·K;

dT/dt = rate of temperature rise of the sapphire, K/h.

A correction factor, the heat capacity of the sample pan, must be considered and was determined by the same procedure.

The shale sample was then placed in the sample pan, which was crimp-sealed to prevent loss of water.

From these three procedures, a plot of dH/dt vs dT/dt was obtained (Fig. 5), and the shale heat capacity at various temperatures was calculated by using the equation

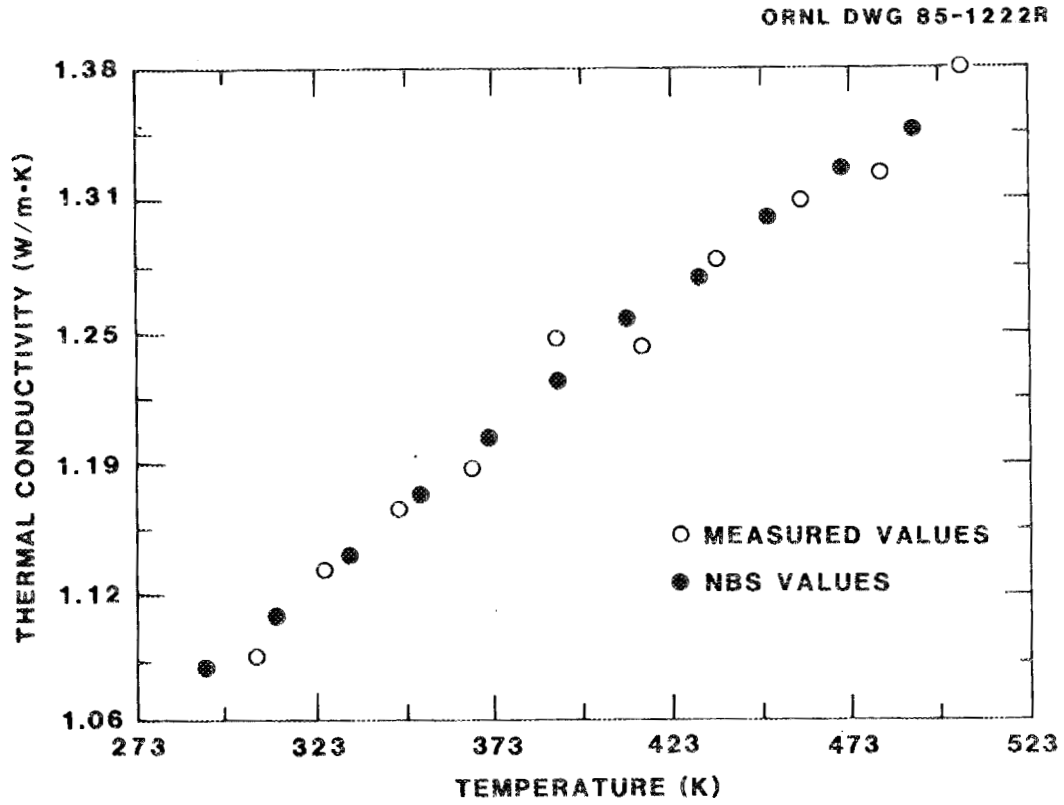


Fig. 4. Typical calibration verification curve using Pyrex 7740 sample.

ORNL DWG 85-1232R

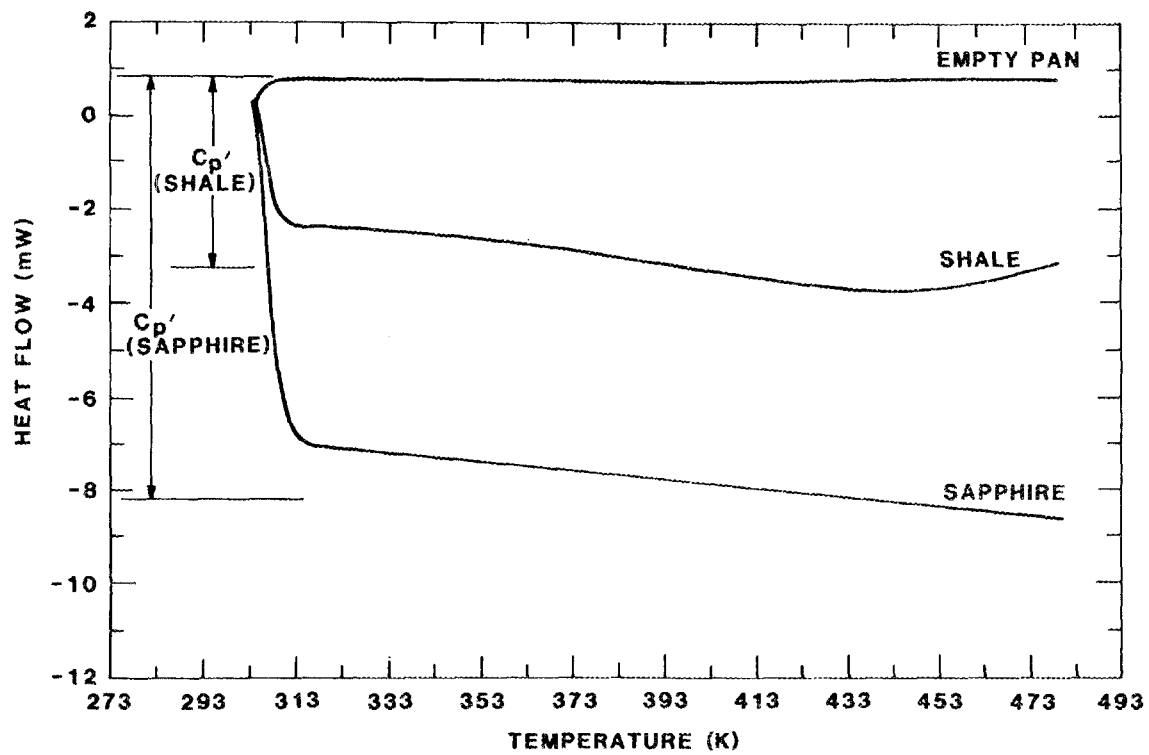


Fig. 5. Typical plot of dH/dt versus dT/dt obtained from the differential scanning calorimeter.

$$C_p = \frac{C_p' M_s}{C_p' M} C_{p_s} \quad (7)$$

where

- C_p = heat capacity of the shale, J/kg·K;
- C_p' = measured heat capacity of the shale, J/kg·K;
- C_{p_s}' = measured heat capacity of the sapphire, J/kg·K;
- C_{p_s} = heat capacity of the sapphire, J/kg·K;
- M_s = mass of sapphire, kg;
- M = mass of shale, kg.

4.3 LINEAR THERMAL EXPANSION

Thermal expansion measurements were made using a NETZSCH Model 402E dilatometer interfaced with a Hewlett-Packard (H-P) Model 9816 data acquisition system (DAS). The reference material used for calibration purposes was Vacromium (a Deutsche Industrial Norms standard metal alloy commonly used for thermal expansion measurement calibrations). The samples were fabricated in the shape of right-circular cylinders, 1.3 cm in diameter and of varying lengths. The specimen was placed in an alumina sample-holder/push-rod device. The sample-holder assembly was covered by a quartz glass tube to isolate the heating zone from air currents. A tube furnace was placed over the entire sample/push-rod assembly. As the sample or standard expanded upon application of heat, the change of length was determined by recording the output voltage of the linear variable differential transformer (LVDT) using the H-P DAS.

The DAS also determined the corrected expansion numbers based on the raw data and measurements obtained from the Vacromium reference material. The corrected expansion data were then expressed as a percentage of original length (at 298 K), as shown in Fig. 6.

5. EXPERIMENTAL RESULTS

The size of the samples received did not permit cores to be obtained parallel to the bedding planes. Thus, all measurements were obtained on

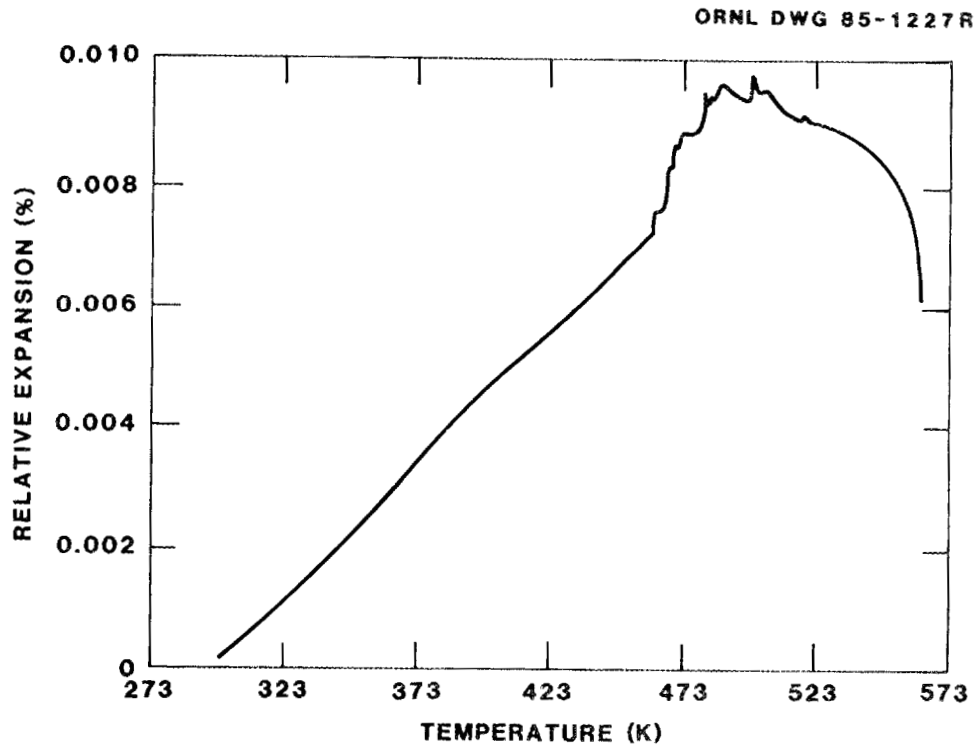


Fig. 6. Typical plot of thermal expansion versus temperature obtained from push-rod dilatometer.

samples perpendicular to the shale bedding planes. As discussed previously (Sect. 2.5), thermal conductivities of samples perpendicular to the bedding planes have been reported to be 30% to 50% lower than values obtained from samples parallel to the bedding planes.

5.1 THERMAL CONDUCTIVITY

Data obtained for thermal conductivity as a function of temperature over the range of ambient to 473 K for all samples are shown in Appendix B. The magnitude of values obtained varied from sample to sample, but the trends exhibited by thermal conductivity as a function of temperature were consistent among all samples. These trends are typical of that shown in Fig. 7 for a sample taken from a well depth of 176.8 m (580 ft) in the EGSP Kentucky No. 5 Well.

As shown in the figure, the relationship between thermal conductivity and temperature (below 473 K) exhibits three distinct regions. First, thermal conductivity increases with increasing temperature below 363 K. However, this temperature dependence is weak, and, in general, all samples exhibited less than a 10% increase in conductivity over the range of ambient to 363 K. The second region occurs between 363 and 423 K. Over this temperature range, there is a decrease in conductivity which may be due to the loss of free, adsorbed, or absorbed water.²⁵ This decrease in thermal conductivity was not as pronounced in the two samples of oil shale from the Green River Formation. The absence of this magnitude of decrease may be attributable to the reported low water content of the oil shale (Sect. 3.3). The third region is over the temperature range of 423–473 K, where conductivity increases with temperature. The relationship between conductivity and temperature appears to be more pronounced than in the first region, with conductivity generally increasing 20%. After one experiment, a single EGSP Kentucky No. 5 Well sample was allowed to cool to ambient temperature, and the procedure was repeated. Because of water sorbed from the surrounding environment during cooling, the shape of the resulting conductivity-vs-temperature curve was similar to that shown in Fig. 7. Significantly, the conductivity values obtained in the second

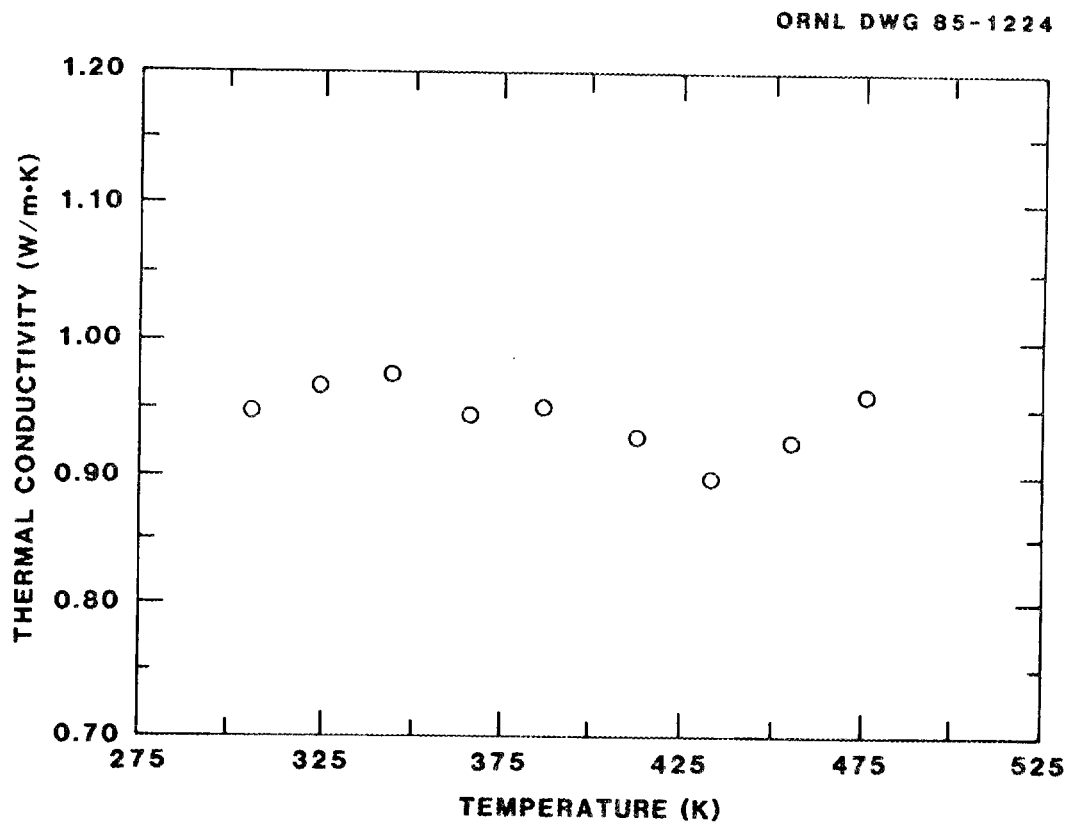


Fig. 7. Thermal conductivity as a function of temperature for shale from 176.8 m (EGSP Kentucky No. 5 Well).

experiment were 10% to 15% lower than those in the first experiment at temperatures below 393 K and within 3% to 5% of those in the first experiment at temperatures above 429 K.

Average thermal conductivities (from data in Appendix B) are shown in Table 2. Also shown are the number of data points and the standard deviation associated with the average thermal conductivity. In addition, the minimum and maximum conductivities, as well as the temperatures at which they occurred, are presented.

The minimum and maximum values and the temperatures at which they occur indicate significant data scatter. That is, some samples exhibited the maximum conductivity at a higher temperature than the minimum conductivity (e.g., Ohio Cleveland shale), while some samples exhibited the opposite trend (e.g., Middle Huron shale). Indeed, the minimum and maximum conductivities are within two standard deviations from the average for all but three samples. Thus the trends with temperature exhibited by Fig. 7 may be due solely to the effects of water movement and evaporation. Based on these data, it appears that the average thermal conductivity is representative of the temperature range studied for these samples.

The average thermal conductivity of 1.07 W/m·K for oil shale samples from the Green River Formation agrees favorably with the range of thermal conductivity values reported by Tihen, Carpenter, and Sohn³—0.69 to 1.56 W/m·K. Significantly, the range of average thermal conductivities shown in Table 2 overlaps for the shale types studied (0.73–1.09 W/m·K for the Devonian samples, 0.68–1.01 for the Pierre samples, and 1.07 for the oil shale samples). Thus the data presented are not sufficient to distinguish between the shale types. Exploring a broader temperature range may allow significant differences in thermal characteristics to be observed, particularly at temperatures above the regime where water evaporation is apparently occurring.

5.2 HEAT CAPACITY

Heat capacity data for all shale samples are shown in Appendix C. Average heat capacity values (obtained from data at 323, 373, 423, and 473 K) are shown in Table 3. In general, heat capacity obtained at these

Table 2. Thermal conductivity (λ) averaged over the temperature range of ambient to 473 K

Type of shale	Depth (m)	No. data points	Average λ (W/m ² K)	Standard deviation	Minimum λ^a	Maximum λ^a
Ohio Cleveland ^b	137.2	8	0.73	0.06	0.67(344)	0.81(473)
Chagrin Three Lick Bed ^b	149.7	7	0.83	0.05	0.78(369)	0.90(456)
Upper Huron ^b	157.3	17	0.86	0.03	0.79(429)	0.89(404)
	157.6	6	0.79	0.04	0.75(405)	0.86(373)
	158.4	10	0.78	0.04	0.73(426)	0.84(373)
	158.5	9	0.91	0.05	0.84(426)	1.02(372)
	158.8	9	0.91	0.05	0.83(430)	1.00(374)
	160.9	9	0.85	0.03	0.81(427)	0.93(375)
	164	5	0.94	0.01	0.93(413)	0.95(389)
Middle Huron ^b	175.6	7	0.87	0.04	0.81(442)	0.93(341)
	176.2	6	1.09	0.04	1.02(445)	1.14(393)
	176.3	9	1.08	0.06	1.05(461)	1.20(374)
	176.3	10	1.05	0.06	0.93(439)	1.17(374)
	176.5	10	0.93	0.03	0.91(431)	1.02(374)
	176.8	8	0.94	0.03	0.90(434)	0.98(345)
Pierre	45.1	4	1.01	0.21	0.75(441)	1.22(348)
	45.3	9	0.68	0.05	0.63(313)	0.76(372)
	45.4	4	0.88	0.08	0.78(417)	0.98(370)
	45.7	9	0.84	0.10	0.76(431)	0.95(316)
	49.1	4	0.87	0.06	0.81(406)	0.96(375)
Oil ^c		8	1.07	0.09	0.98(311)	1.23(451)

^aThe value in parentheses is the temperature (K) at which the thermal conductivity was measured.

^bFrom EGSP Kentucky No. 5 Well.

^cFrom Green River Formation.

four temperatures followed the trend shown in Fig. 8 for all samples. As seen in the figure, heat capacity increases with temperature to 423 K and then exhibits a minor decrease from 423 to 473 K. The minimum and maximum values shown in Table 3 are within one standard deviation of the average. The absence of the data scatter observed with the thermal conductivity measurements may be due to procedural differences. Unlike the

Table 3. Heat capacity (Cp) averaged over the temperature range of ambient to 473 K^a

Type of shale	Depth (m)	Average Cp (J/kg·K)	Standard deviation	Minimum Cp ^b	Maximum Cp ^b
Ohio Cleveland ^c	137.2	1214.2	209.3	963 (323)	1423.5(423)
	137.2	1256	167.5	1046.7(323)	1465.4(423)
	137.3	1046.7	125.6	879.2(323)	1214.2(473)
	137.4	1214.2	167.5	1046.7(323)	1381.6(473)
Chagrin Three Lick Bed ^c	149.4	1130.4	167.5	963 (323)	1297.9(473)
Upper Huron ^c	155.4	1256	209.3	1004.8(323)	1465.4(423)
	157	1088.6	167.5	879.2(323)	1297.9(423)
	157.4	1130.4	167.5	963 (323)	1297.9(423)
	161.5	1172.3	167.5	963 (323)	1297.9(423)
Pierre	44.8	1381.6	293.1	1088.6(323)	1674.7(473)
	45.1	1256	209.3	1004.8(323)	1507.2(473)
	45.7	1256	293.1	963 (323)	1591 (473)
Oil ^c		1256	125.6	963 (323)	1591 (473)

^aAverages are taken from heat capacity values obtained at 323, 373, 423, and 473 K.

^bThe values in parentheses are the temperatures at which the heat capacity was determined.

^cFrom EGSP Kentucky No. 5 Well samples.

conductivity measurements, the heat capacity measurements were performed in an airtight container, which prevents loss of volatile components, such as water. As with thermal conductivity, the average heat capacities overlapped for the shale types studied (1046.7–1256 J/kg·K for the Devonian samples, 1256–1381.6 for the Pierre samples, and 1256 for the Green River Formation samples).

5.3 THERMAL EXPANSION

Linear thermal expansion data were obtained on four samples from the Kentucky No. 5 Well; these data are plotted in Figs. 9–12. The samples

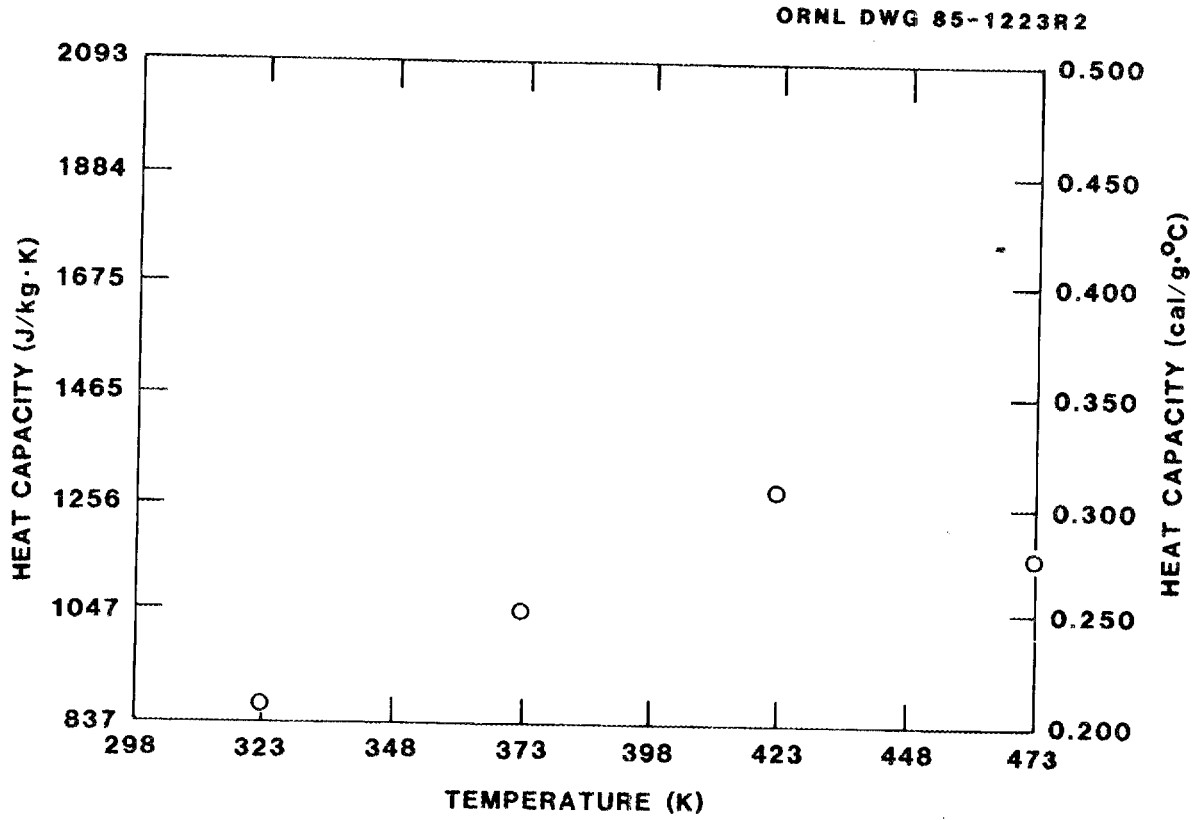


Fig. 8. Heat capacity as a function of temperature for shale from 187.8 m (EGSP Kentucky No. 5 Well).

ORNL DWG 85-1225R

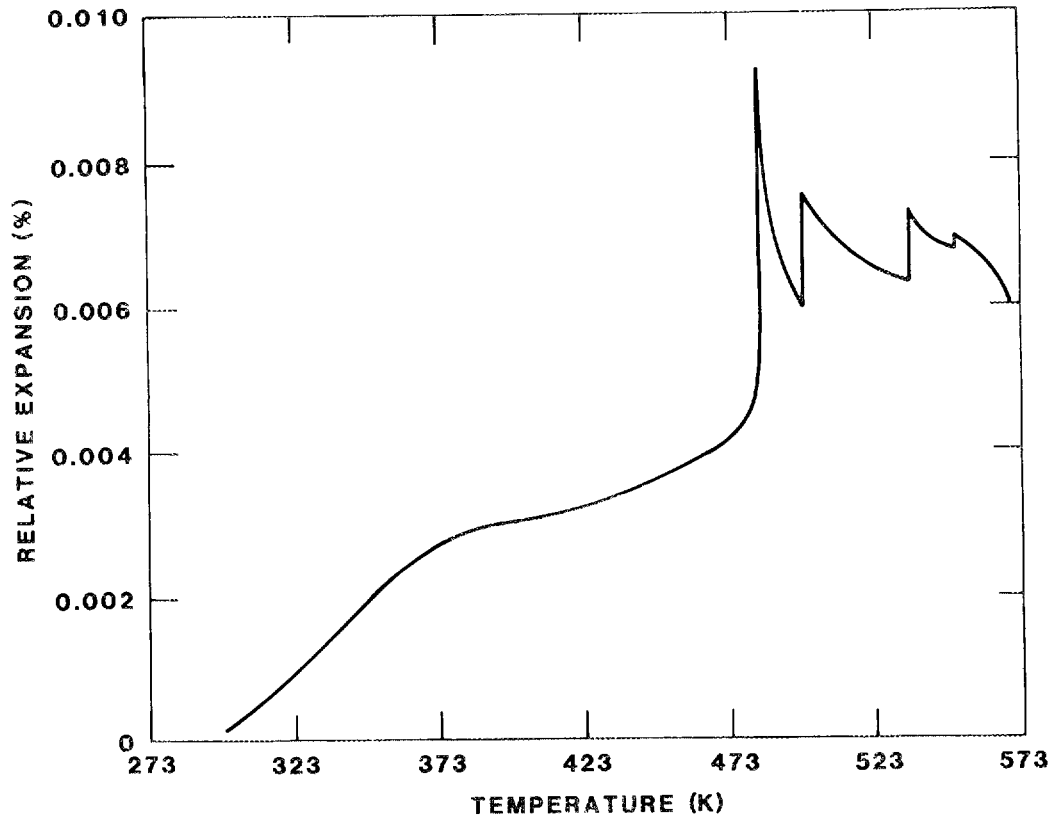


Fig. 9. Thermal expansion data for shale from 157 m (EGSP Kentucky No. 5 Well).

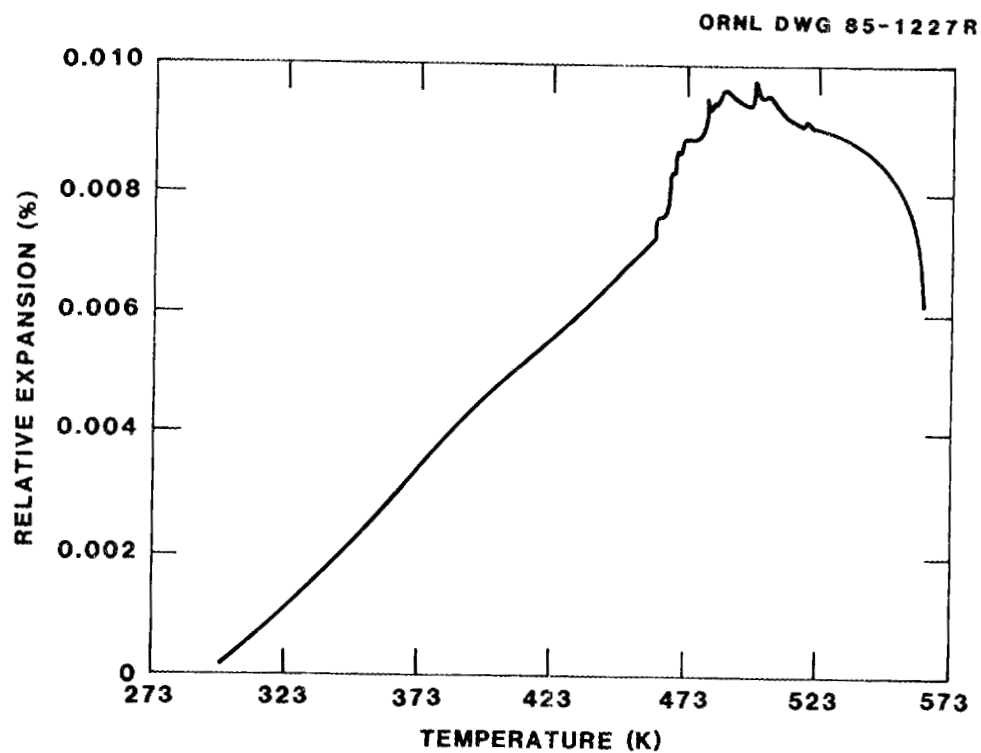


Fig. 10. Thermal expansion data for shale from 157.1 m (EGSP Kentucky No. 5 Well).

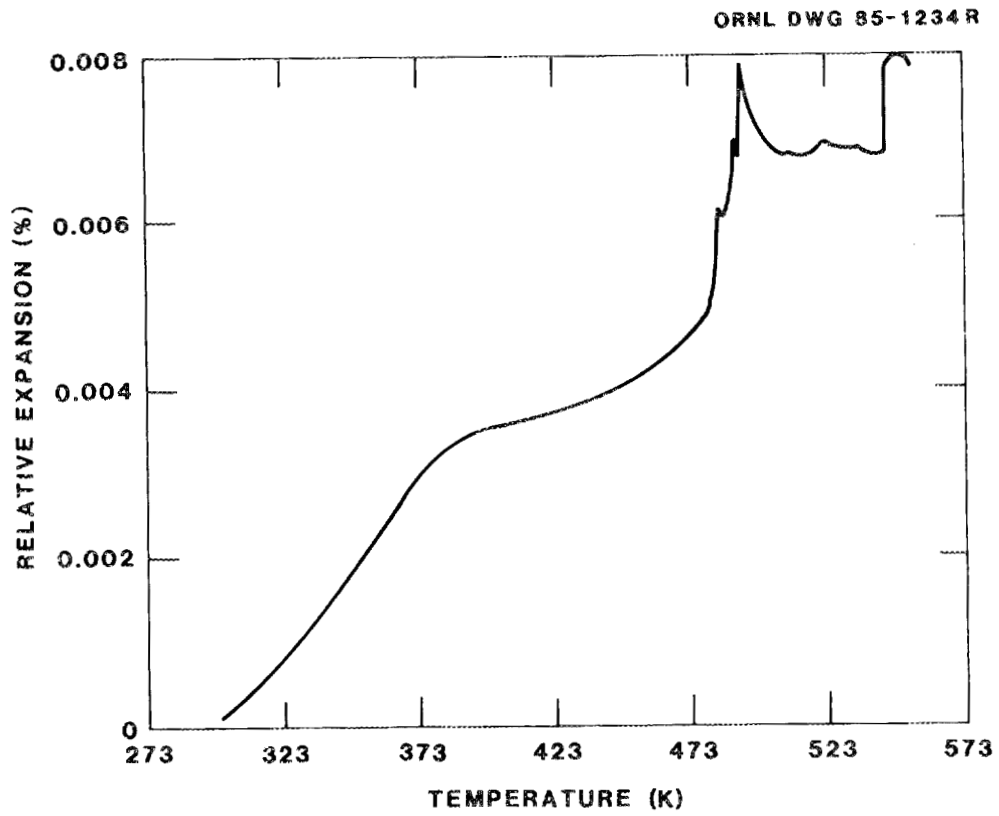


Fig. 11. Thermal expansion data for shale from 157.4 m (EGSP Kentucky No. 5 Well).

ORNL DWG 85-1229R

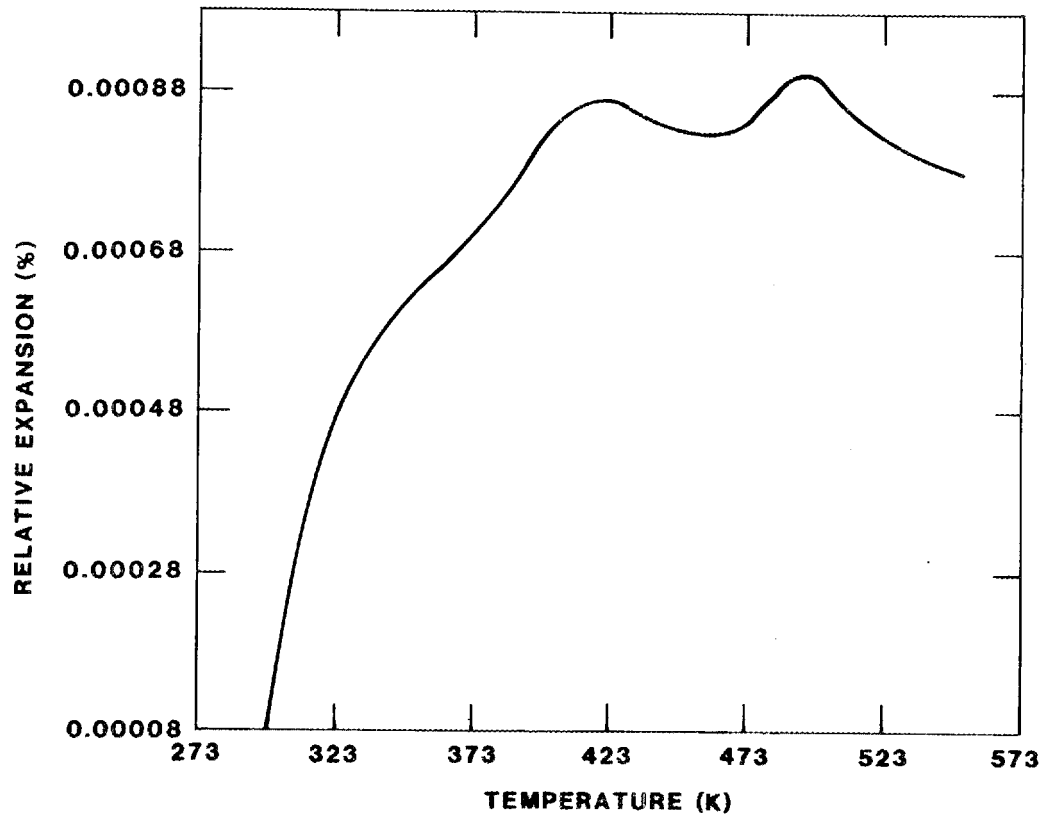


Fig. 12. Thermal expansion data for shale from 191.6 m (EGSP Kentucky No. 5 Well).

were taken from depths of 157, 157.1, 157.4, and 191.6 m. Additional data are shown in Appendix D.

Relative expansion increases with temperature up to ~ 473 K for all samples except the one obtained at 191.6 m, which showed an increase up to ~ 413 K. Maximum relative expansion values of 0.0075% and 0.0094% were recorded at 488 K for the 157- and 157.1-m samples, respectively. Maximum relative expansion values for the 157.4- and 191.6-m samples were 0.0071% (at 502 K) and 0.0009% (at 413 and 501 K), respectively.

Above 473 K, the samples underwent deformation, as indicated by the decrease in relative expansion (Figs. 9-12). The collapse of contained clay may have contributed to this deformation. For example, illitic clays exhibit a reduction of the spacing between platelets (from 13 to 10 Å) at a temperature of ~ 473 K.²⁶ Other clay types exhibit similar behavior at elevated temperatures.²⁶ The magnitude of the effect on relative expansion of the shale sample will be dependent on the type and quantity of the contained clays.

Thermal expansion coefficients may be obtained by differentiating data in Figs. 9-12 with respect to temperature. The values so obtained at various temperatures are reported in Appendix D (as alpha). Average expansion coefficients over the temperature range of ambient to 473 K (18 data points at each depth) are as follows:

<u>Shale depth (m)</u>	<u>Average expansion (%/K)</u>
157	23×10^{-6}
157.1	48×10^{-6}
157.4	34×10^{-6}
191.6	9×10^{-6}

6. SUMMARY

Thermal conductivity, heat capacity, and thermal expansion were measured for selected shale samples using comparative thermal conductivity, differential scanning calorimetry, and push-rod dilatometry techniques. Based on a literature survey, this equipment represents well-established, accepted thermal measurement techniques with accuracy and

precision comparable to those of alternative methods. These three techniques have been applied in the measurement of thermal properties of other geologic media. The literature survey indicated that the thermal properties of geologic media may be dependent on temperature, pressure, porosity, density, and composition.

On the basis of this survey, the study presented here was focused on thermal characteristics as a function of temperature. Data are presented on Devonian shale, Pierre shale, and oil shale from the Green River Formation. The majority of data were obtained on the Devonian shale samples. However, in general, data from the other samples were in agreement with trends established by the Devonian samples.

Experiments were performed over the temperature range of ambient to 473 K. In general, thermal conductivity, heat capacity, and thermal expansion increased with temperature. However, in the case of thermal conductivity and heat capacity, this temperature dependence was weak, with all values within two and one standard deviations from the average, respectively. The ranges of average thermal characteristics are shown in Table 4.

Relative thermal expansion increased with temperature over the range of ambient to 473 K with the exception of one sample (where the increase stopped at ~413 K). Above 473 K, all samples underwent deformation, as indicated by a significant decrease in relative expansion.

Data on samples from the Green River Formation are consistent with results reported by Tihen, Carpenter, and Sohn.³ In addition, data presented in Table 4 agree reasonably well with generic averages reported by Croff et al.²⁷—heat capacity of 837.4 J/kg•K and thermal conductivity of 1.4 W/m•K. It should be noted that the reported thermal conductivity of 1.4 W/m•K is an average from two samples—one with an average conductivity of 0.8 W/m•K and the other with an average conductivity of 2.0 W/m•K.²⁸

The literature search revealed no systematic comparison of thermal characteristics of different shale types which addressed variables that may potentially affect these thermal characteristics. Such a study is necessary for a quantitative comparison of thermal characteristics of different shale types in order to understand, and ultimately to predict,

Table 4. Ranges in average thermal characteristics over the temperature range of ambient to 473 K

Shale	Thermal property		
	Thermal conductivity (W/m·K)	Heat capacity (J/kg·K)	Thermal expansion coefficient (%/K)
Devonian	0.73-1.09	879.2-1046.7	9-48 ($\times 10^{-6}$)
Pierre	0.68-1.01	1046.7-1088.6	
Green River Formation	1.07	1046.7	

thermal behavior. Variables of potential interest which have been identified include temperature, composition, pressure, and anisotropy. Future studies need to include these variables in order to explain differences in thermal behavior in a manner suitable for predictive modeling.

7. REFERENCES

1. J. J. Dell'Amico, F. K. Captain, and S. H. Chansky, Characterization and Thermal Conductivities of Some Samples of Conasauga Shale, ORNL-MIT-20, Oak Ridge National Laboratory, Mar. 29, 1967.
2. R. Nottenburg et al., "Measurement of Thermal Conductivity of Green River Oil Shales by a Thermal Comparator Technique," FUEL 57 (December 1978).
3. S. S. Tihen, H. C. Carpenter, and H. W. Sohn, Thermal Conductivity and Thermal Diffusivity of Green River Oil Shale, Laramie Petroleum Research Center, Laramie, Wyoming, National Bureau of Standards Special Publication No. 302, 1968.
4. M. Prats and S. M. O'Brien, J. Petrol. Technol. 97 (1975).
5. M. J. Gavin and L. H. Sharp, USBM Rep. Invest. 2152, U.S. Bureau of Mines, 1920.

6. T. A. Sladek, "A Determination of the Composition and Temperature Dependencies of Thermal Conductivity Factors for Green River Oil Shale," Ph.D. dissertation, Colorado School of Mines, 1971.
7. F. Birch, "Thermal Conductivity, Climatic Variation and Flow near Columet, Michigan," Am. J. Sci. 252, 1 (1954).
8. W. H. Diment and E. C. Robertson, "Temperature, Thermal Conductivity, and Heat Flow in a Drilled Hole near Oak Ridge, Tennessee," J. Geophys. Res. 68, 5035 (1963).
9. W. H. Somerton, "Some Thermal Characteristics of Porous Rocks," J. Petrol. Technol. 10, 61 (1958).
10. W. H. Somerton, "Thermal Characteristics of Porous Rocks at Elevated Temperatures," J. Petrol. Technol. 12, 77 (1960).
11. Environmental Impact Statement - Management of Commercially Generated Radioactive Waste, DOE/EIS-0046-D, U.S. DOE, April 1979.
12. Dames and Moore, Baseline Rock Properties - Shale, Y/OWI/TM-336, Office of Waste Isolation, Union Carbide Corporation, Nuclear Division, Oak Ridge, Tennessee, 1976.
13. C. E. Weaver, Geothermal Alteration of Clay Minerals and Shales: Diagenesis, ONWI-21, Office of Nuclear Waste Isolation, Battelle Memorial Institute, 1979.
14. E. C. Robertson, Thermal Conductivity of Rocks, USGS Open File Report 79-356, U.S. Geological Survey, 1979.
15. E. H. Ratcliffe, "Thermal Conductivities of Fused and Crystalline Quartz," Brit. J. Appl. Phys. 10, 22 (1959).
16. F. Birch and H. Clark, "The Thermal Conductivity of Rocks and Its Dependence upon Temperature and Composition," Am. J. Sci. 238, 529 (1940).
17. M. T. Morgan and G. A. West, Thermal Conductivity of the Rocks in the Bureau of Mines Standard Rock Suite, ORNL/TM-7052, Oak Ridge National Laboratory, 1980.
18. D. C. Larson, Thermal Conductivity 16, Plenum Press, New York, 1983.
19. E. I. Parkhomenko, Electrical Properties of Rocks, Plenum Press, New York, 1967.
20. P. W. Bridgman, The Physics of High Pressure, G. Bell and Sons, London, 1958.

21. J. N. Sweet, "Pressure Effects on Thermal Conductivity and Expansion of Geologic Materials, SAND 78, 1991 (1979).
22. Cliffs Minerals, Inc., Eastern Gas Shales Project Kentucky #5 Well - Rowan County Phase II, Report Preliminary Laboratory Results, April 1982.
23. F. D. Homan, Oak Ridge National Laboratory, letter to T. F. Lomenick, Oak Ridge National Laboratory, Oct. 7, 1985 [letter RSI(RCO)-087/10-85/209].
24. F. D. Hansen, RE/SPEC, Inc., letter to T. F. Lomenick, Oak Ridge National Laboratory, Sept. 11, 1985 [letter RSI(RCO)-087/9-85/265].
25. R. W. Grimshaw, The Chemistry and Physics of Clays and Allied Ceramic Materials, John Wiley & Sons, New York, 1971.
26. C. E. Weaver and L. D. Pollard, The Chemistry of Clay Minerals, Vol. 5, Elsevier Scientific Publishing Co., New York, 1973.
27. A. G. Croff et al., Evaluation of Five Sedimentary Rocks Other Than Salt for Geologic Repository Siting, ORNL-6241/V3, Oak Ridge National Laboratory, 1985.
28. Office of Waste Isolation Progress Report, Y/OWI/TM-43/2, Office of Waste Isolation, Union Carbide Corporation, Nuclear Division, Oak Ridge, Tennessee, November 1977.

APPENDIX A:
TECHNIQUES FOR THE MEASUREMENT OF THERMAL PROPERTIES

In evaluating the suitability of geologic media for a repository, the thermal properties of interest are thermal conductivity, thermal expansion, and heat capacity. A wide variety of experimental techniques is available to measure these three parameters. A discussion of these techniques is presented in this appendix.

THERMAL CONDUCTIVITY

Thermal conductivity is measured by two general methods: absolute and comparative. In absolute methods, the sample of interest is placed in a configuration such that the heat flow through the sample can be modeled by an explicit mathematical equation. The equation is then used to calculate thermal conductivity directly. Conversely, in comparative methods, the sample of interest and a reference sample of known thermal conductivity are placed in such a way that heat flow through the sample and reference can be modeled by an implicit mathematical equation. The equation is used to calculate the sample's thermal conductivity relative to that of the reference.

Absolute Methods

Although many different procedures may be used to obtain thermal conductivity data by absolute methods, most methods of this type measure heat flow in the radial direction. For radial flow procedures, the sample is normally fabricated in the shape of a right-circular cylinder with provision for placing a heating element at the vertical axis of the cylinder. Thermocouples are then placed in the sample at varying radial distances from the heater (Fig. A.1). When heat is applied, the temperature is allowed to stabilize, and measurements are made to determine the power output of the heater. This information, along with the thermocouple readings, is used to calculate the thermal conductivity (λ) of the sample by using the equation

$$\lambda = \frac{P \ln(r_2/r_1)}{2\pi L(T_1 - T_2)} \quad , \quad (\text{A.1})$$

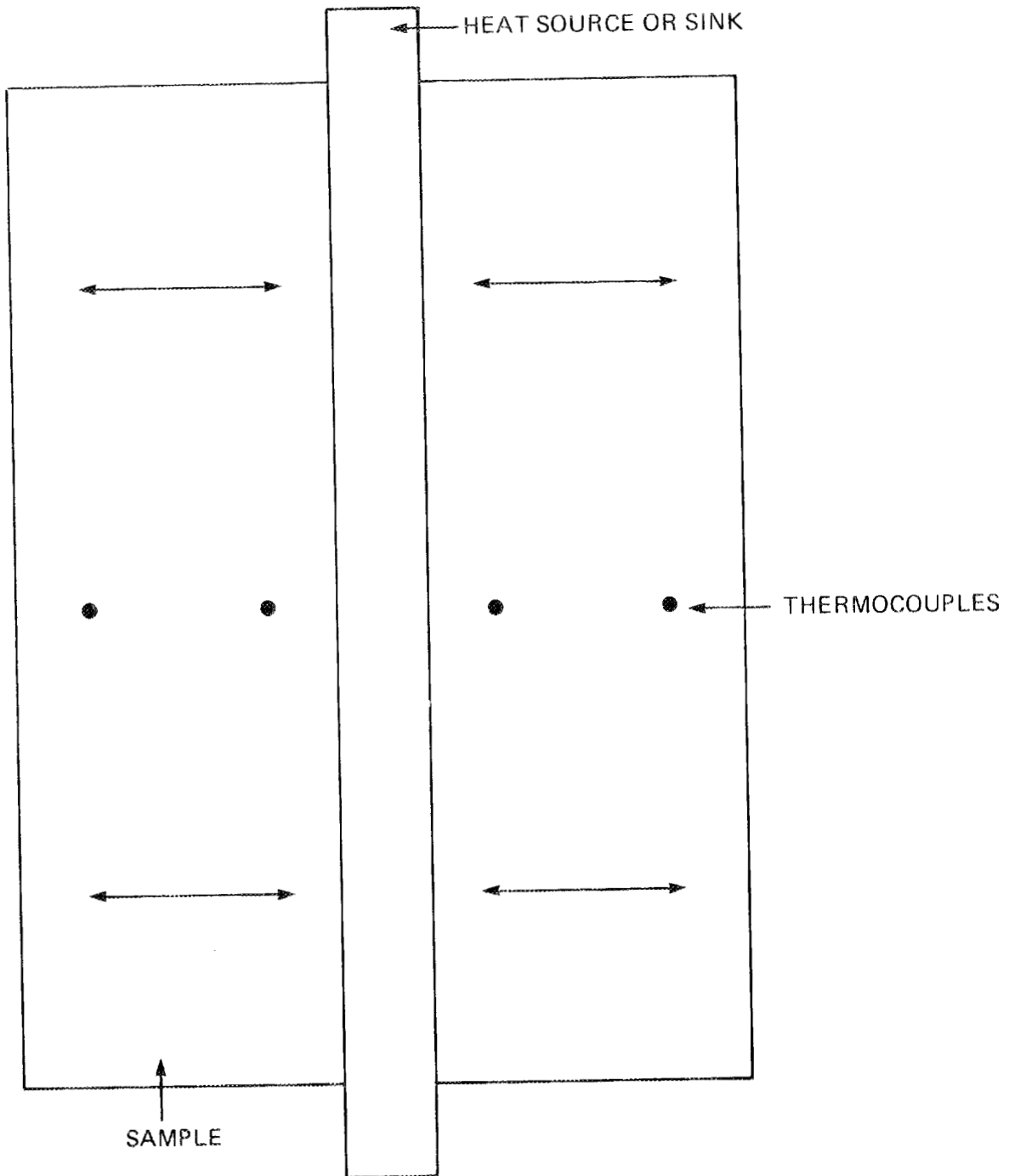


Fig. A.1. Schematic of radial heat flow method for the measurement of thermal conductivity.

where

- P = power output of heater,
- r_1 = radial distance from the heat source,
- T_1 = temperature at point r_1 ,
- L = sample length.

This procedure and the associated mathematical model are accurate only if the sample approximates a cylinder of infinite length. In investigations by Kingery,¹ an $L/2r$ ratio of 12 was used to minimize end effects at higher temperatures. Slack and Glassbrenner² employed an $L/2r$ ratio of 5 when measuring the thermal conductivity of germanium.

A modified version of this procedure has been developed to overcome infinite length constraints. In this method, known as the guarded end-plate procedure, plate-type heaters are used at each end of the sample to duplicate the core heater temperature at the top and bottom of the cylinder, thereby minimizing heat losses in the axial direction (Fig. A.2). The accuracy and precision of this technique have been reported to be from 3% to 12%.^{3,4}

Comparative Methods

In comparative methods, Pyrex 7740 or Pyroceram 9606 is typically used as a standard reference material (SRM). Axial heat flow methods are more widely used than radial methods for comparative measurements because of the relative ease of sample and reference material fabrication. This procedure is currently used for thermal conductivity measurements of geologic specimens by the Engineered Waste Disposal Technology (EWD) Group at ORNL. The EWD Group uses the Dynatech Model TCFCM-N20 thermal conductivity instrument, whose general configuration is shown in Fig. A.3.

The sample and reference materials are normally fabricated in the shape of a 0.005- × 0.005-m square or a cylinder of 0.005 m diam and of varying lengths. The sample and reference materials are fitted with thermocouples, as depicted in Fig. A.4. The sample is placed in a test stack consisting of a heat source, two identical reference materials, and a heat sink, as shown in Fig. A.3. The annulus between the test stack and guard heaters is filled with insulating material. The heater and heat

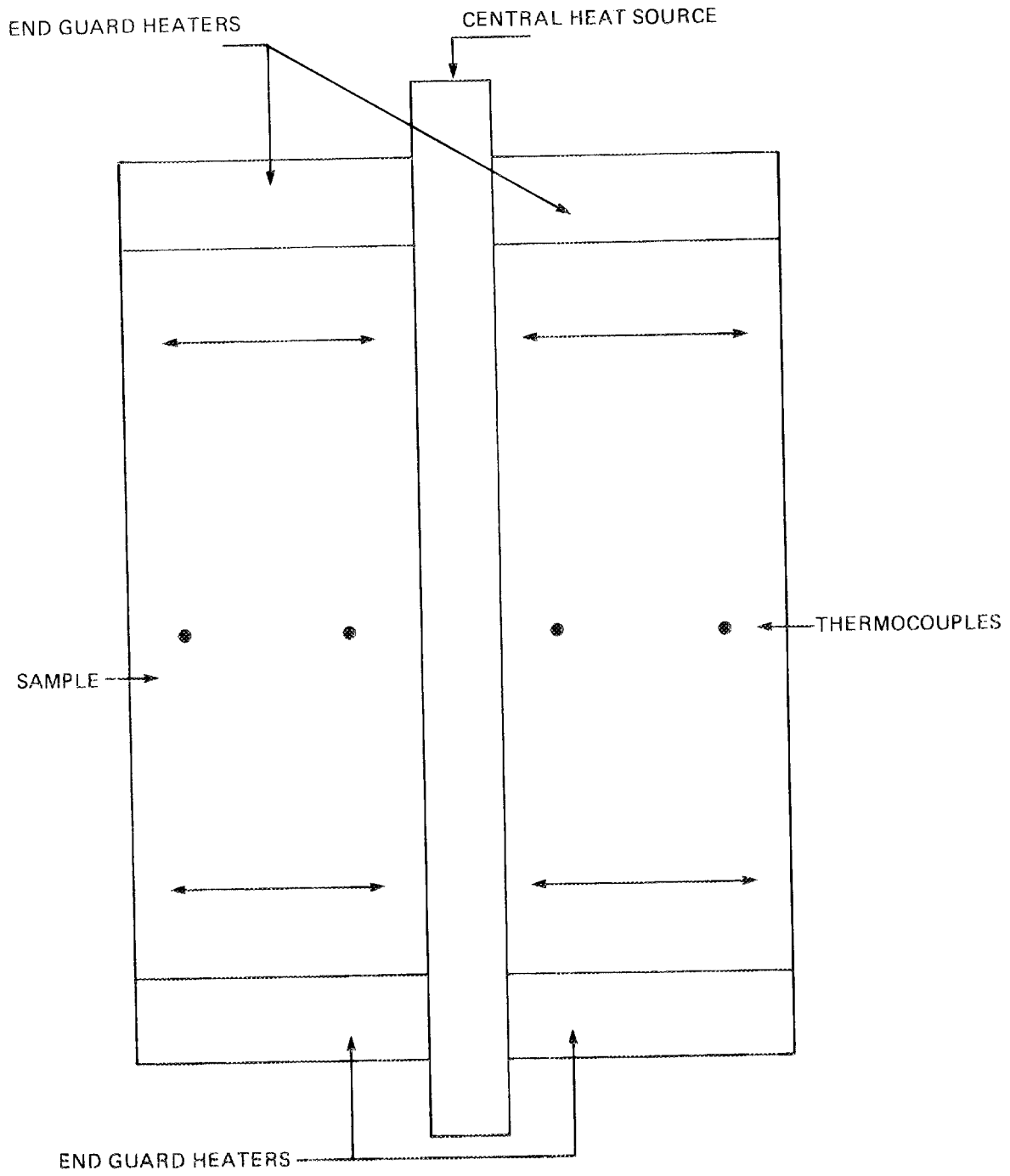
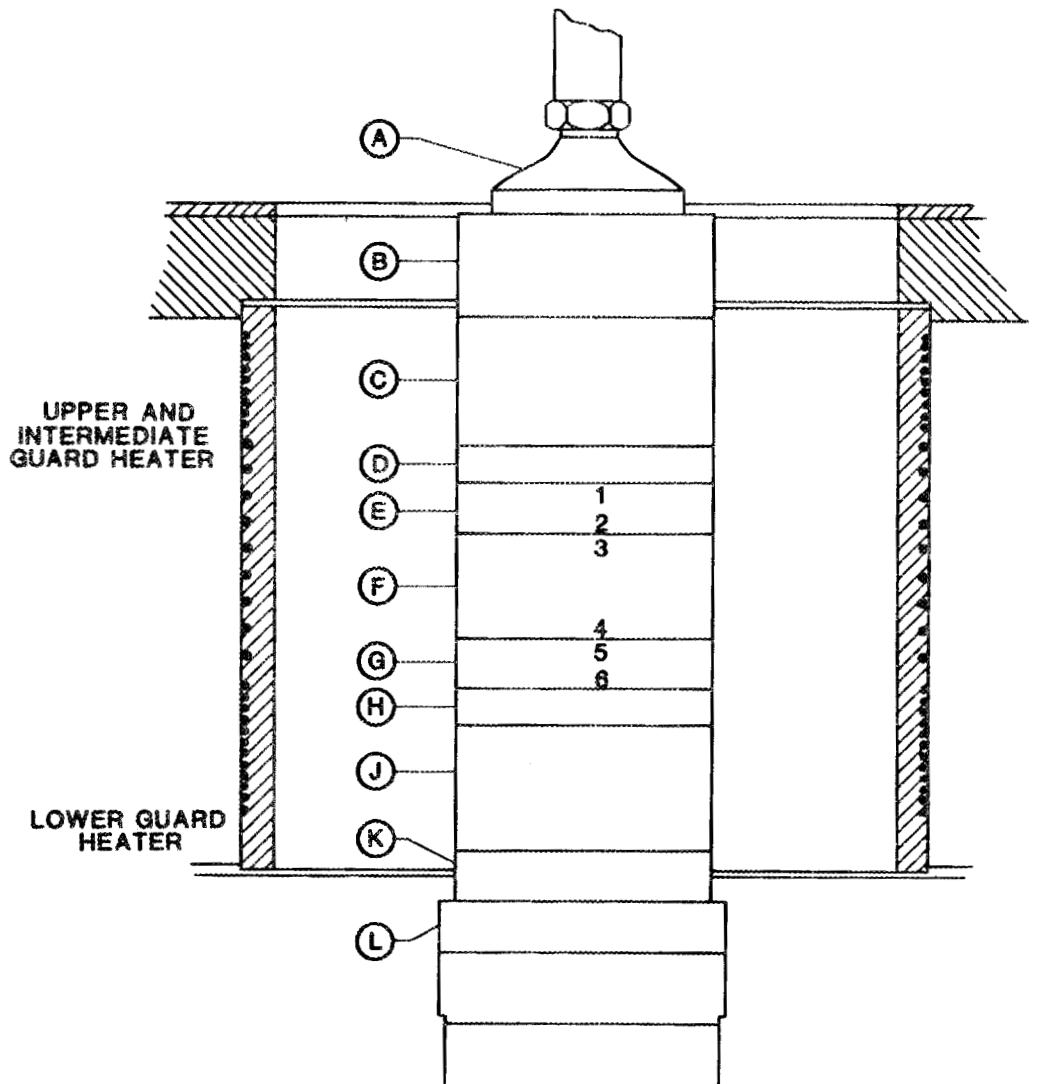


Fig. A.2. Schematic of radial heat flow method with guard heaters.



- | | |
|---------------------------|---|
| A. PRESSURE PAD | G. BOTTOM REFERENCE STANDARD |
| B. INSULATION | H. SURFACE PLATE |
| C. MAIN HEATER | J. AUXILIARY HEATER |
| D. SURFACE PLATE | K. SPACER |
| E. TOP REFERENCE STANDARD | L. HEAT SINK |
| F. TEST SAMPLE | NOS. 1, 2, 3, 4, 5, 6, •: THERMOCOUPLES |

Fig. A.3. Schematic of thermal conductivity analyzer.

ORNL DWG 86-198R2

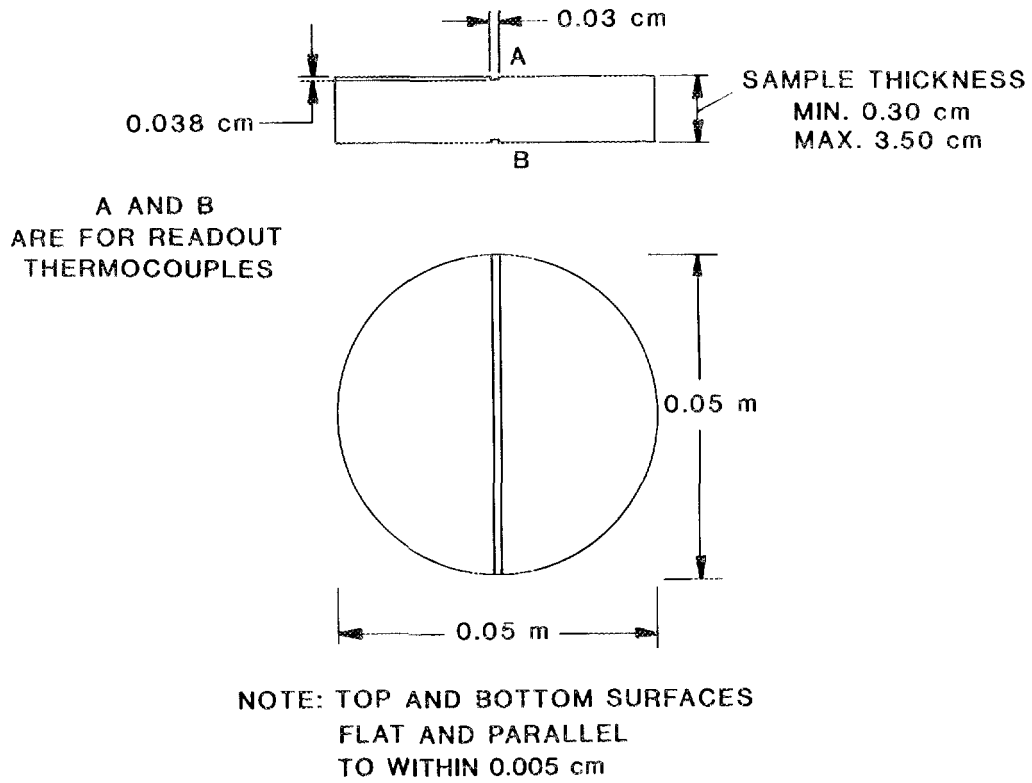


Fig. A.4. Thermal conductivity sample configuration.

sink control the magnitude of the thermal gradient, and the guard heaters, together with the insulating material, minimize heat losses in the radial direction. A thermal gradient is applied to the stack, and sufficient time is allowed for the temperature readings from the thermocouples to stabilize. The thermal conductivity of the sample may then be calculated by using the equation

$$\lambda_{\text{sample}} = \frac{1}{2} \left(\frac{\Delta X}{\Delta T} \right)_{\text{sample}} \left[\left(\frac{\lambda \Delta T}{\Delta X} \right)_{\text{top reference}} + \left(\frac{\lambda \Delta T}{\Delta X} \right)_{\text{bottom reference}} \right], \quad (\text{A.2})$$

where

λ = thermal conductivity,

ΔX = thickness of material,

ΔT = temperature drop across ΔX .

The accuracy and precision of this method have been reported to be 3%.⁵

THERMAL EXPANSION

The most widely used method of measuring thermal expansion is push-rod dilatometry.⁶ For measurements of this type, the sample (or reference material for calibration purposes) is placed in a sample holder fabricated from a material of low thermal expansion. Heat is supplied by a tube furnace that slides into position around the sample/holder. As heat is applied, the change in sample length is represented by the output of a probe rod and linear variable differential transformer (LVDT) assembly, as shown in Fig. A.5. The outputs of the transformer and a thermocouple placed in close proximity to the sample are recorded on a standard x-y plotter. The thermal expansion coefficient of the sample is derived by comparing the plot of the sample's behavior with a plot of that from a known reference. Typical maximum sensitivity of this method is 1×10^{-4} m of sample length change per meter of recorder chart deflection.

DWG. NO. K/G-87-297(A)

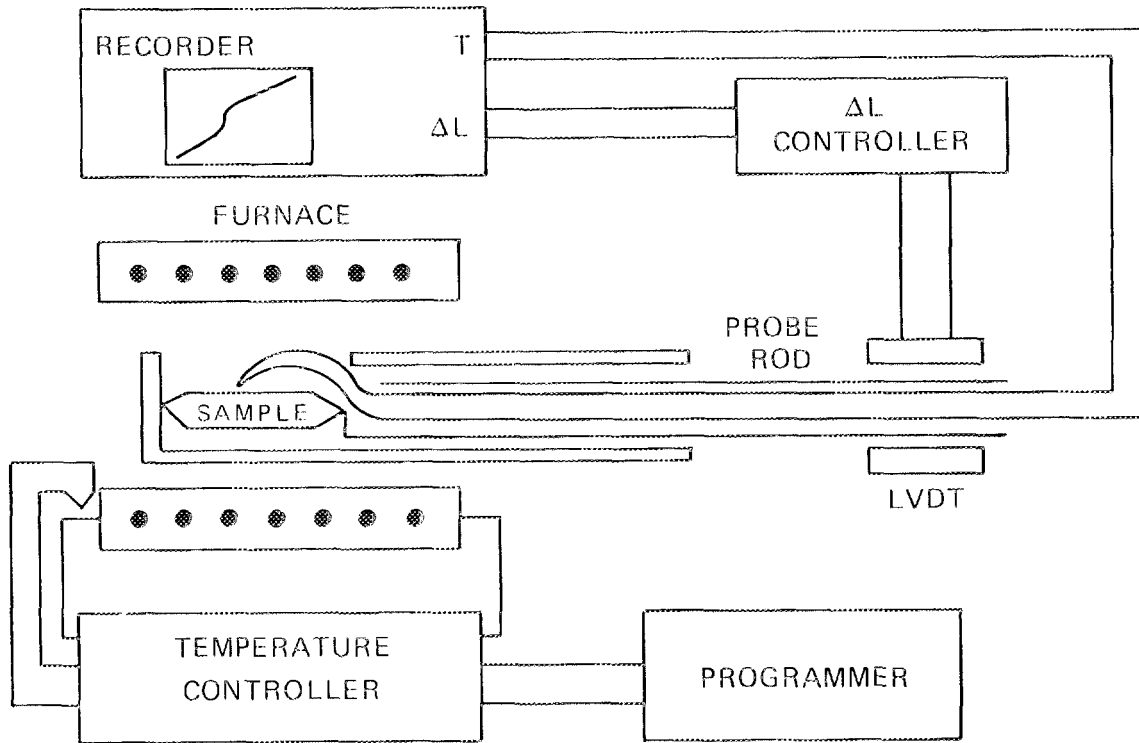


Fig. A.5. Block diagram of push-rod dilatometer.

In 1967, the structure and materials panel of the Advisory Group for Aerospace Research and Development initiated a cooperative measurement program to determine the accuracy of data and experimental techniques for thermophysical properties of solid material at high temperatures.⁷ Sixteen laboratories participated in this program.⁸ As part of this program, thermal expansion measurements up to 1000°C using push-rod techniques were evaluated.

The results of this evaluation have been reported by Fitzer and Wisenburger.⁹ As a basis for comparison, "absolute" expansion data using optical and x-ray techniques were obtained for gold and platinum and compared with data reported in the literature.¹⁰⁻¹³ For all data, the absolute deviations from the means were $\leq +0.005\%$. Data obtained by the participants using push-rod techniques showed deviations from the means of 0.015% expansion at 300°C and a maximum of 0.030% expansion at 900°C. The report indicated that the increase in deviations was due to individual laboratory systematic calibration errors. Similar measurements on alumina and AXM-5Q graphite resulted in maximum deviations of ± 0.005 and 0.010%, respectively. This report concluded that the accuracy of push-rod techniques was dependent on the accuracy of the calibration but was approximately equal to a relative deviation of 0.3% from the mean thermal expansion value.

An ultraprecise method of measuring thermal expansion has been developed at the Optical Sciences Center of The University of Arizona.¹⁴ This method is based on the principle of laser interferometry. In this method, the sample is fashioned in the shape of a hollow right-circular cylinder. In this form, the sample serves as the spacer for a Fabry-Perot etalon (Figs. A.6 and A.7). The etalon serves as a resonator for an He-Ne red laser. The change in sample length arising from a change in sample temperature alters the resonance frequency of the etalon. The change in resonance frequency is related to the thermal expansion coefficient by the equation

$$\alpha = \frac{1}{L} \frac{\Delta L}{\Delta T} = \frac{1}{v} \frac{\Delta v}{\Delta T} \quad , \quad (\text{A.3})$$

DWG. NO. K/G-87-1189

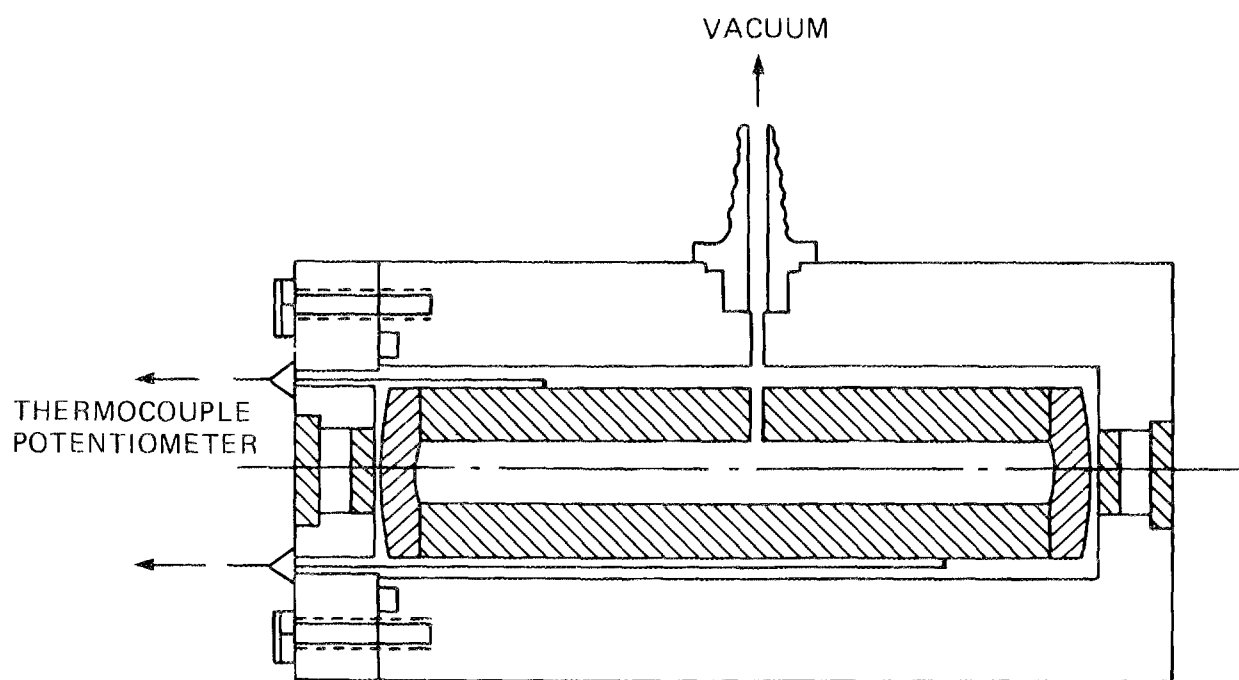


Fig. A.6. Fabry-Perot etalon.

DWG. NO. K/G-87-1190

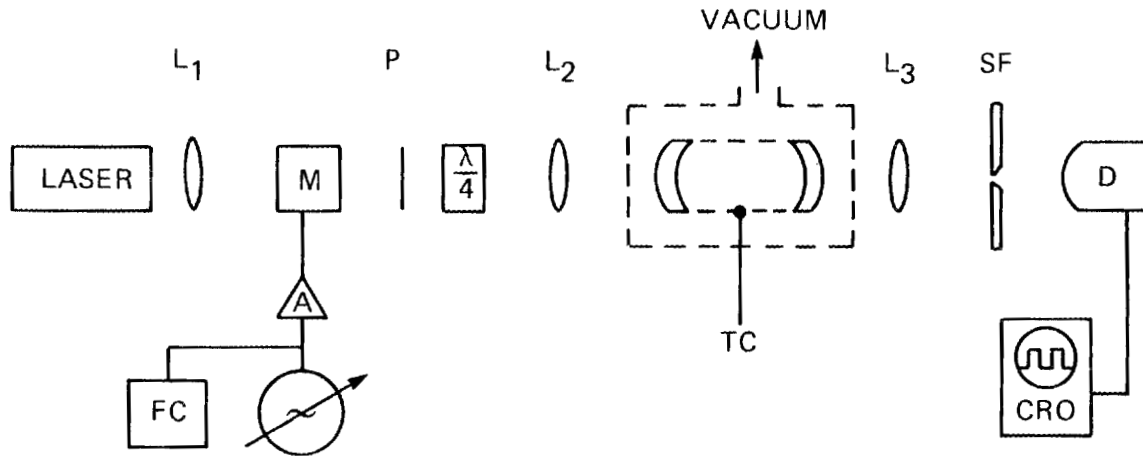


Fig. A.7. Block diagram of Fabry-Perot etalon.

where

α = coefficient of thermal expansion,

ν = resonance frequency of etalon,

L = length of sample,

T = temperature of sample.

Both the reproducibility and precision of this method have been reported to be 1 part in 1,000,000,000.

HEAT CAPACITY

Drop calorimetry and differential scanning calorimetry are the commonly used methods for determining the specific heat of solids. These two methods will be described.

Drop Calorimetry

For drop calorimetry measurements, the sample is heated to the desired temperature and transferred to a calorimeter containing a quantity of solid (such as ice) or liquid of known thermal properties. If a solid is used, then the temperature of the calorimeter well must be maintained at the melting point of the solid (0°C for ice or 26.9°C for diphenyl ether). Specific heat determinations are made, based on the amount of heat evolved from the sample during cooling. The quantity of heat evolved is determined by the amount of solid which melts or by the temperature increase of the liquid. The specific heat of the sample can be calculated on the bases of the mass of the sample and the quantity of heat transferred to the calorimeter.*

Differential Scanning Calorimetry

The differential scanning calorimeter (DSC) compares the amount of energy required to raise the temperature of a known weight of a standard reference material at a predetermined heatup rate to a predetermined temperature with the amount of energy required to raise the temperature of

*For a more detailed treatment of this method, the reader is referred to Treatise on Analytical Chemistry, Part I, Vol. 8, I. M. Kolthoff and P. J. Elving, Wiley Interscience, 1968.

the sample under identical conditions. As such, the DSC is not restricted by the thermal properties of the reference material, as in the case of drop calorimetry.

The sample (S) and reference material (R) are placed in the DSC as shown in Fig. A.8. As heat is applied, the temperatures of the sample and reference material vs power input are plotted on an x-y chart plotter (see Fig. A.9). The specific heat of the sample may be calculated from the ratio of the temperature increase of the sample to the corresponding temperature increase of the reference material. This comparison yields a factor that is multiplied by the specific heat of the reference material to obtain the specific heat of the sample (see Fig. A.9).

Differential scanning calorimetry has been used successfully to determine specific heats of geologic materials by N. D. Topor and L. V. Mel'chakova of Moscow University.¹⁵ Reported reproducibility of this method is 2% to 3%, with a general accuracy of 2% to 3%.

REFERENCES

1. W. D. Kingery, J. Am. Ceram. Soc. 38, 3 (1954).
2. G. A. Slack and G. Glassbrenner, Phys. Rev. 120, 782 (1960).
3. A. M. Banaev and V. Ya. Chekhovskoi, Teplofizika Vysokikh Temperature 3, 47 (1965).
4. A. D. Feith, Advances in Thermophysical Properties at Extreme Temperatures and Pressures, pp. 328-35, American Society of Mechanical Engineers, New York, 1985.
5. D. R. Flynn, "Thermal Conductivity of Ceramics," Mechanical and Thermal Properties of Ceramics, National Bureau of Standards Special Publication No. 303, p. 63, 1969.
6. Harrop Laboratories, Instruction Manual for Thermal Dilatometric Analyzer Harrop Model TD-712, Columbus, Ohio, 1977.
7. E. Fitzer, AGARD Report No. 12, Advisory Group for Research and Development, Nevelly-sur-Seine, France, 1967.
8. E. Fitzer, AGARD Report No. 31, Advisory Group for Research and Development, Nevelly-sur-Seine, France, 1971.

DWG. NO. K/G-87-294(A)

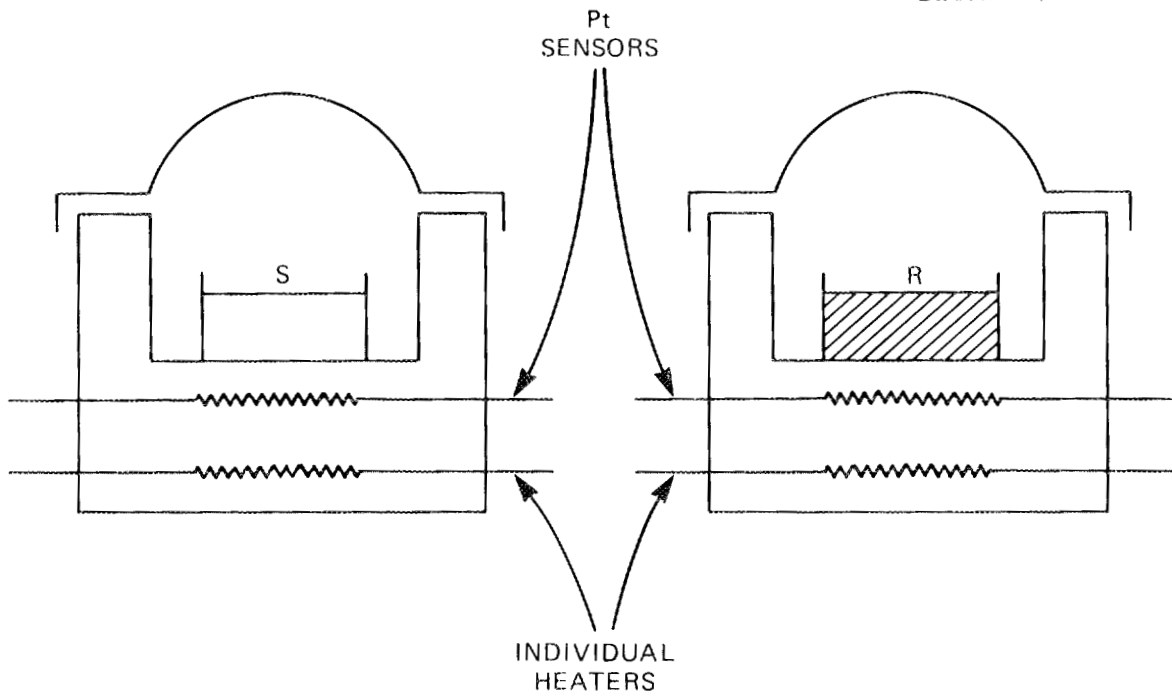


Fig. A.8. Arrangement of sample and reference material for determination of heat capacity by DSC.

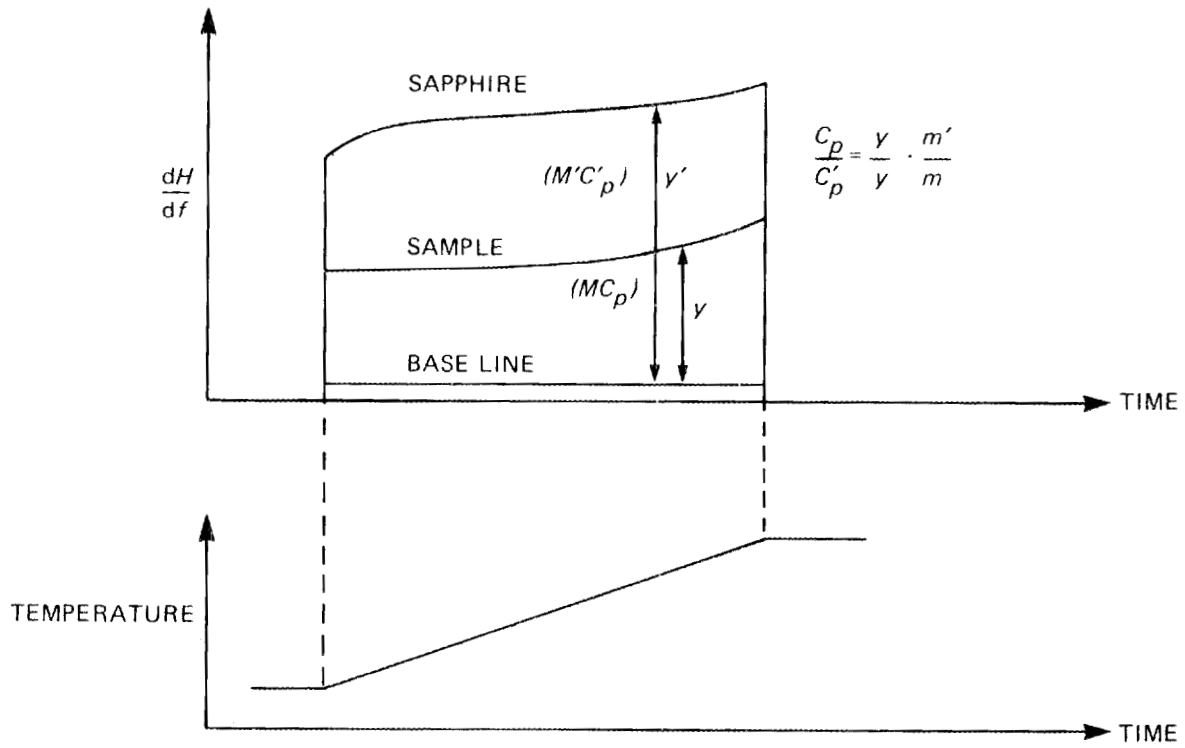


Fig. A.9. Specific heat determination by DSC using sapphire as a reference material.

9. E. Fitzer and S. Wisenburger, "Cooperative Measurement of the Thermal Expansion Behavior of Different Materials up to 1000°C by Pushrod Dilatometers," Proceedings of the AIP Conference on Thermal Expansion, Corning, New York, 1972.
10. R. O. Simmons and R. W. Balluffi, Phys. Rev. 125(3), 862-72 (1962).
11. R. G. Merryman and C. P. Kempter, J. Am. Ceram. Soc. 48(4), 202 (April 1965).
12. E. Kaelble, Handbook of X-Rays, McGraw-Hill, New York, 1967.
13. AIP Handbook, 3rd ed., Sects. 4-66, McGraw-Hill, New York, 1969.
14. S. F. Jacobs et al., "Ultraprecise Measurement of Thermal Expansion Coefficients - Recent Progress," Proceedings of the AIP Conference on Thermal Expansion, 1971.
15. N. D. Topor and L. V. Mel'chakova, Measurement of Cp of Minerals in the Scanning Regime by the Method of Quantitative Differential Thermal Analysis, Moscow University Geology Bulletin 37, p. 6, 1982.

APENDIX B:

THERMAL CONDUCTIVITY DATA FOR SHALE SAMPLES

This appendix presents the thermal conductivity data on all shale samples. Average values and conclusions presented in the text were taken from these data.

APPENDIX B.1. THERMAL CONDUCTIVITY DATA FOR DEVONIAN SHALE SAMPLES
FROM EGSP KENTUCKY NO. 5 WELL

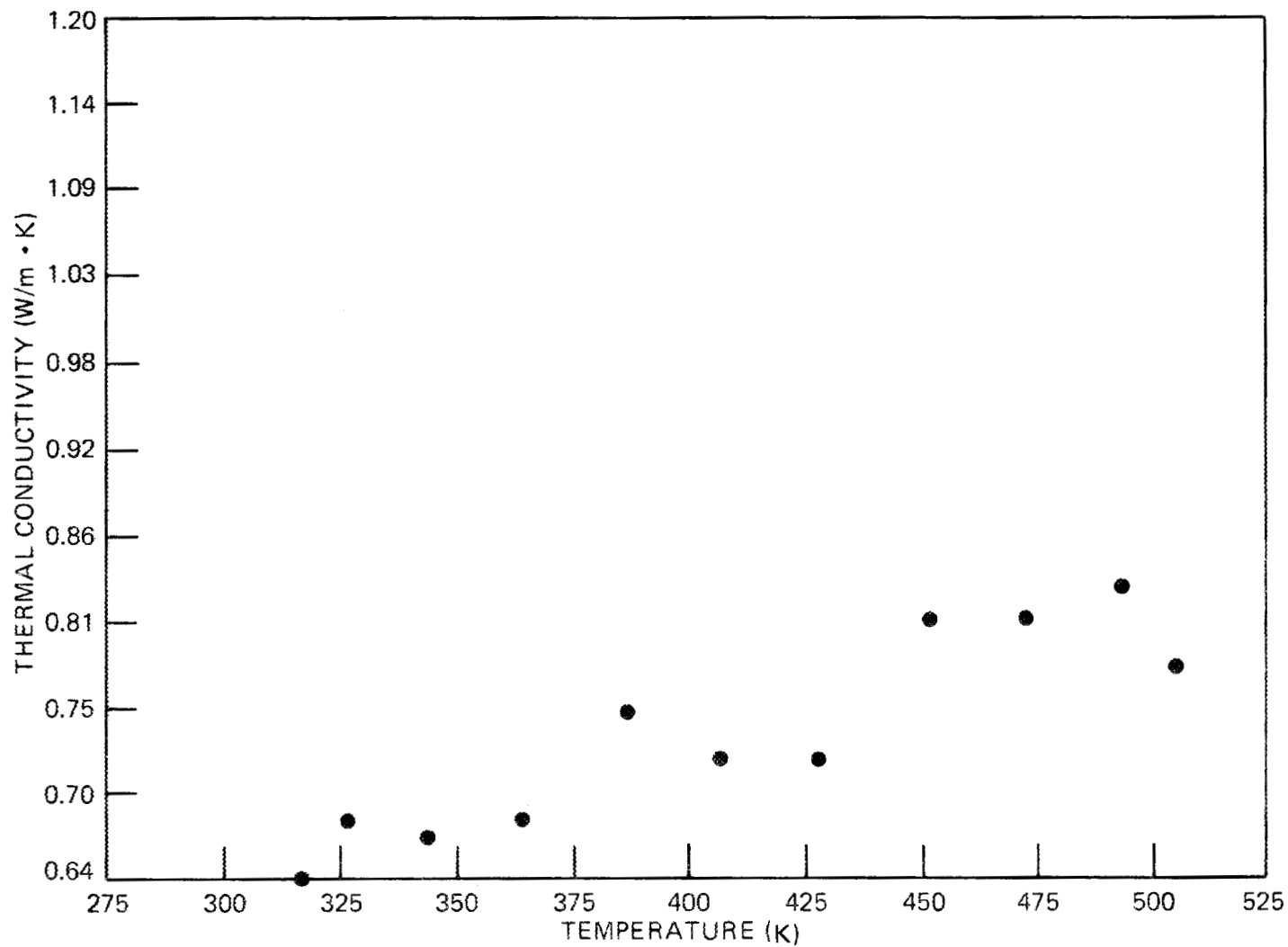


Fig. B.1. Thermal conductivity as a function of temperature for shale from 137.2 m (450 ft).

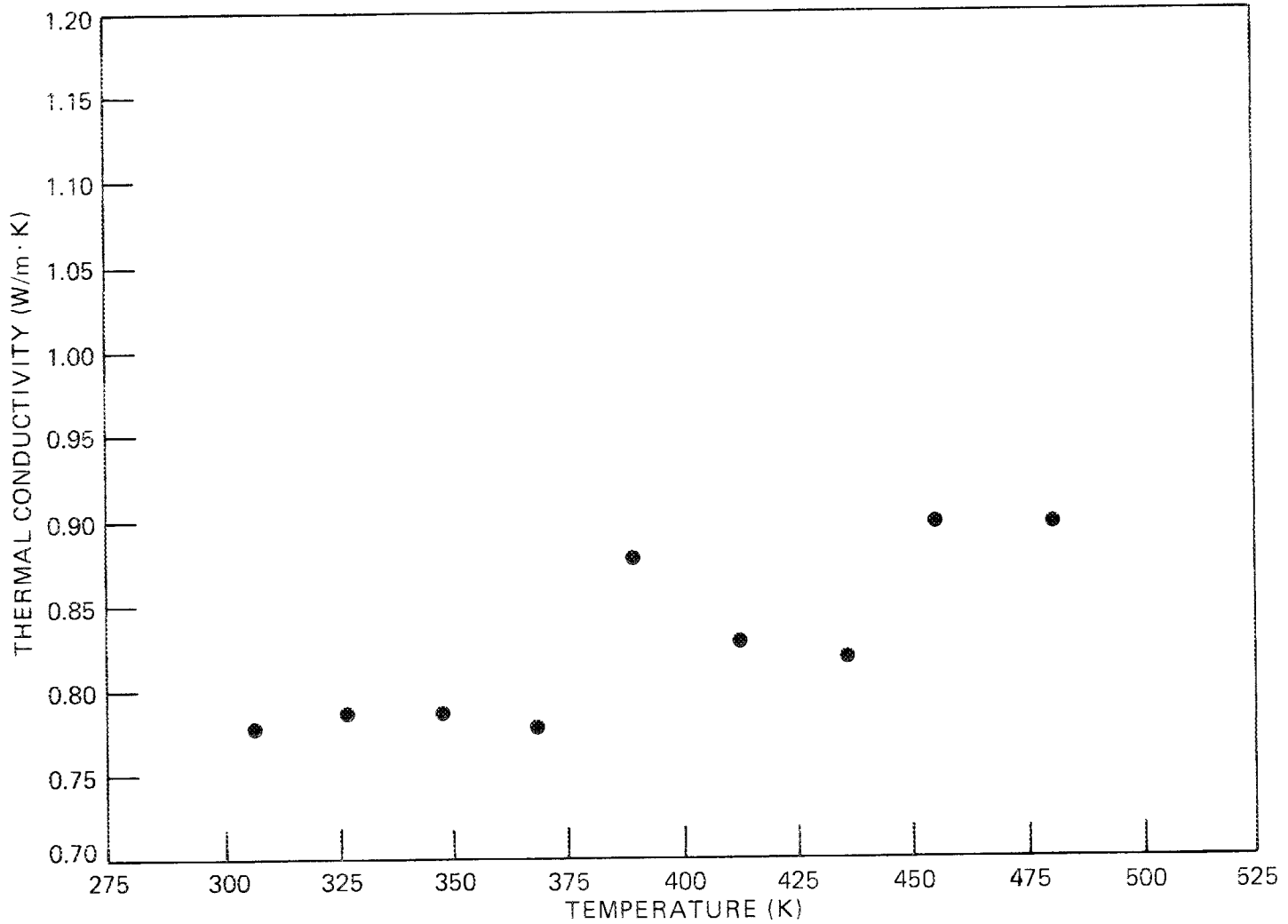


Fig. B.2. Thermal conductivity as a function of temperature for shale from 149.7 m (491 ft).

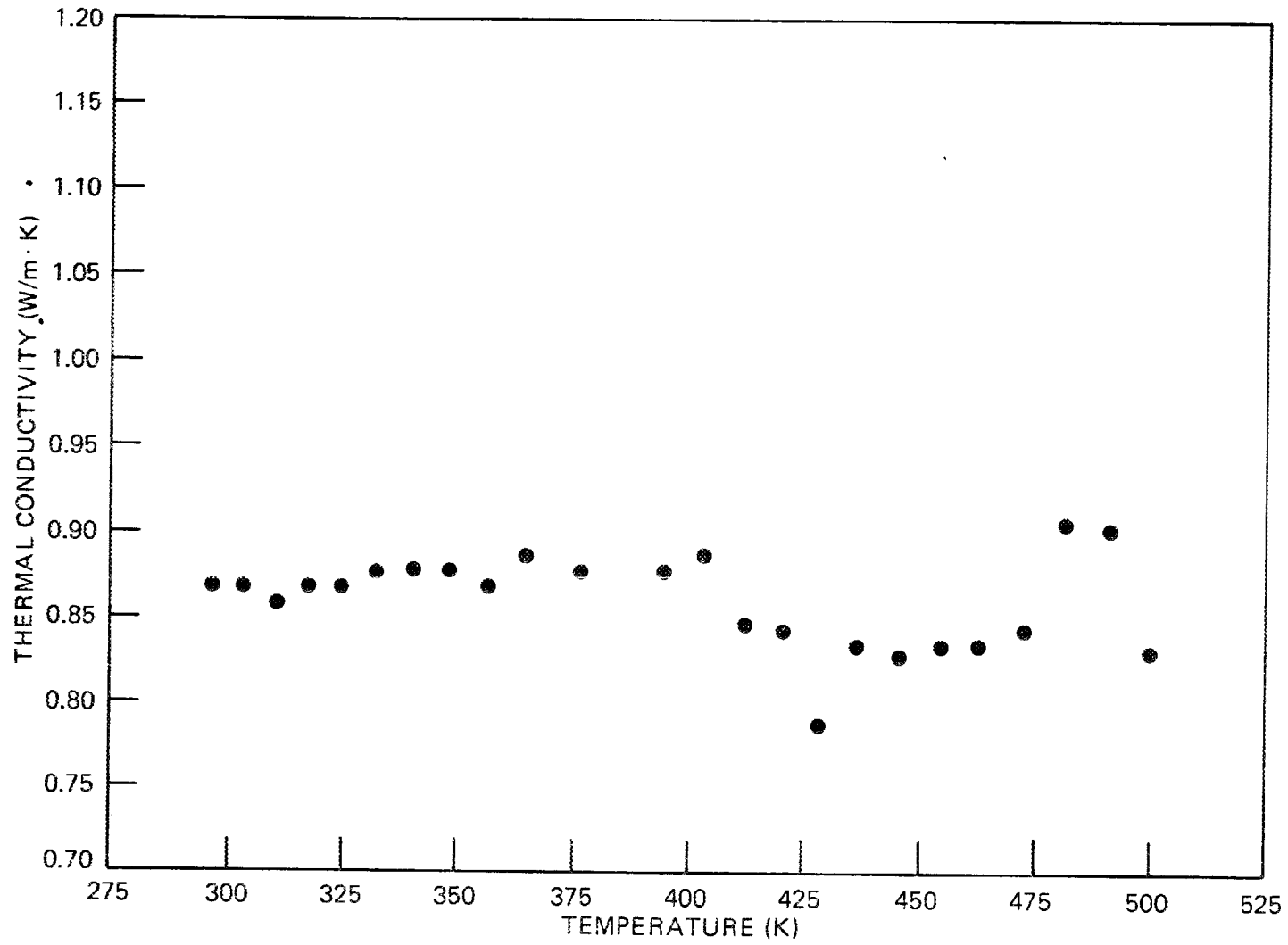


Fig. B.3. Thermal conductivity as a function of temperature for shale from 157.3 m (516 ft).

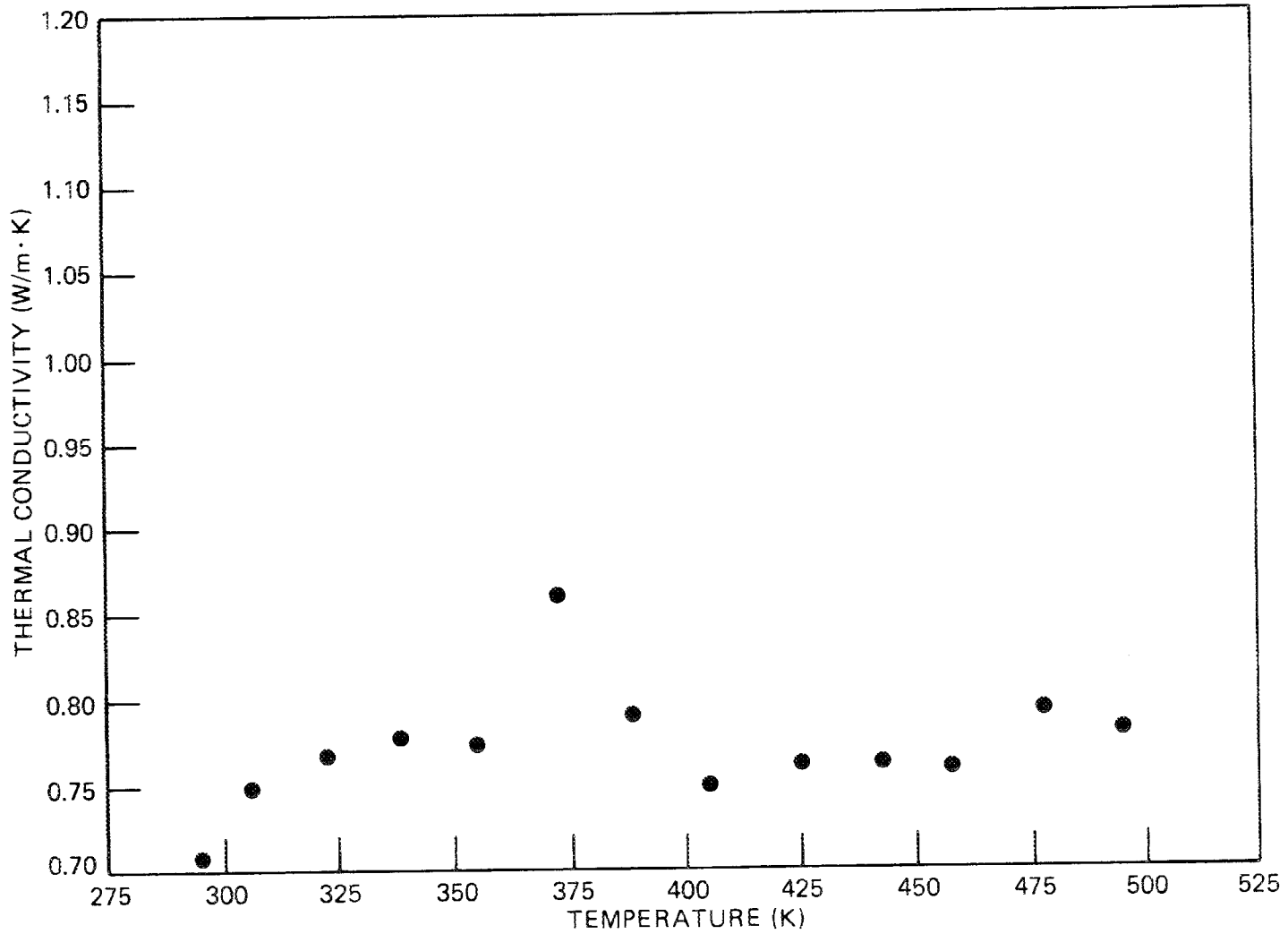


Fig. B.4. Thermal conductivity as a function of temperature for shale from 157.6 m (517 ft).

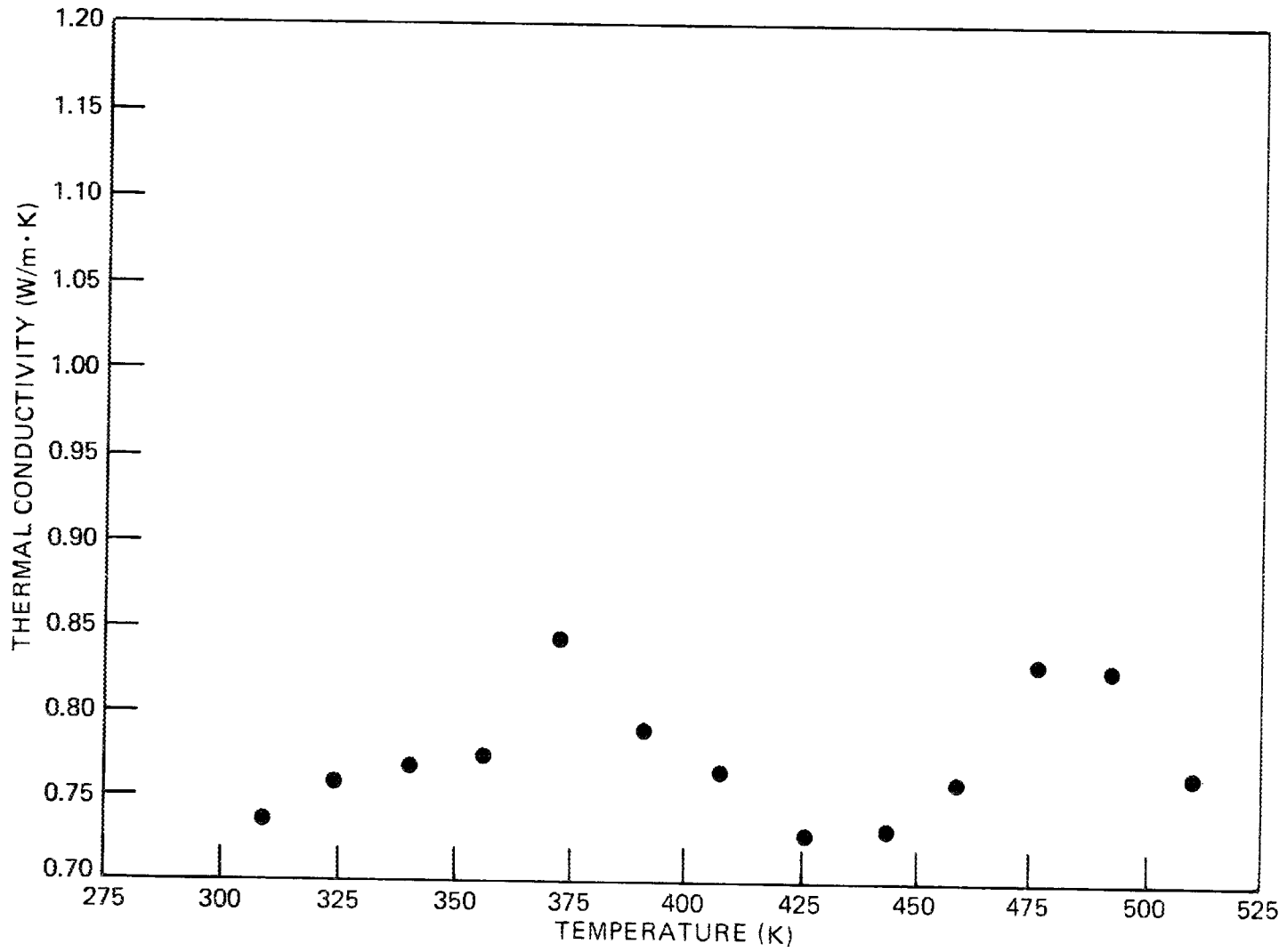


Fig. B.5. Thermal conductivity as a function of temperature for shale from 158.4 m (519.6 ft).

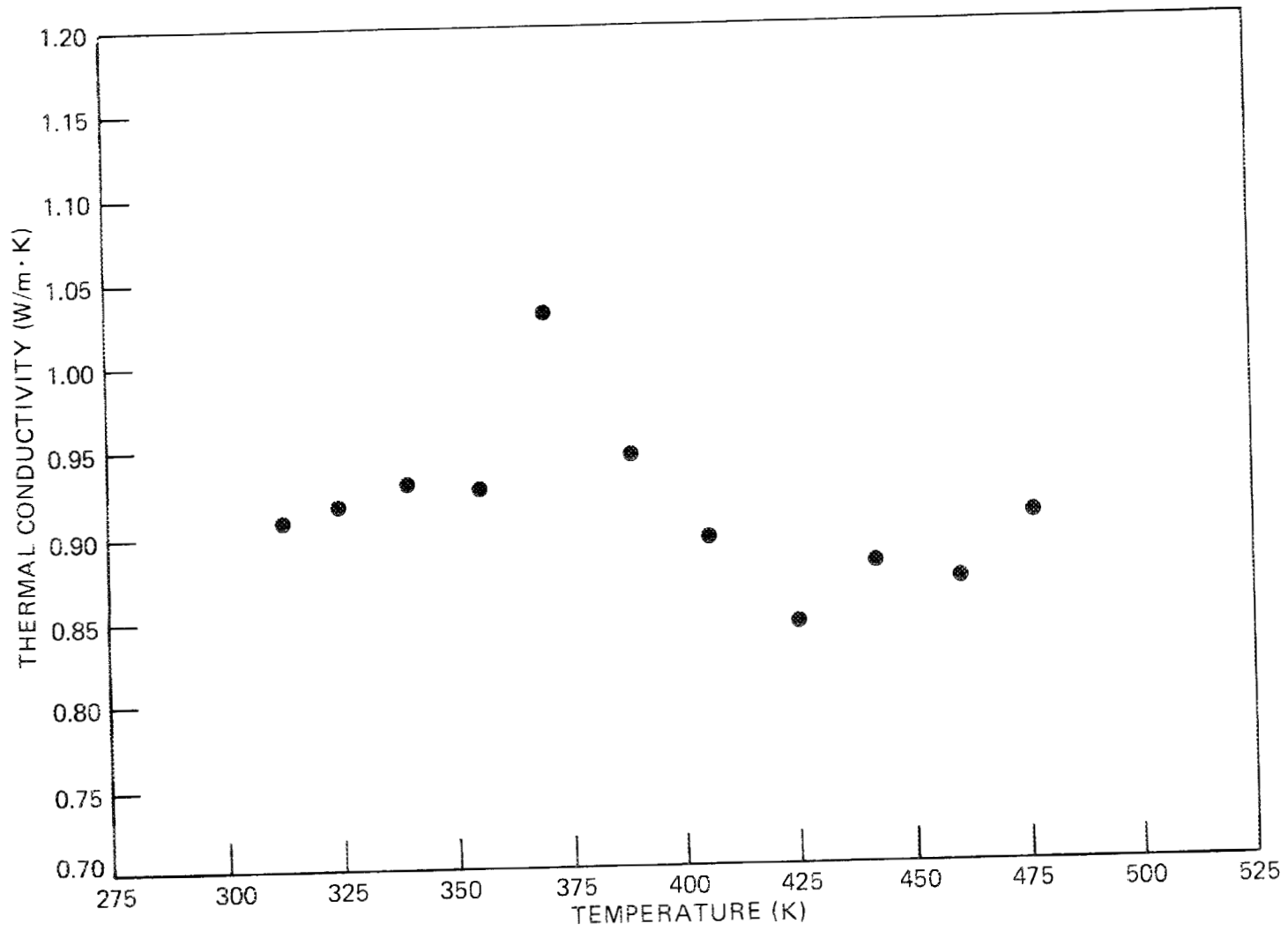


Fig. B.6. Thermal conductivity as a function of temperature for shale from 158.5 m (520 ft).

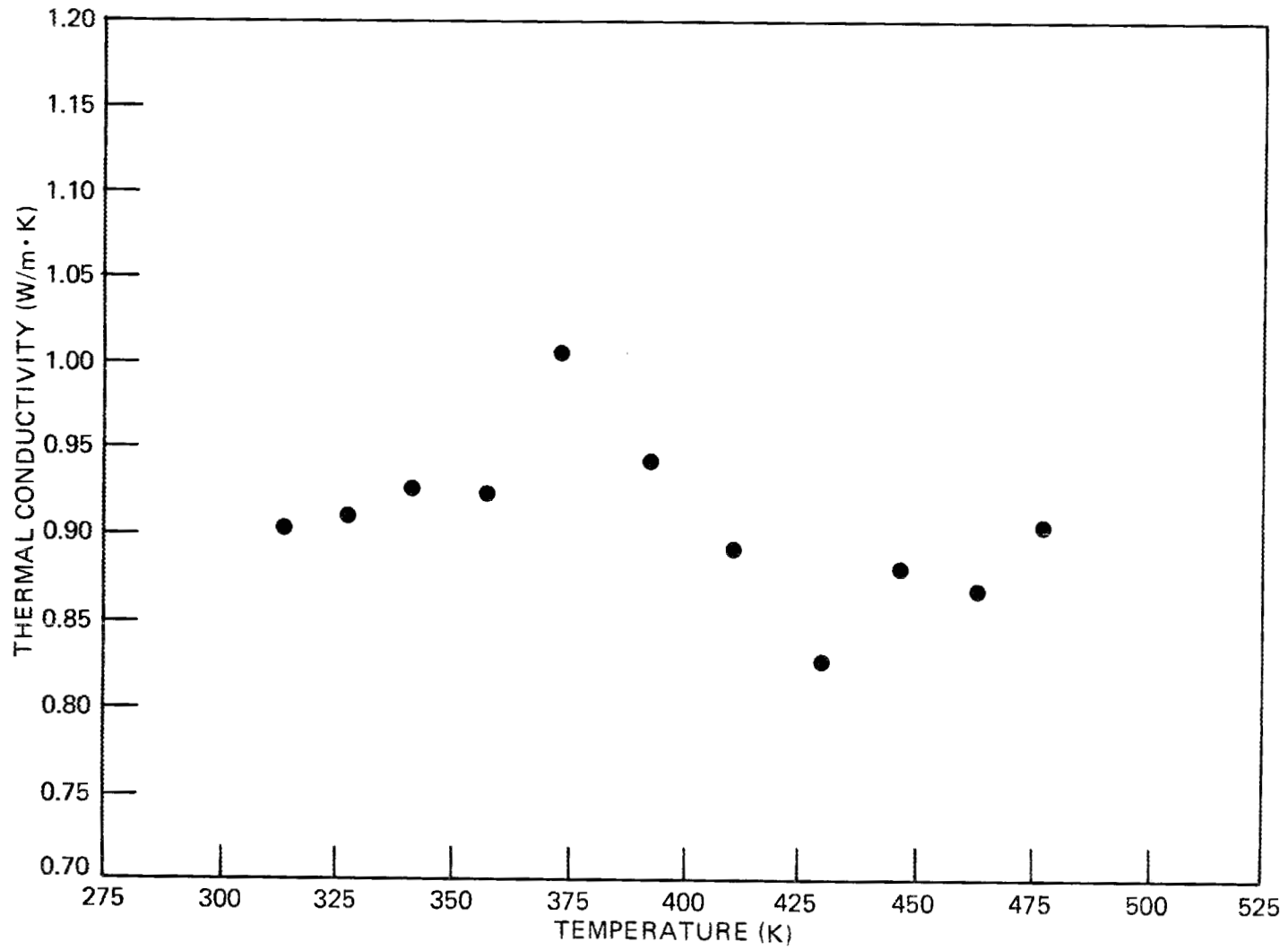


Fig. B.7. Thermal conductivity as a function of temperature for shale from 158.8 m (521 ft).

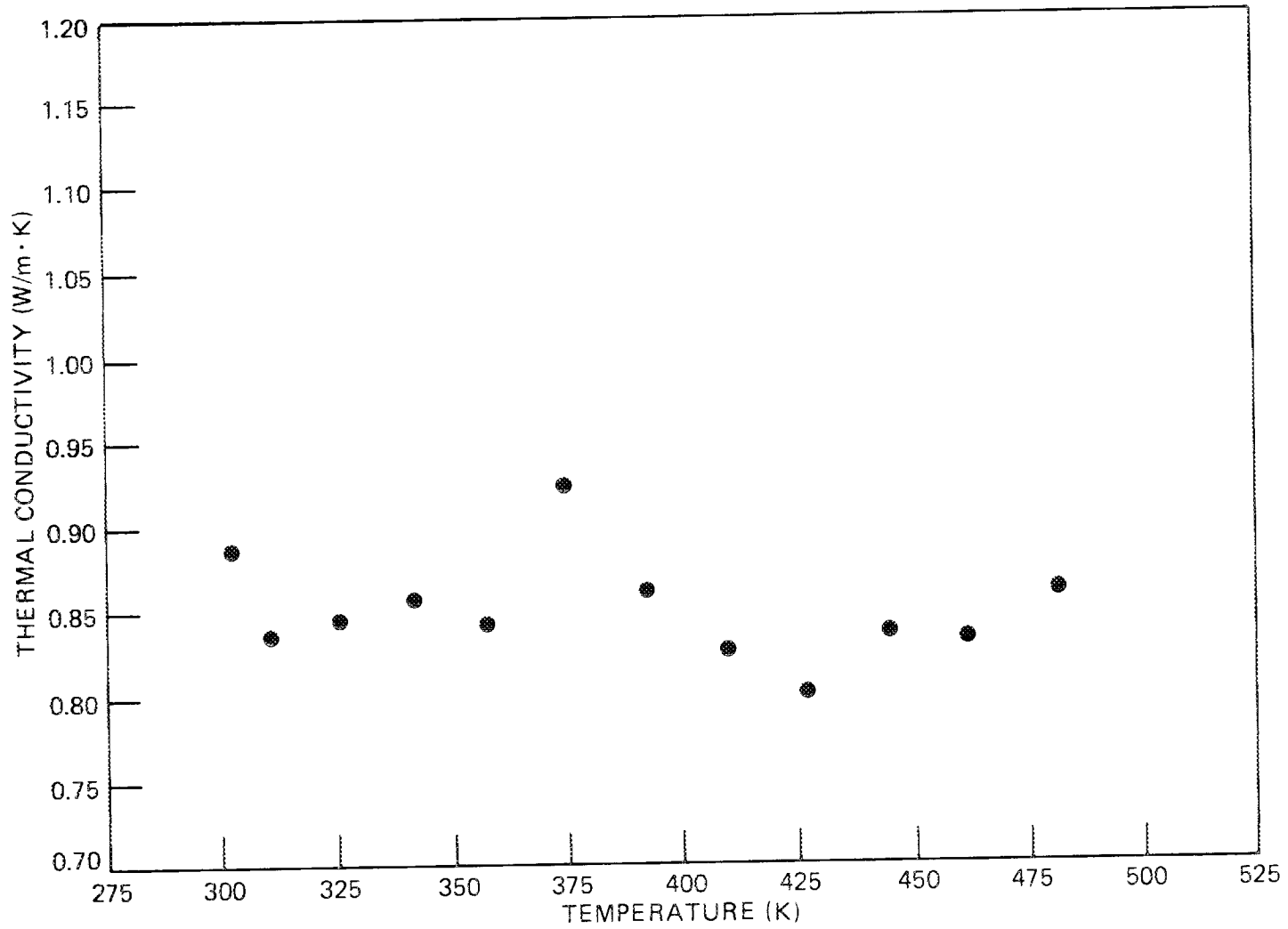


Fig. B.8. Thermal conductivity as a function of temperature for shale from 160.9 m (528 ft).

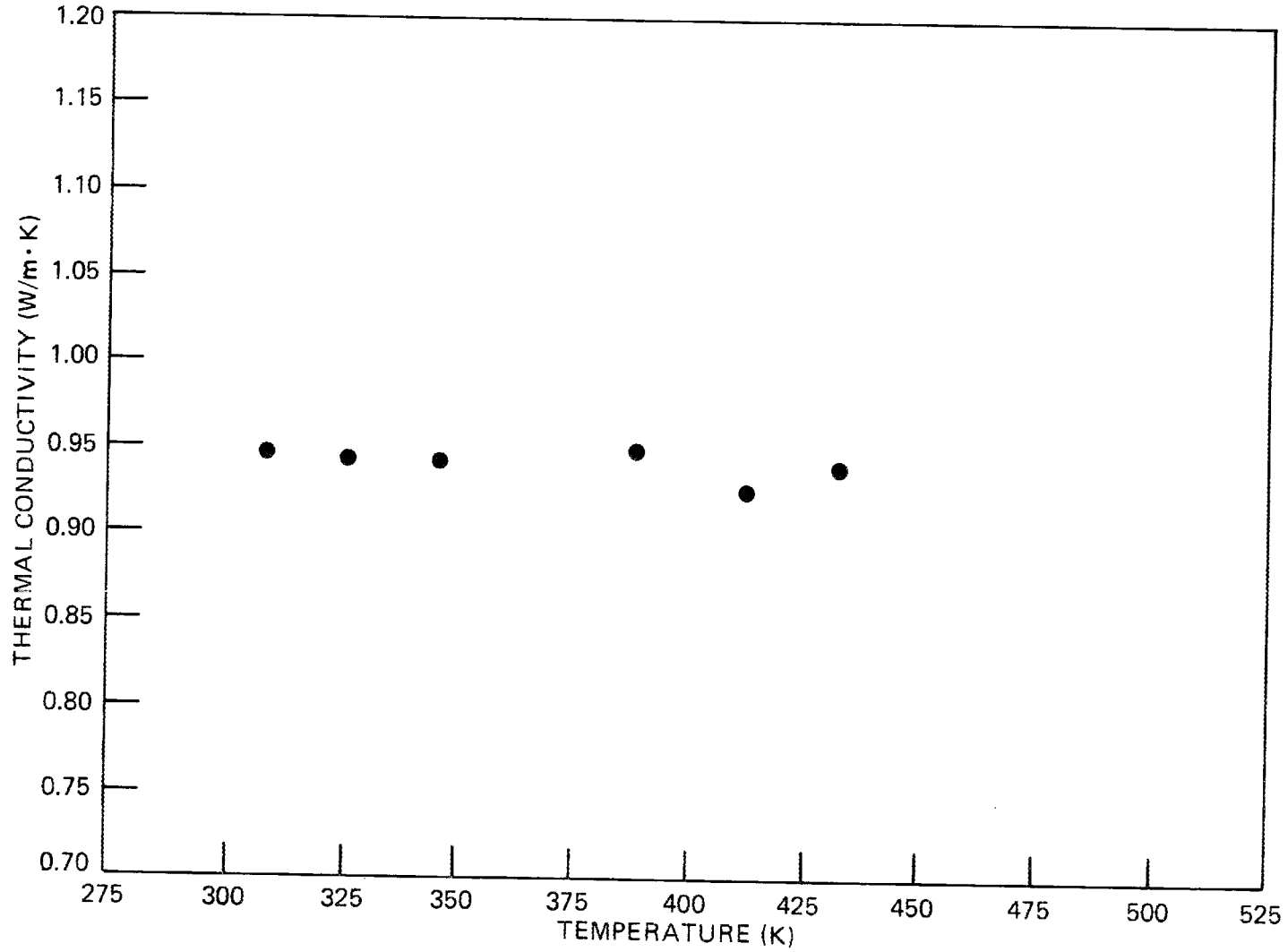


Fig. B.9. Thermal conductivity as a function of temperature for shale from 164 m (538 ft).

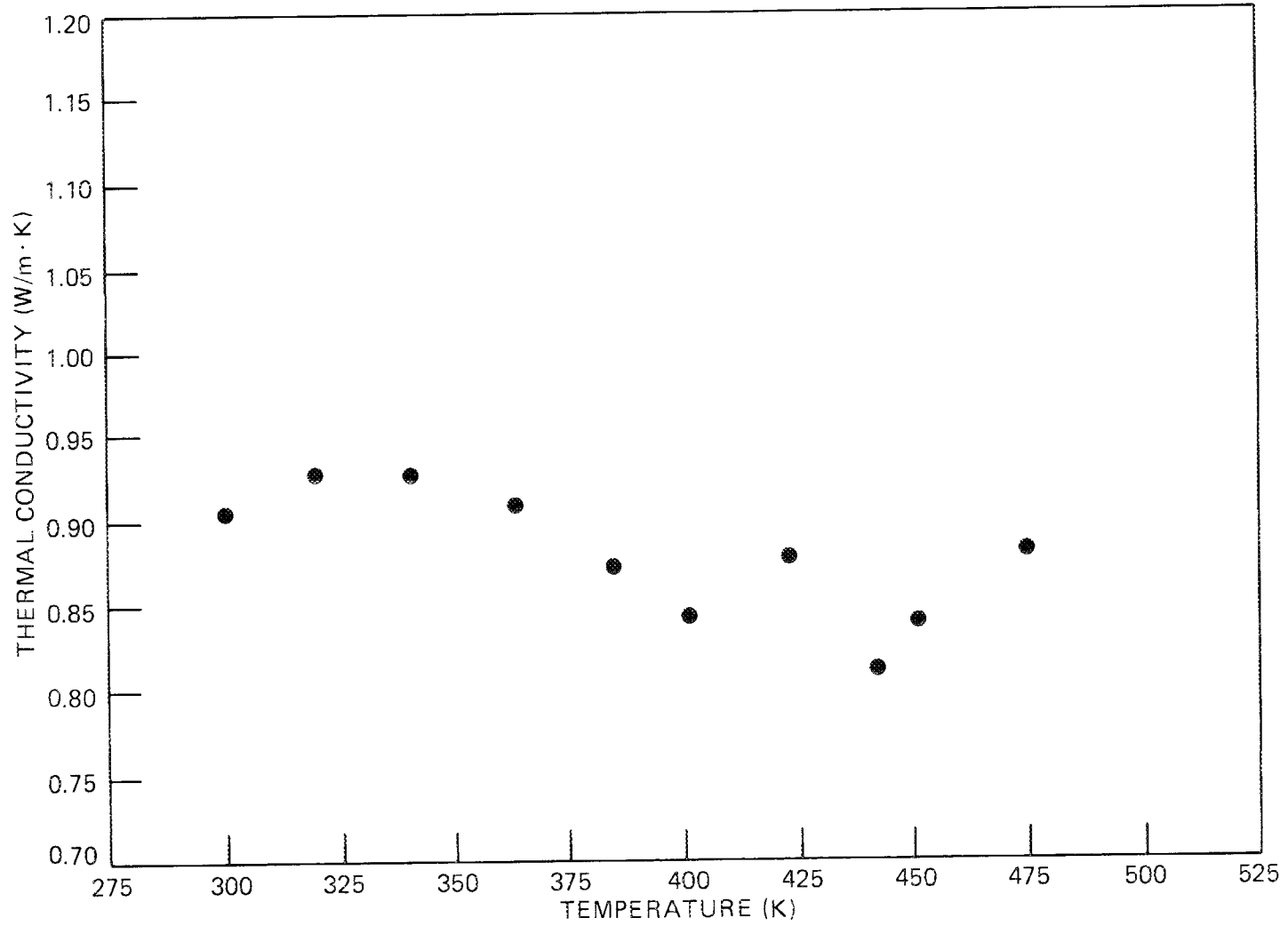


Fig. B.10. Thermal conductivity as a function of temperature for shale from 175.6 m (576 ft).

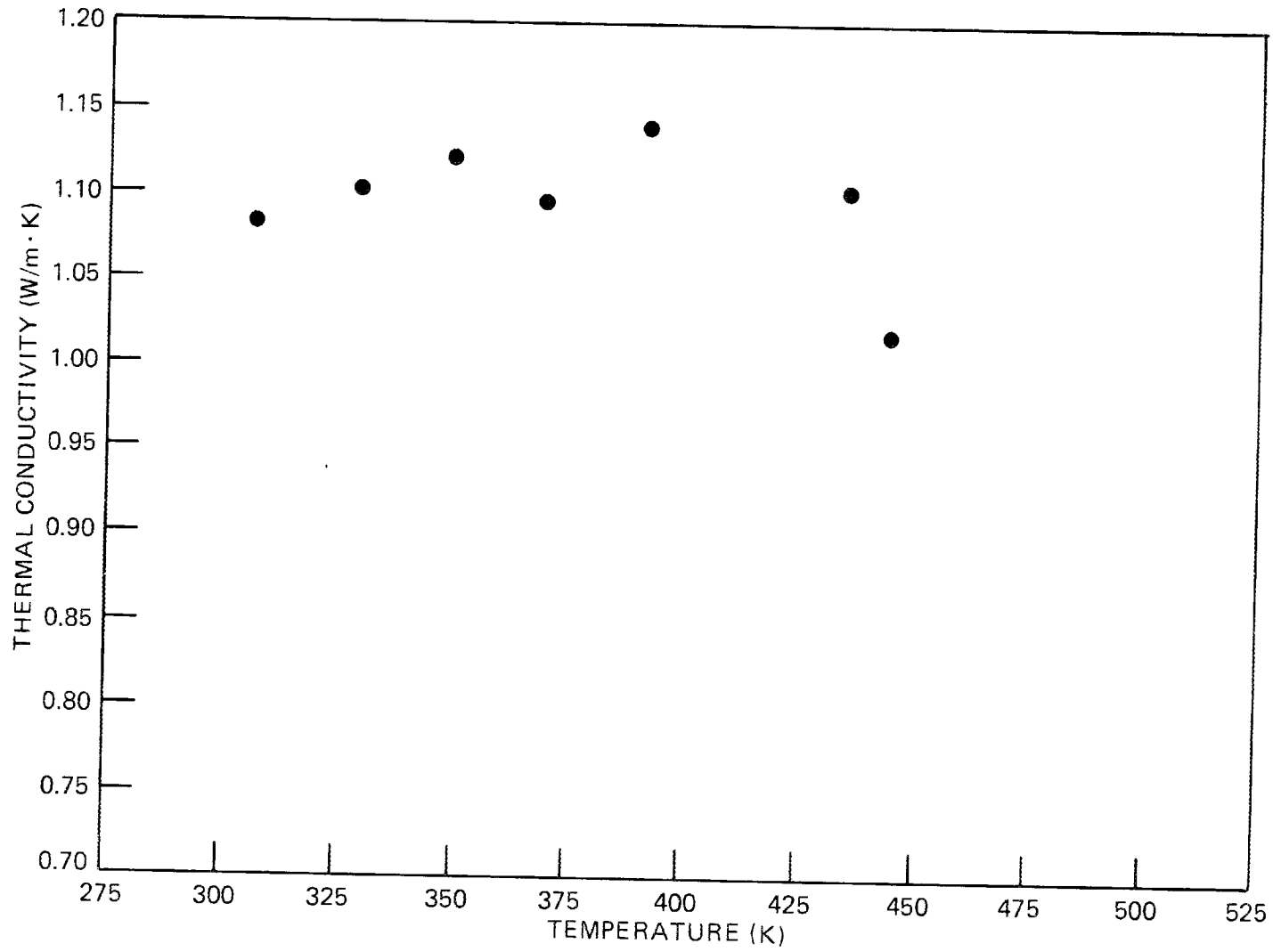


Fig. B.11. Thermal conductivity as a function of temperature for shale from 176.2 m (578 ft).

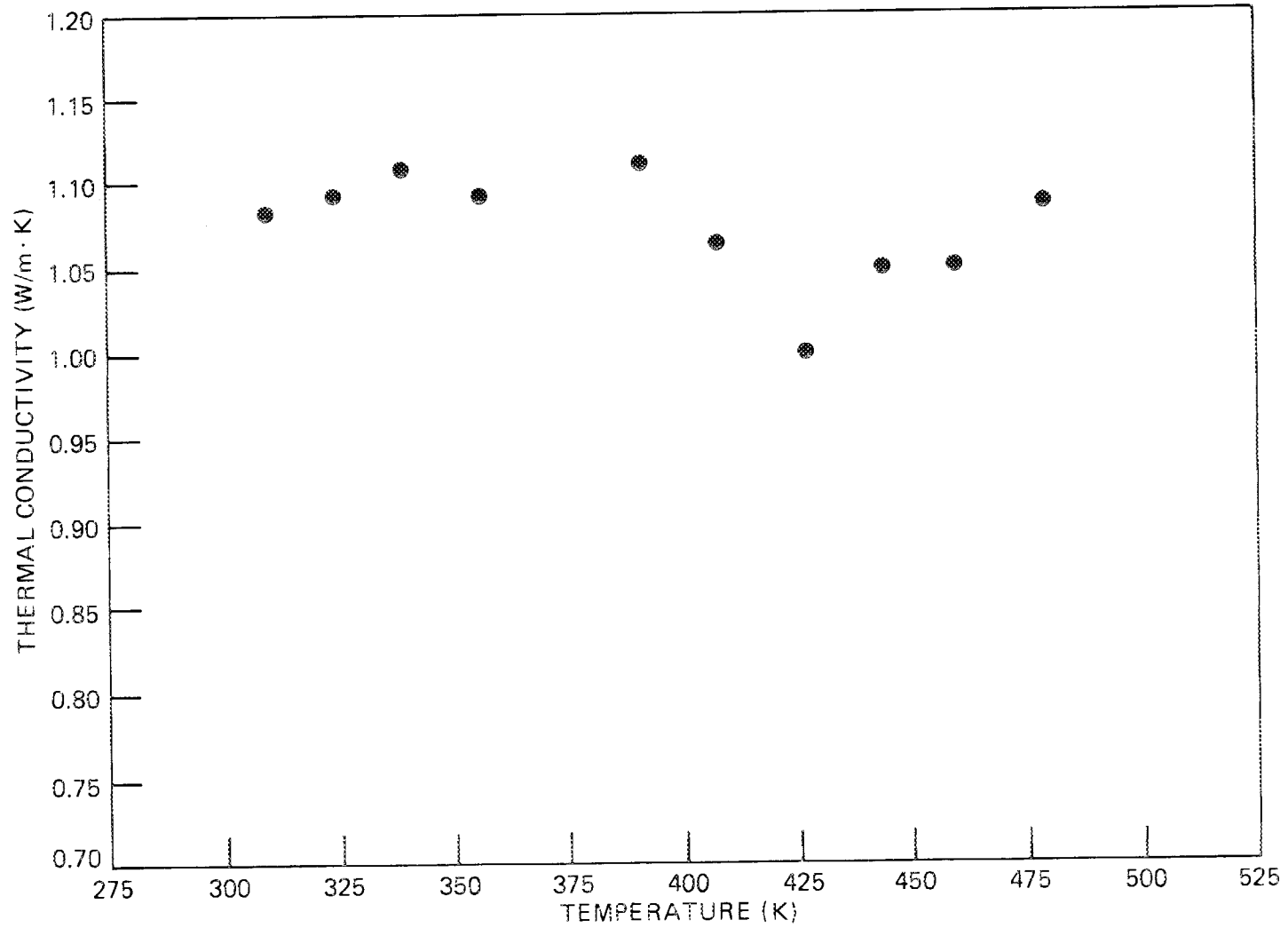


Fig. B.12. Thermal conductivity as a function of temperature for shale from 176.3 m (578.3 ft).

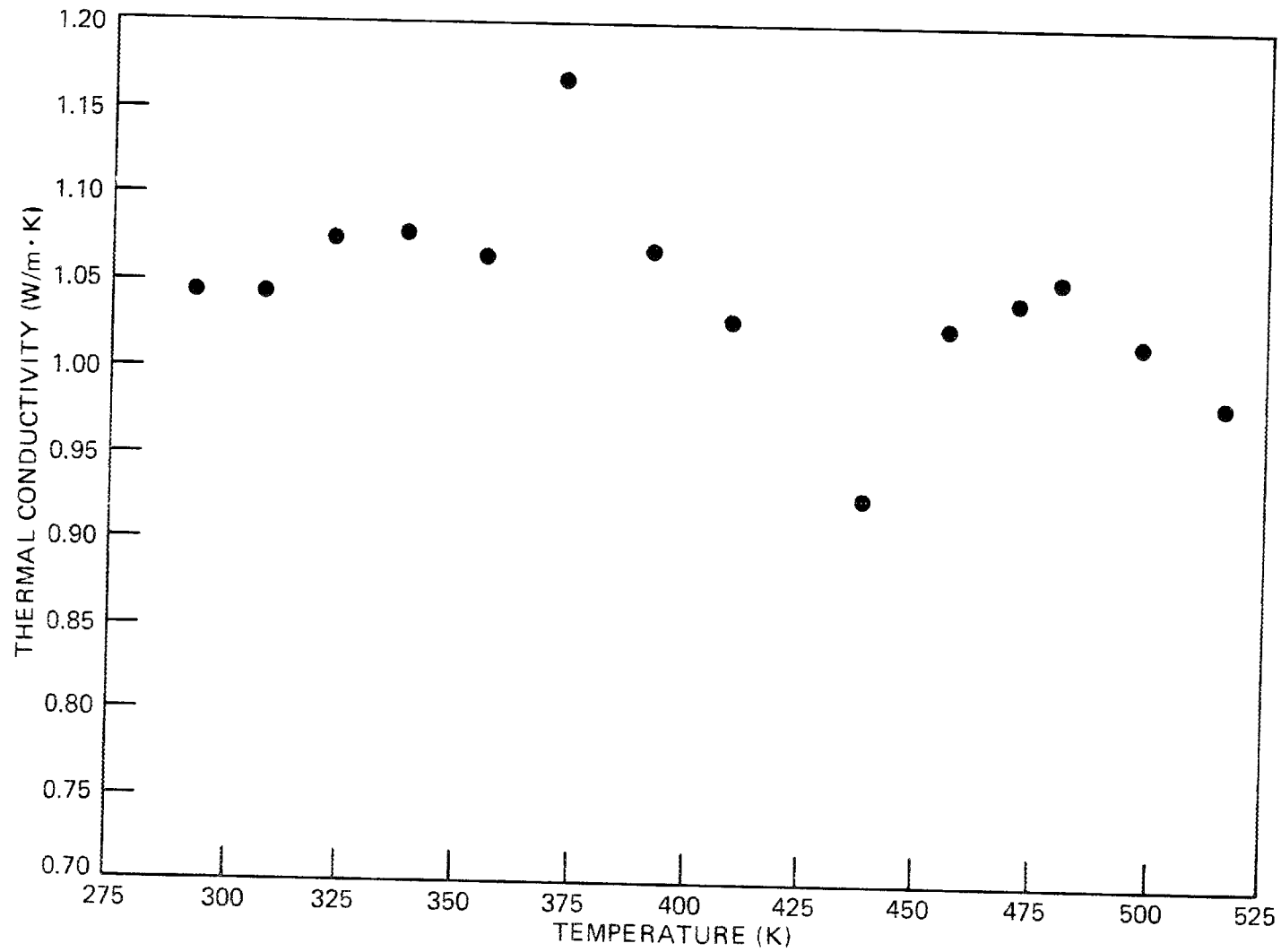


Fig. B.13. Thermal conductivity as a function of temperature for shale from 176.3 m (578.5 ft).

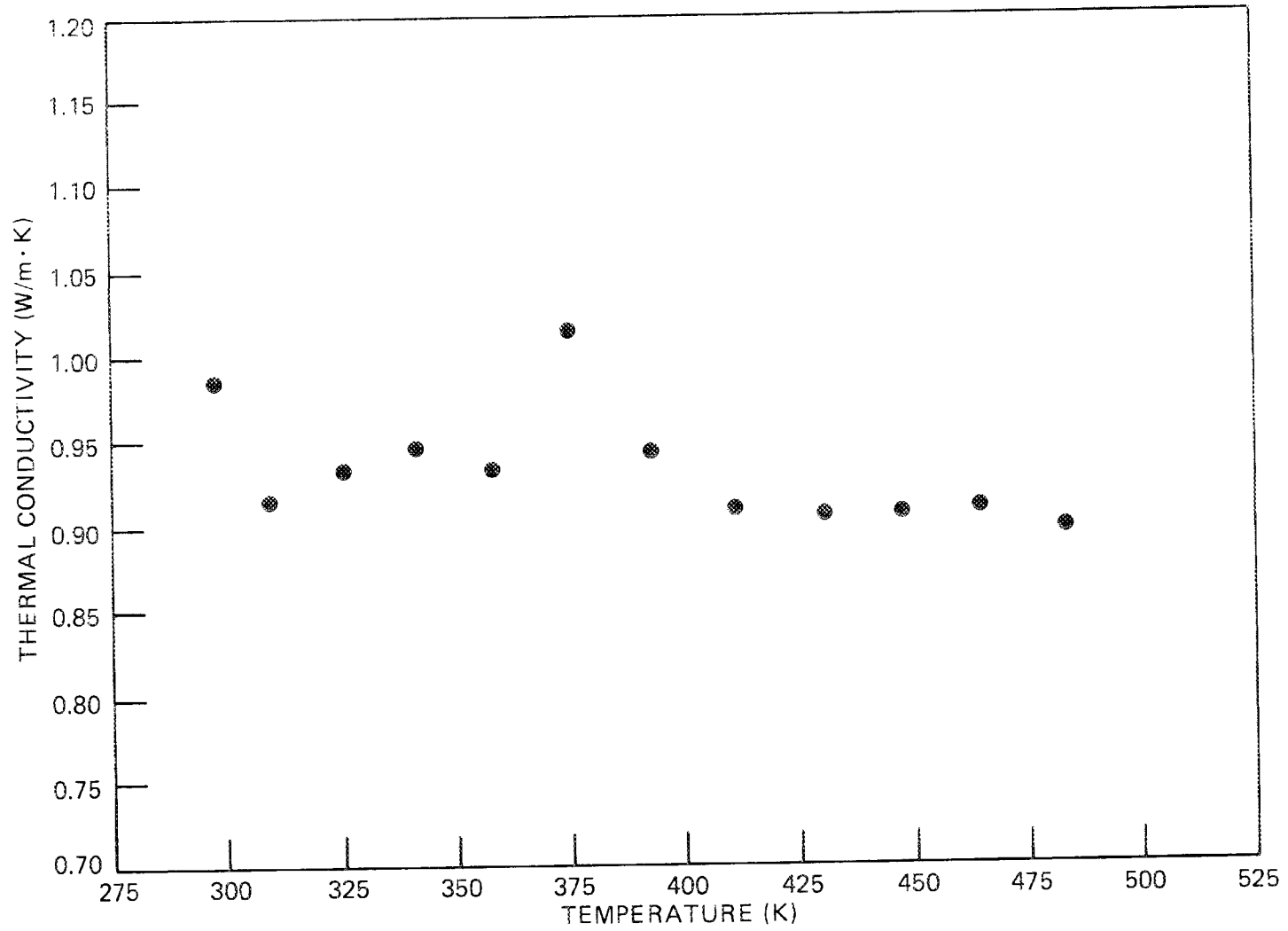


Fig. B.14. Thermal conductivity as a function of temperature for shale from 176.5 m (579 ft).

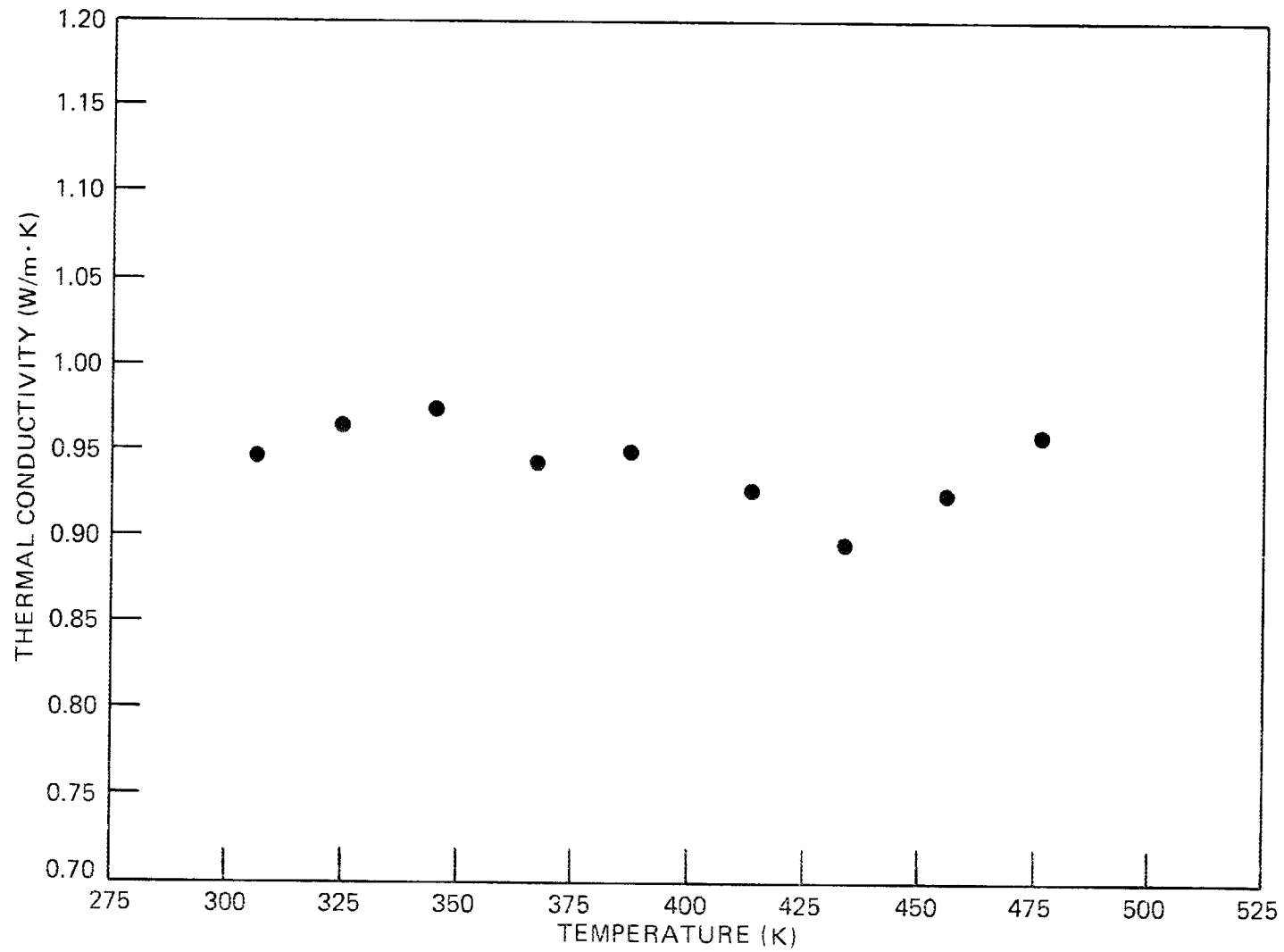


Fig. B.15. Thermal conductivity as a function of temperature for shale from 176.8 m (580 ft).

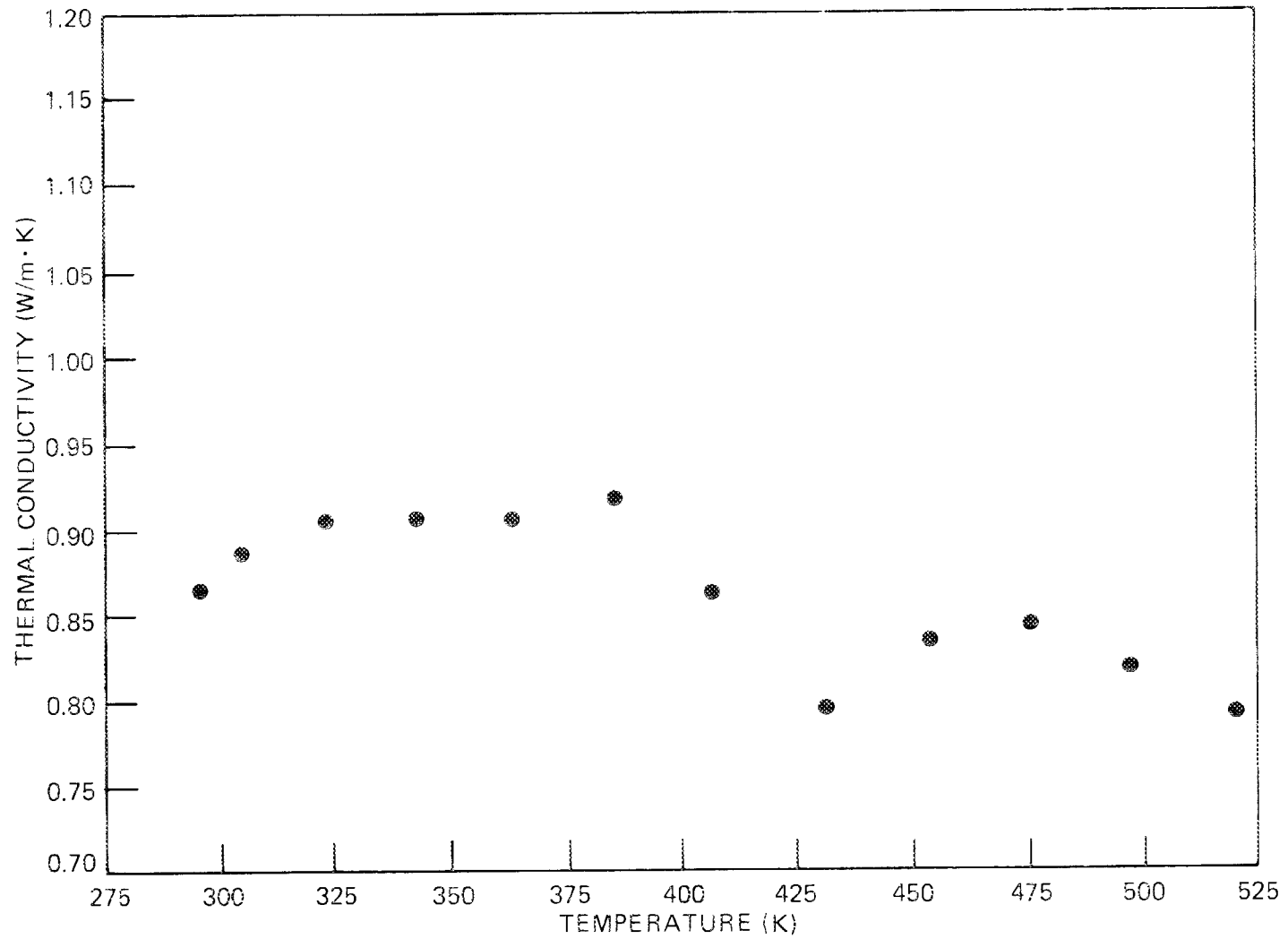


Fig. B.16. Thermal conductivity as a function of temperature for shale sample.

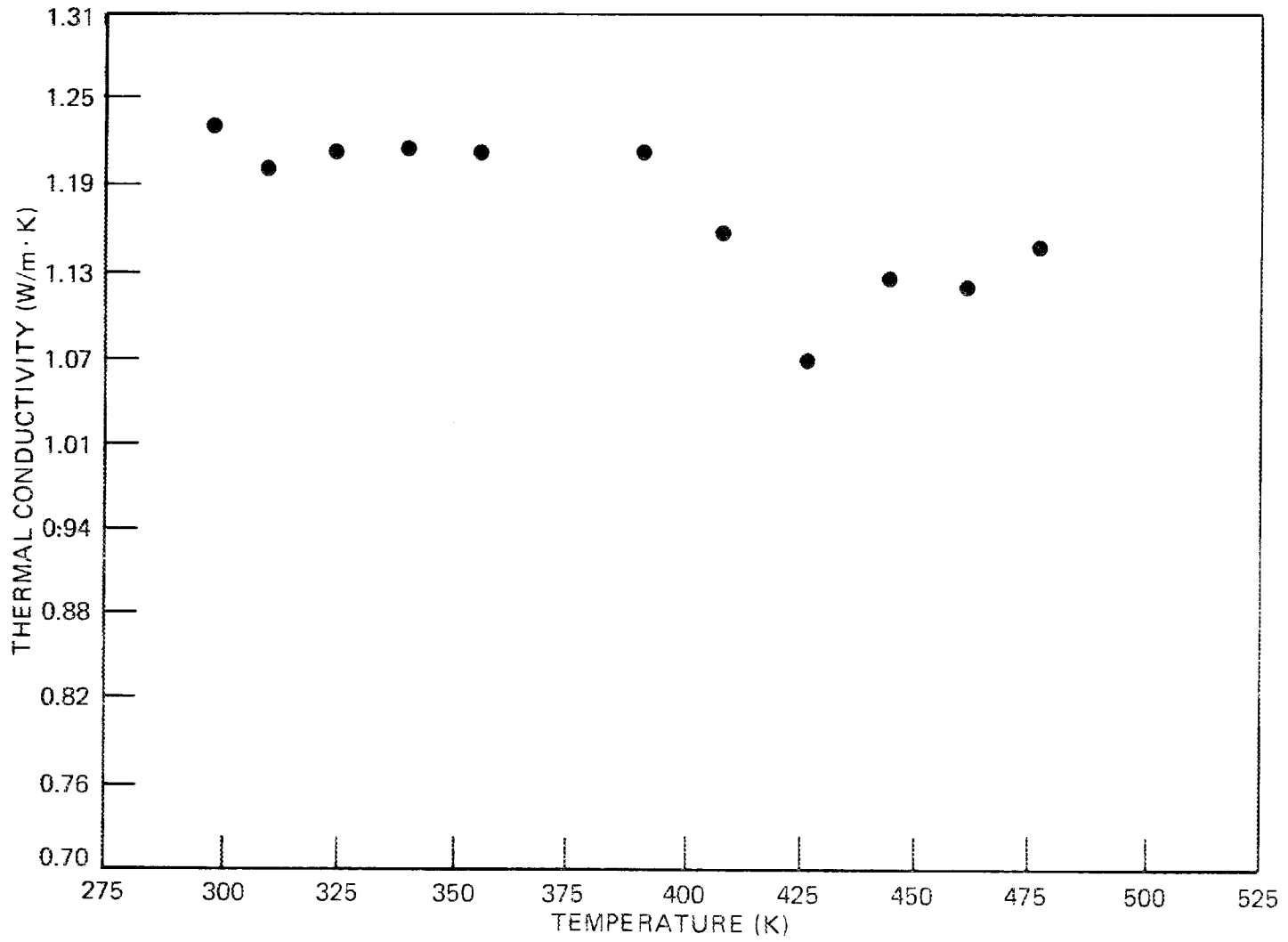


Fig. B.17. Thermal conductivity as a function of temperature for shale sample.

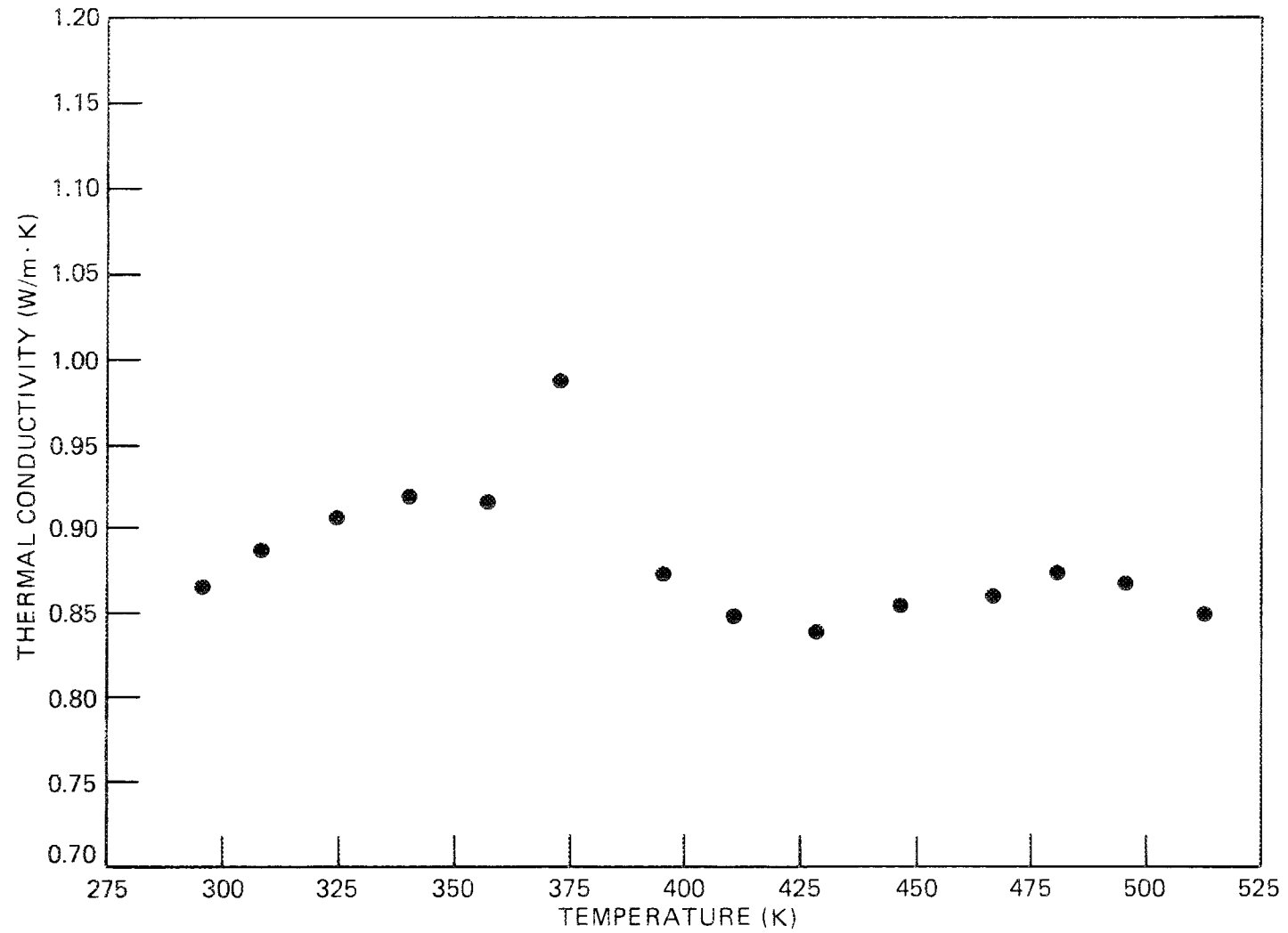


Fig. B.18. Thermal conductivity as a function of temperature for shale sample.

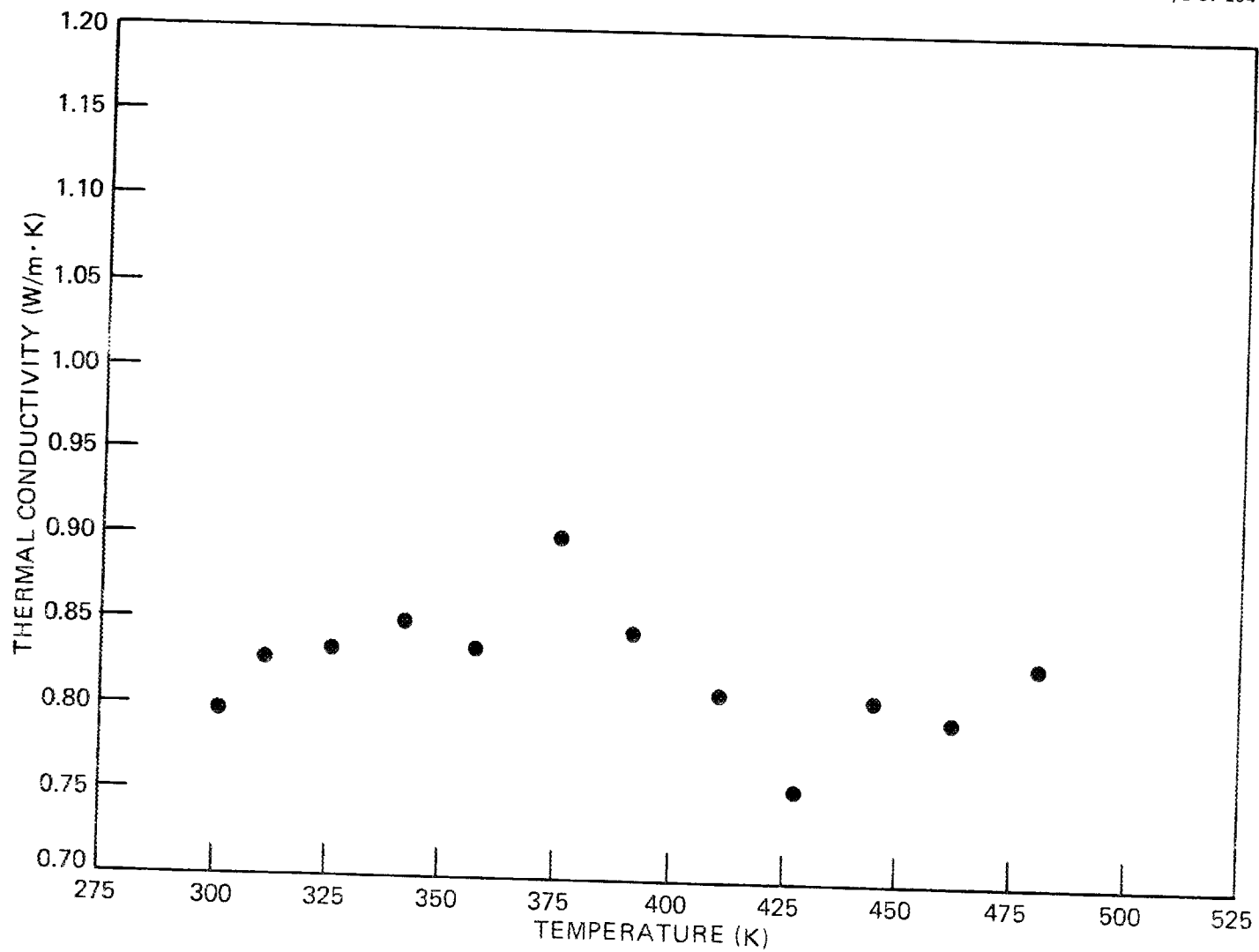


Fig. B.19. Thermal conductivity as a function of temperature for shale sample.

APPENDIX B.2. THERMAL CONDUCTIVITY DATA FOR PIERRE SHALE SAMPLES

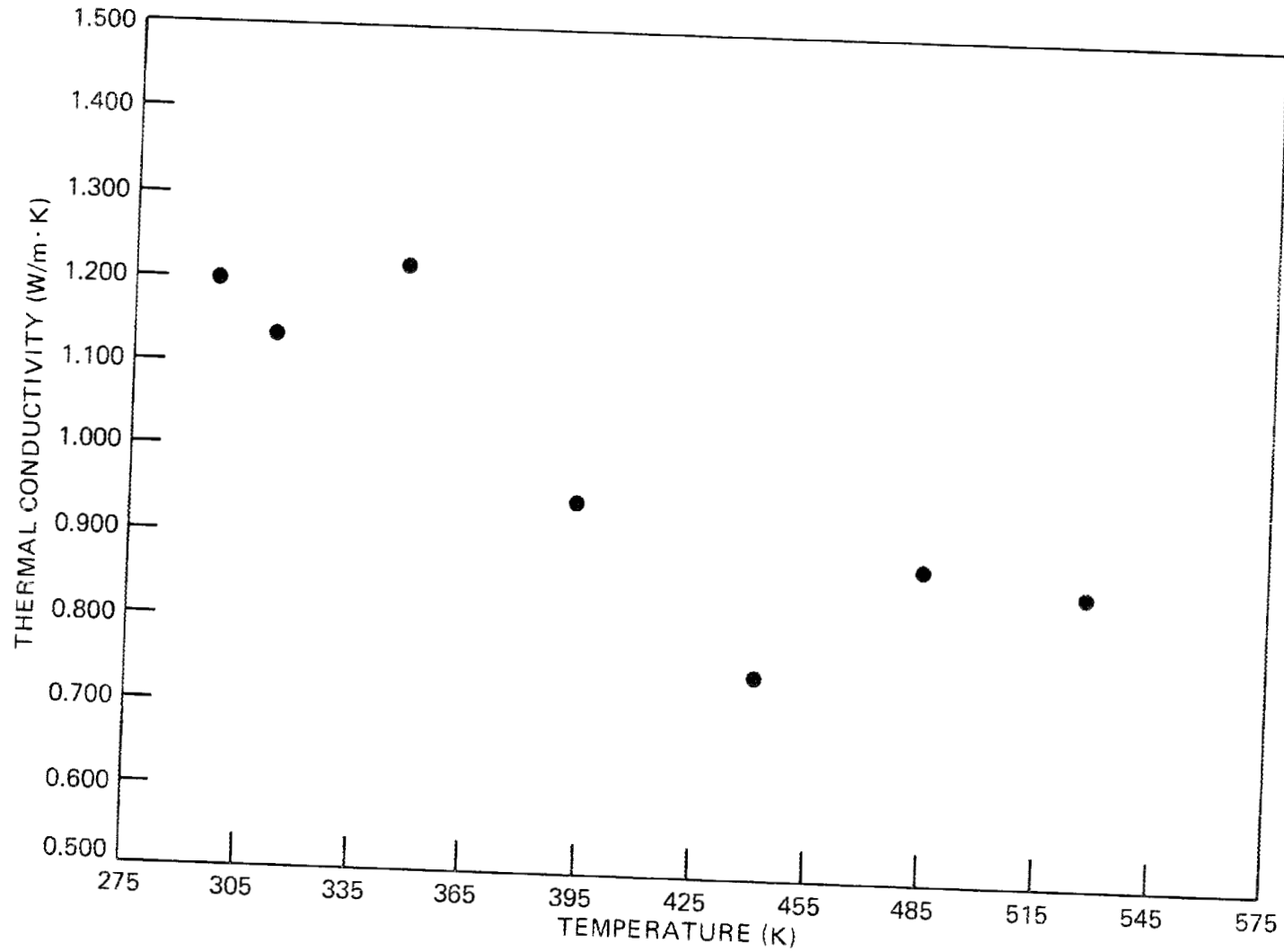


Fig. B.20. Thermal conductivity as a function of temperature for shale from 45.1 m (148 ft).

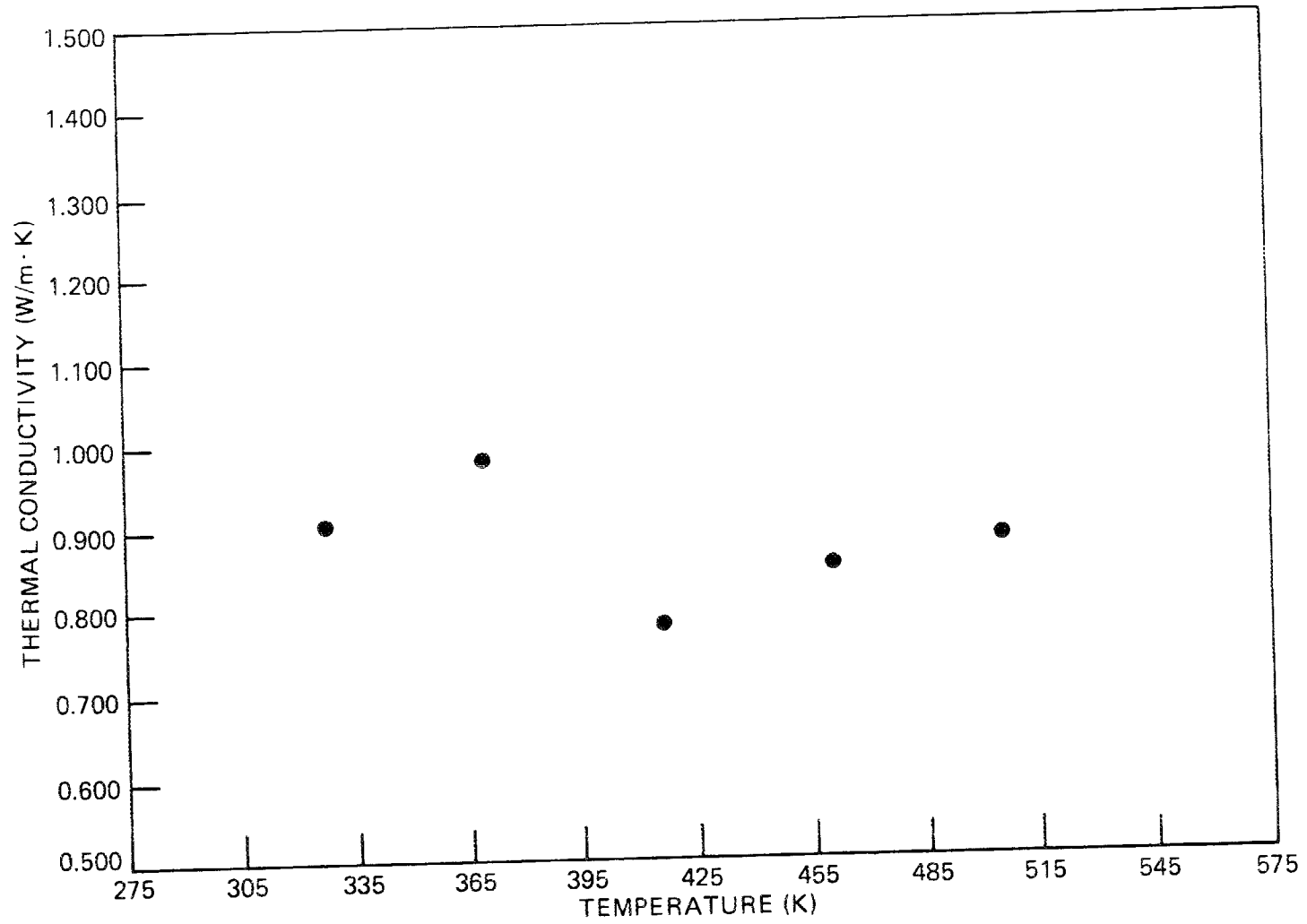


Fig. B.21. Thermal conductivity as a function of temperature for shale from 45.4 m (149 ft).

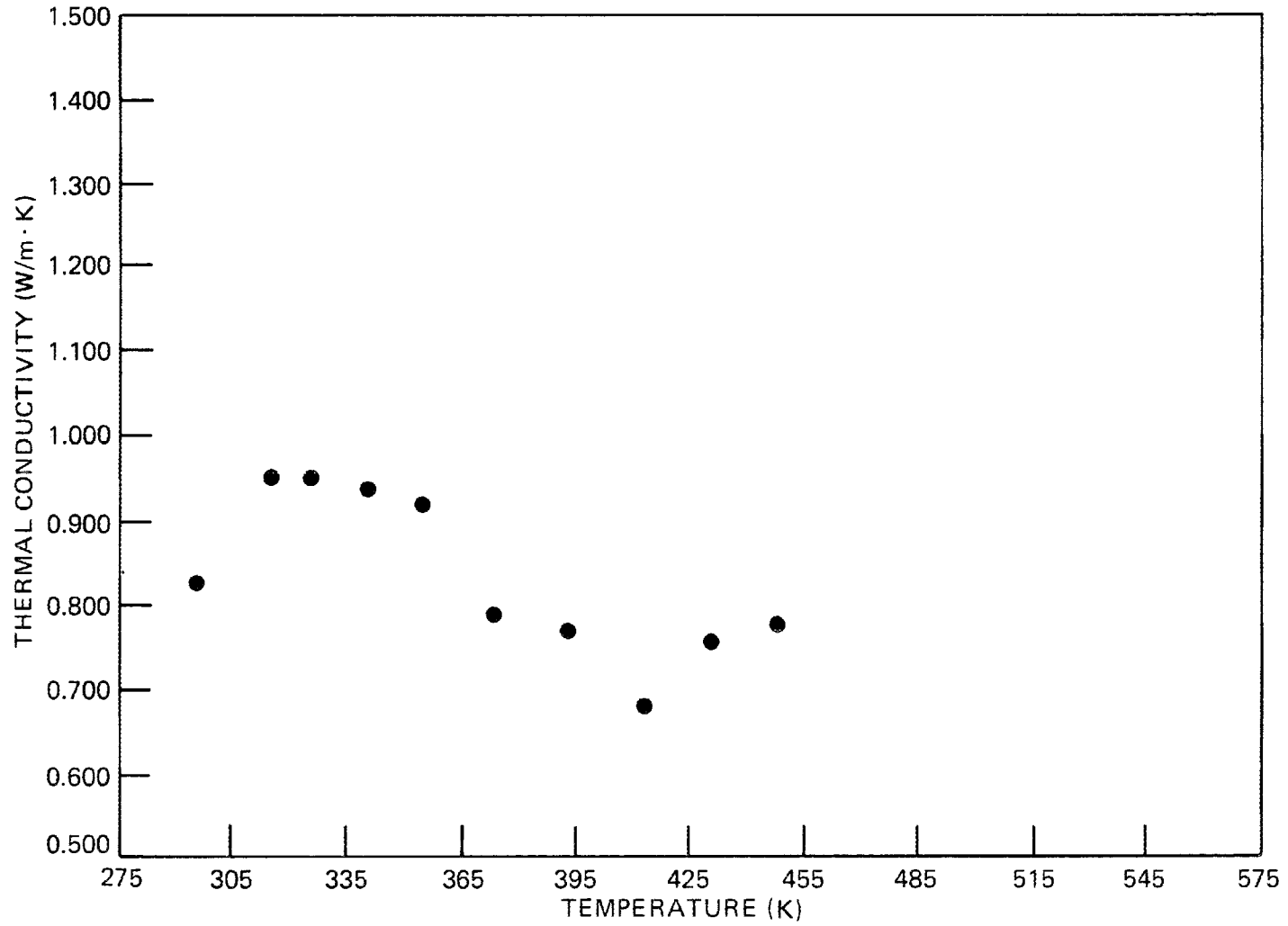


Fig. B.22. Thermal conductivity as a function of temperature for shale from 45.7 m (150 ft).

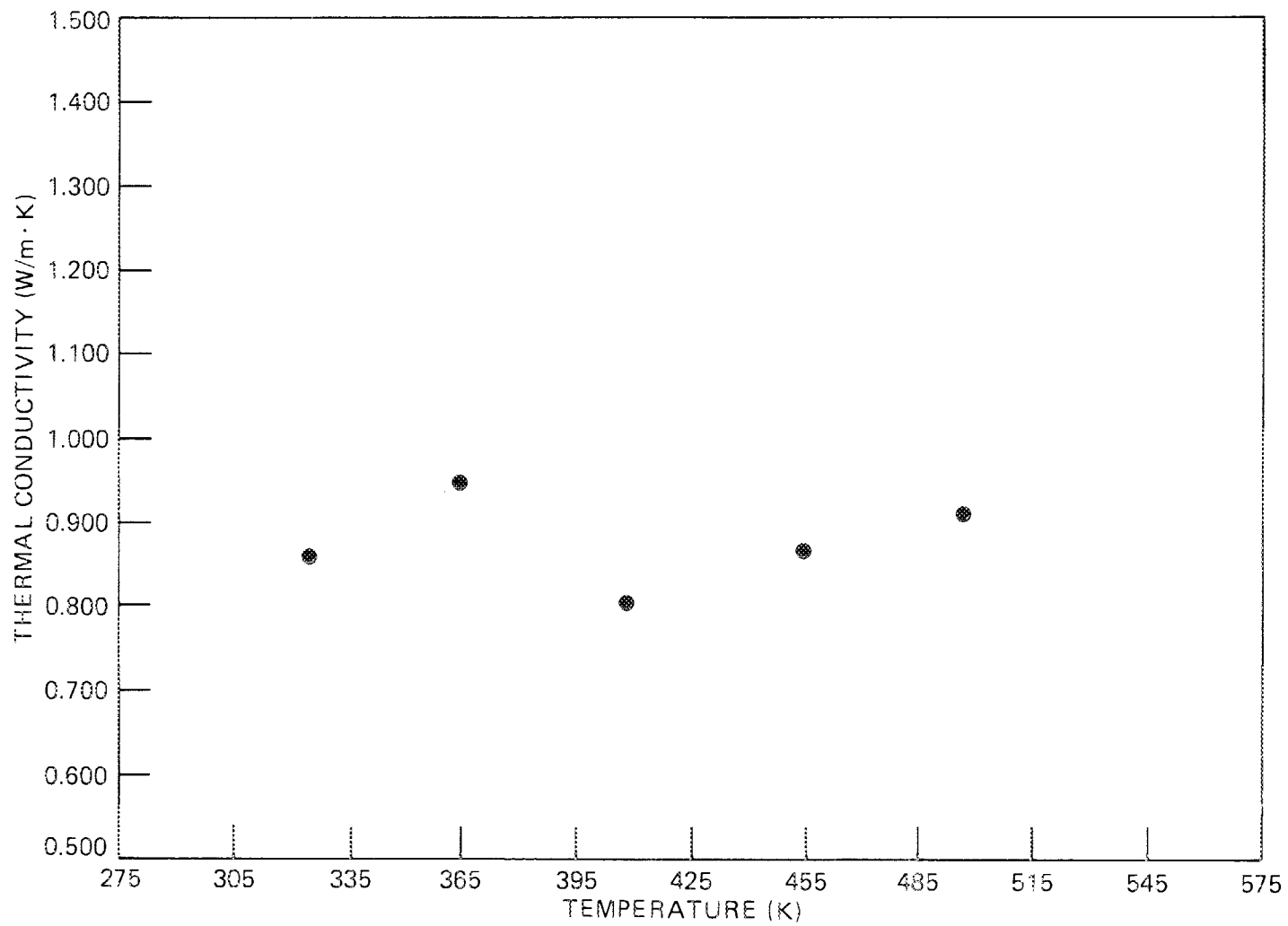


Fig. B.23. Thermal conductivity as a function of temperature for shale from 49.1 m (161 ft).

APPENDIX B.3. THERMAL CONDUCTIVITY DATA FOR GREEN RIVER FORMATION SHALE
SAMPLES

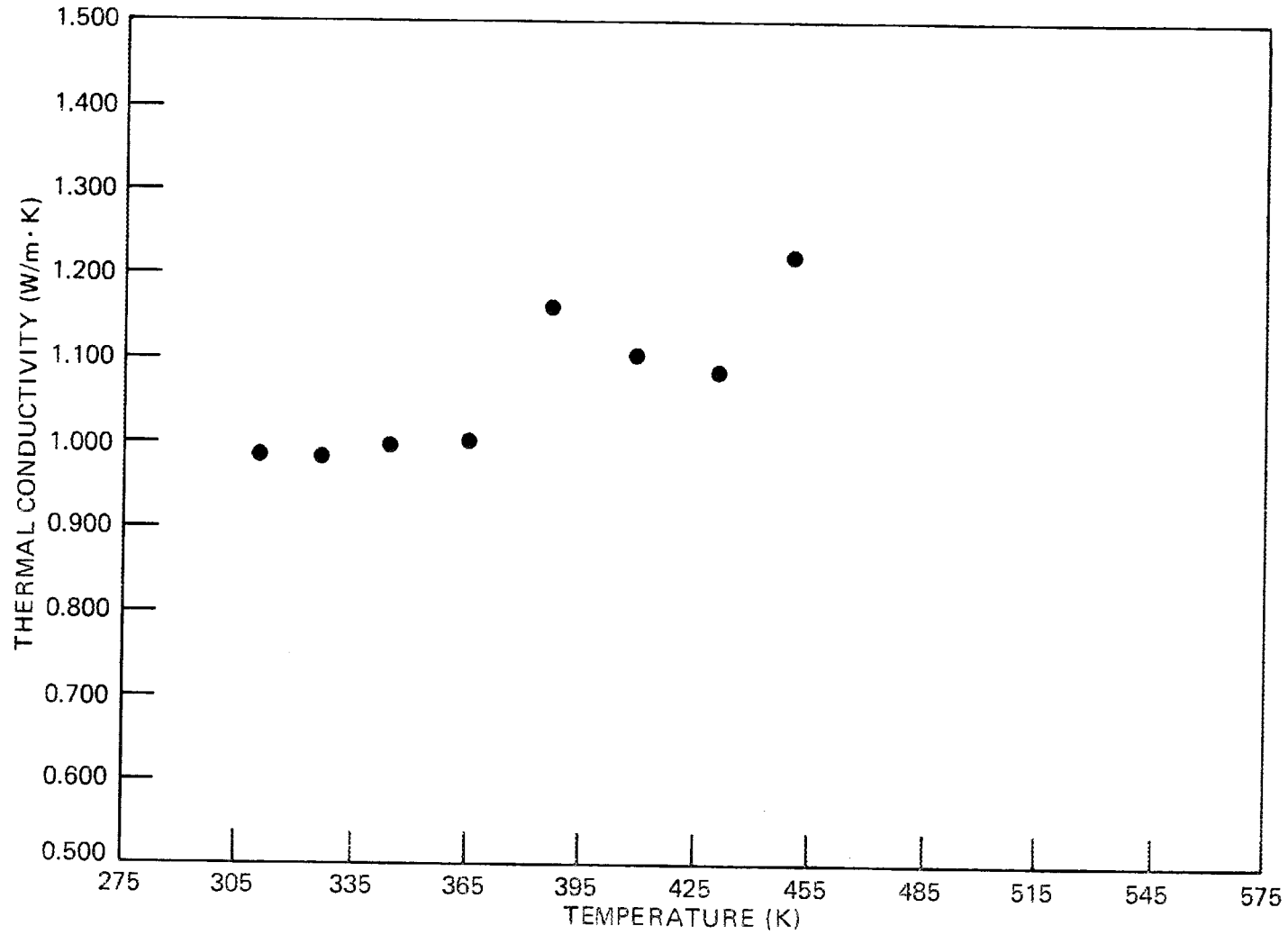


Fig. B.24. Thermal conductivity as a function of temperature.

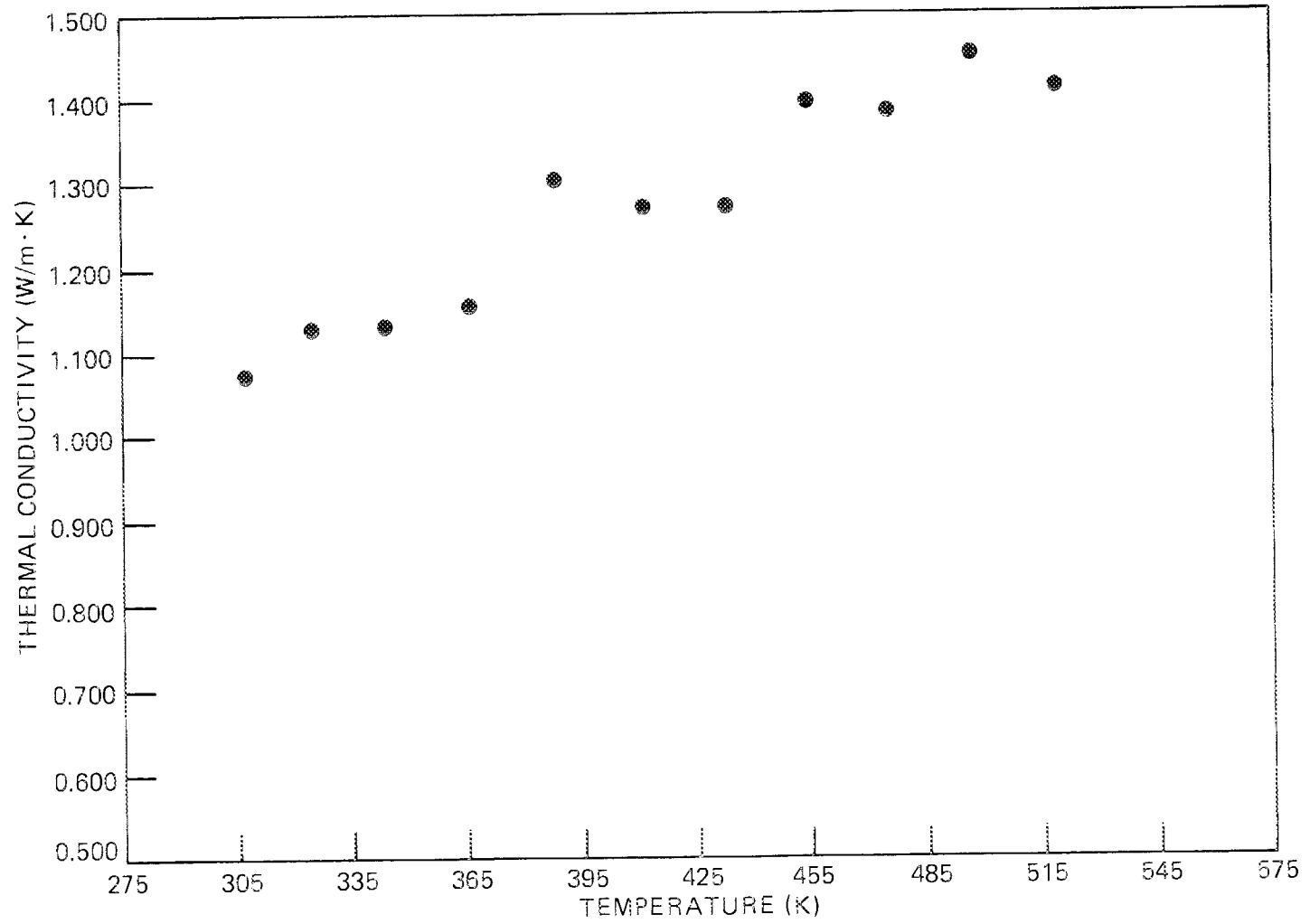


Fig. B.25. Thermal conductivity as a function of temperature.

APPENDIX C:
HEAT CAPACITY DATA FOR SHALE SAMPLES

This appendix presents the heat capacity data for all shale samples. Average values and conclusions presented in the text were taken from these data.

APPENDIX C.1. HEAT CAPACITY DATA FOR DEVONIAN SHALE SAMPLES
FROM EGSP KENTUCKY NO. 5 WELL

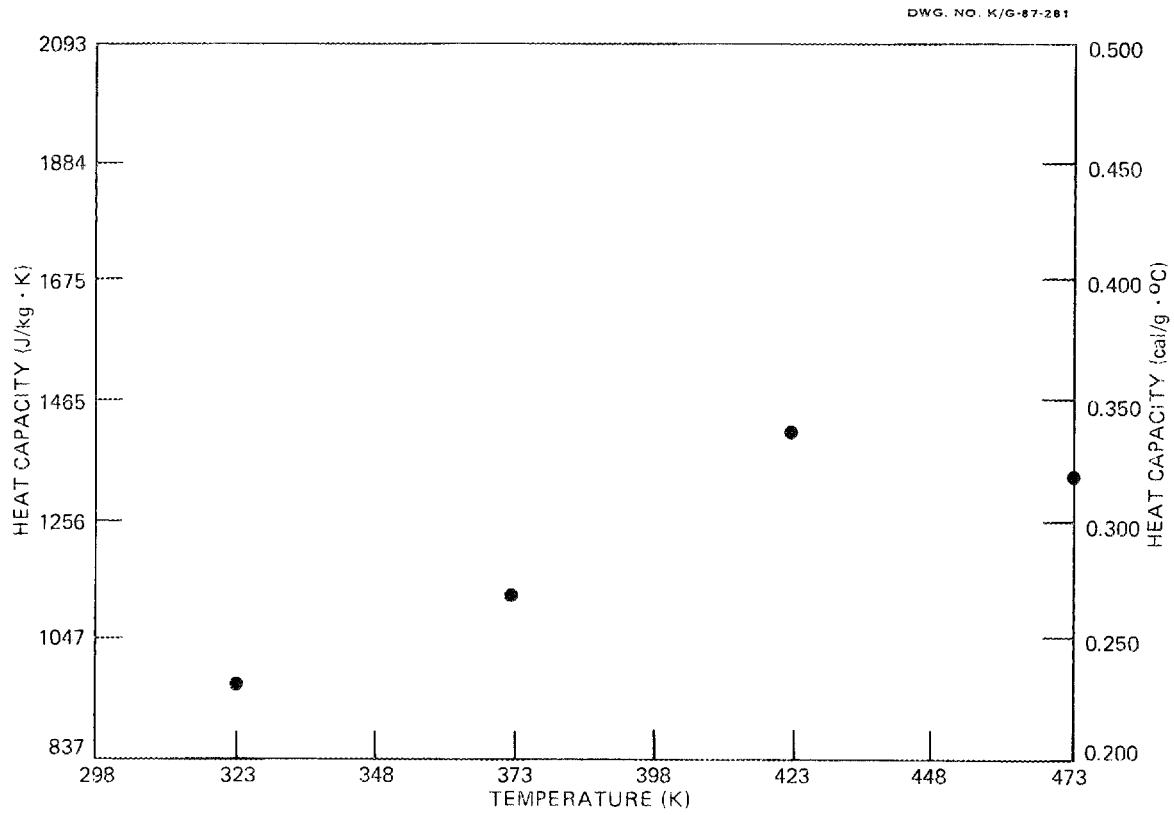


Fig. C.1. Selected heat capacity as a function of temperature for shale from 137.2 m (450 ft).

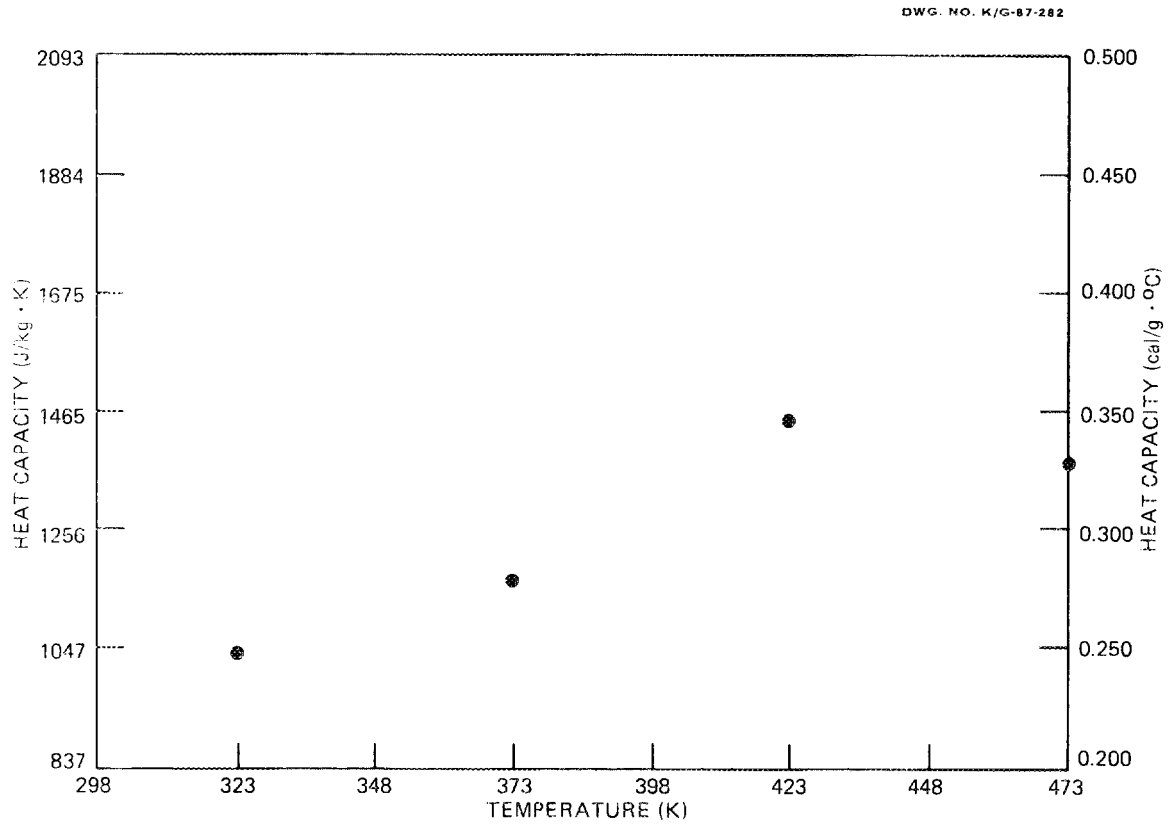


Fig. C.2. Selected heat capacity as a function of temperature for shale from 137.2 m (450.1 ft).

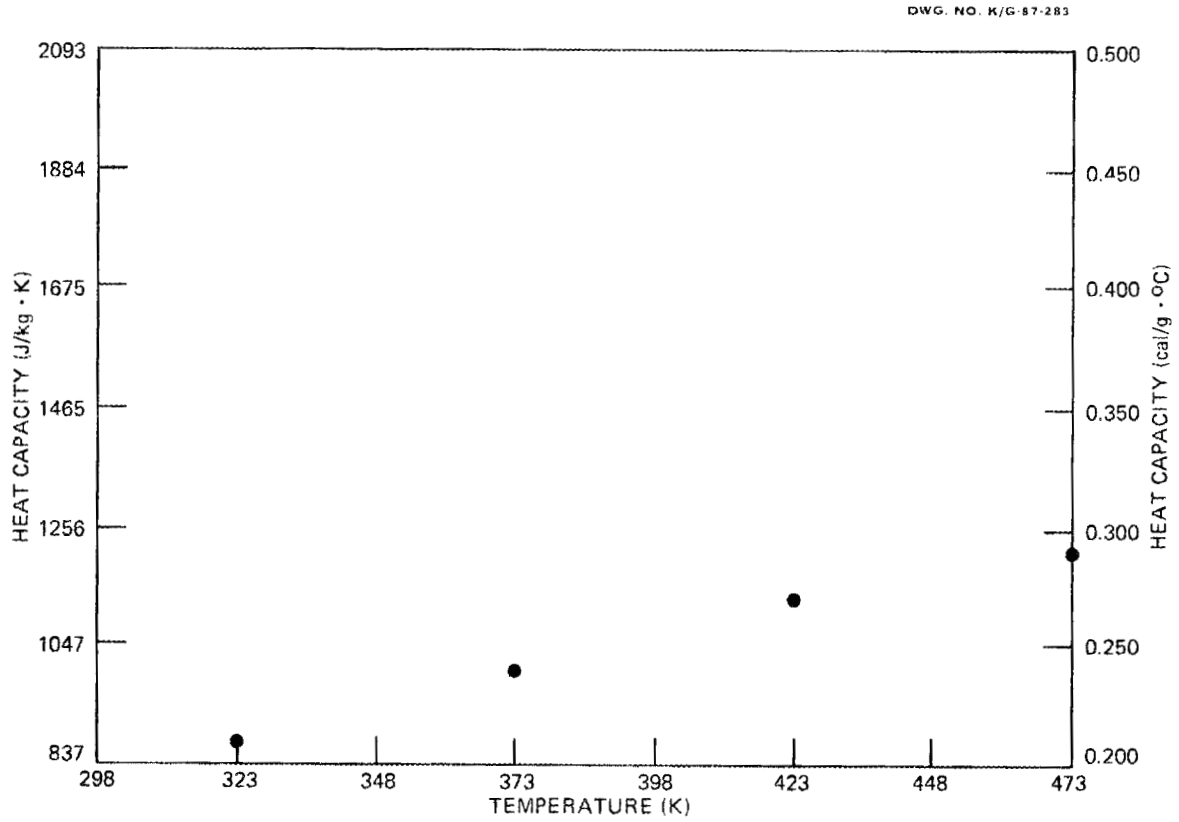


Fig. C.3. Selected heat capacity as a function of temperature for shale from 137.3 m (450.4 ft).

DWG. NO. K/G-87-293

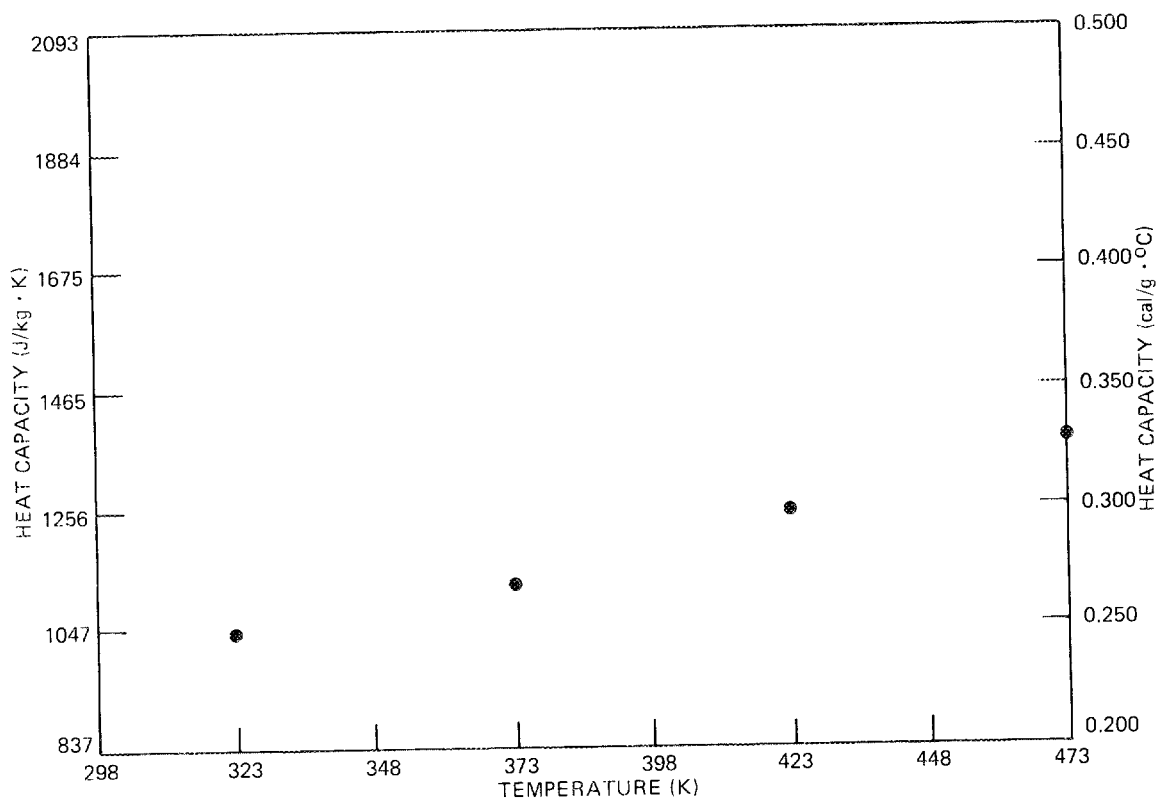


Fig. C.4. Selected heat capacity as a function of temperature for shale from 137.4 m (450.7 ft).

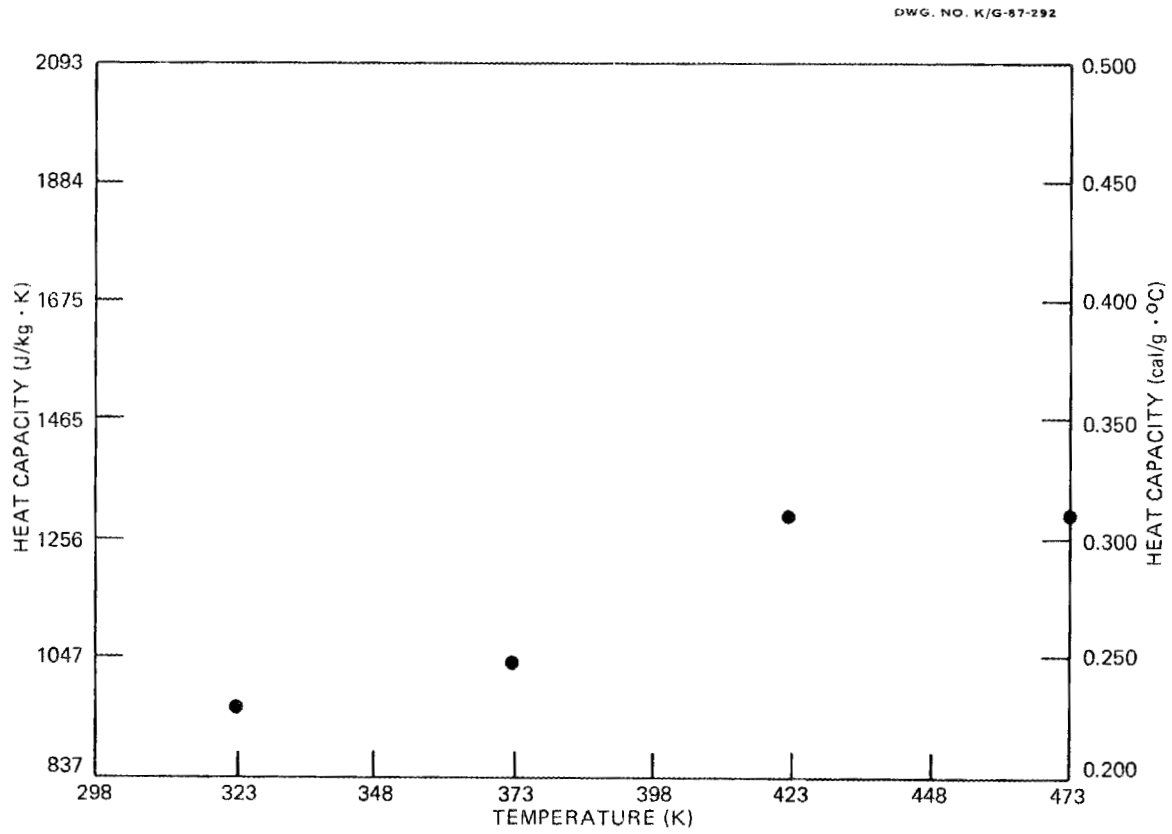


Fig. C.5. Selected heat capacity as a function of temperature for shale from 149.4 m (490 ft).

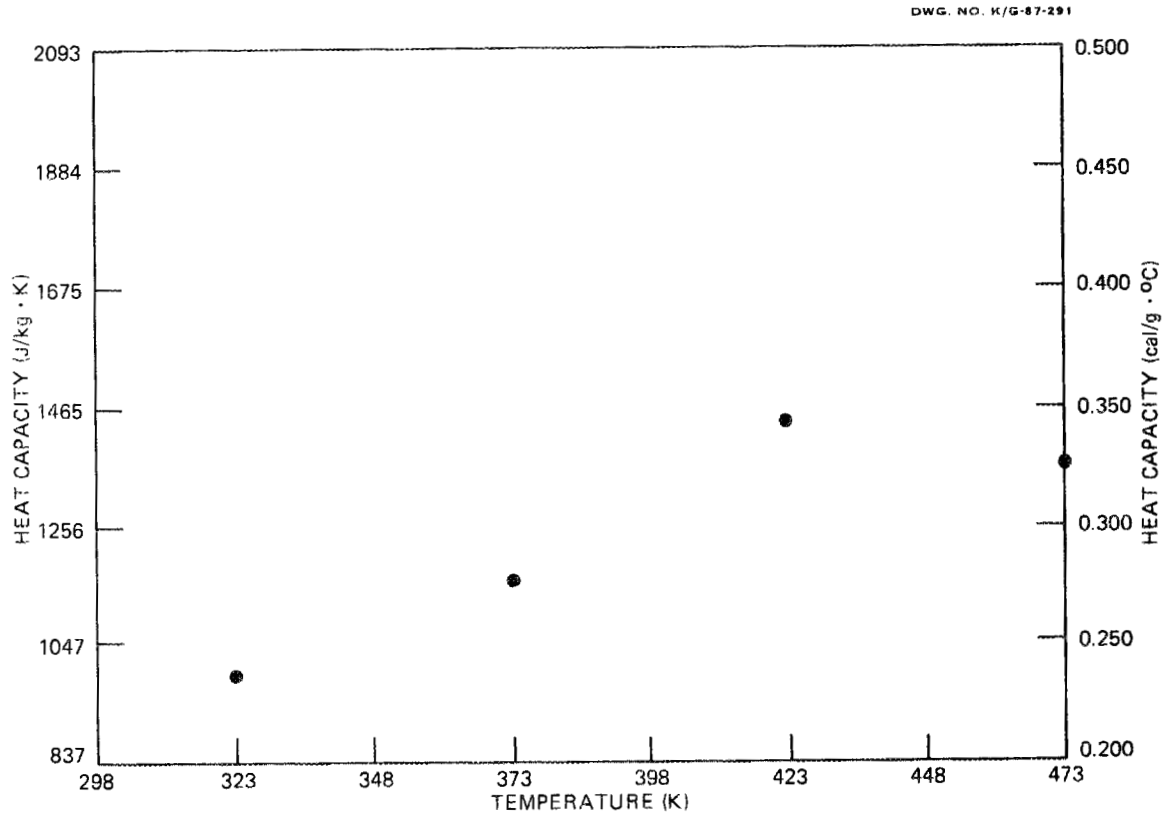


Fig. C.6. Selected heat capacity as a function of temperature for shale from 155.4 m (510 ft).

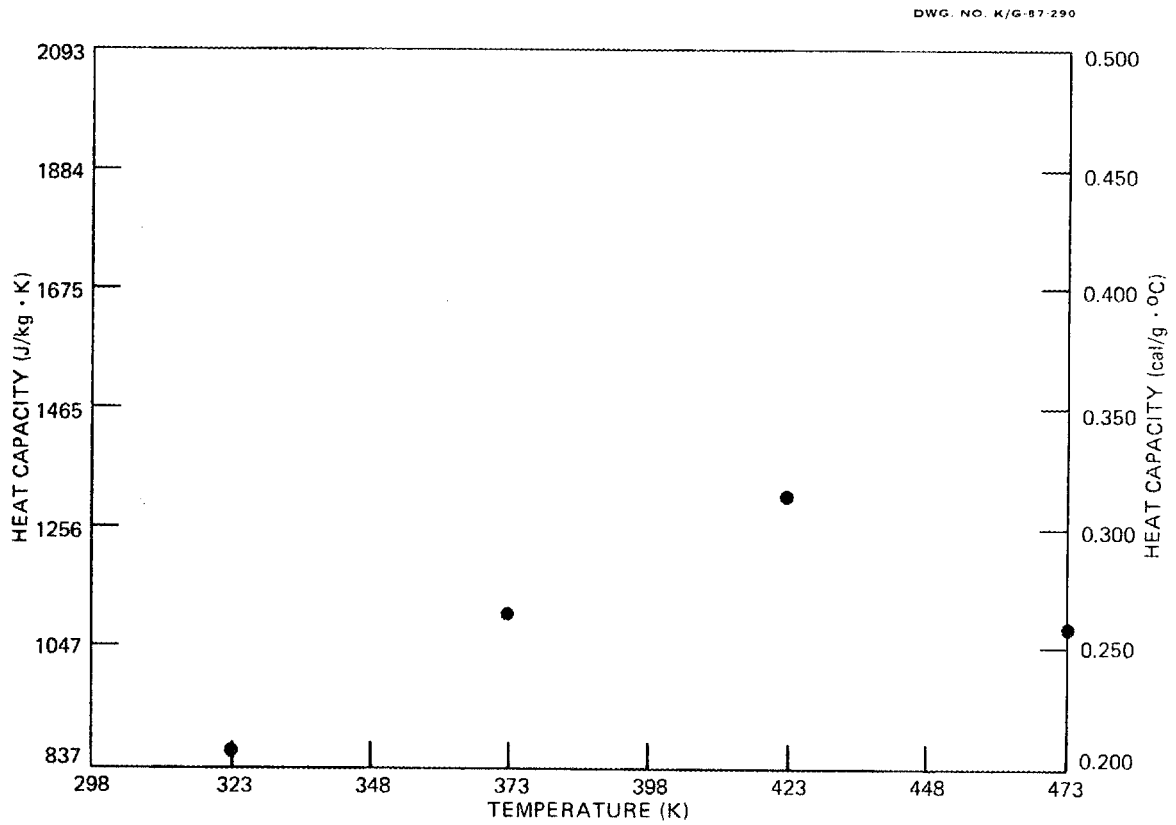


Fig. C.7. Selected heat capacity as a function of temperature for shale from 157 m (515 ft).

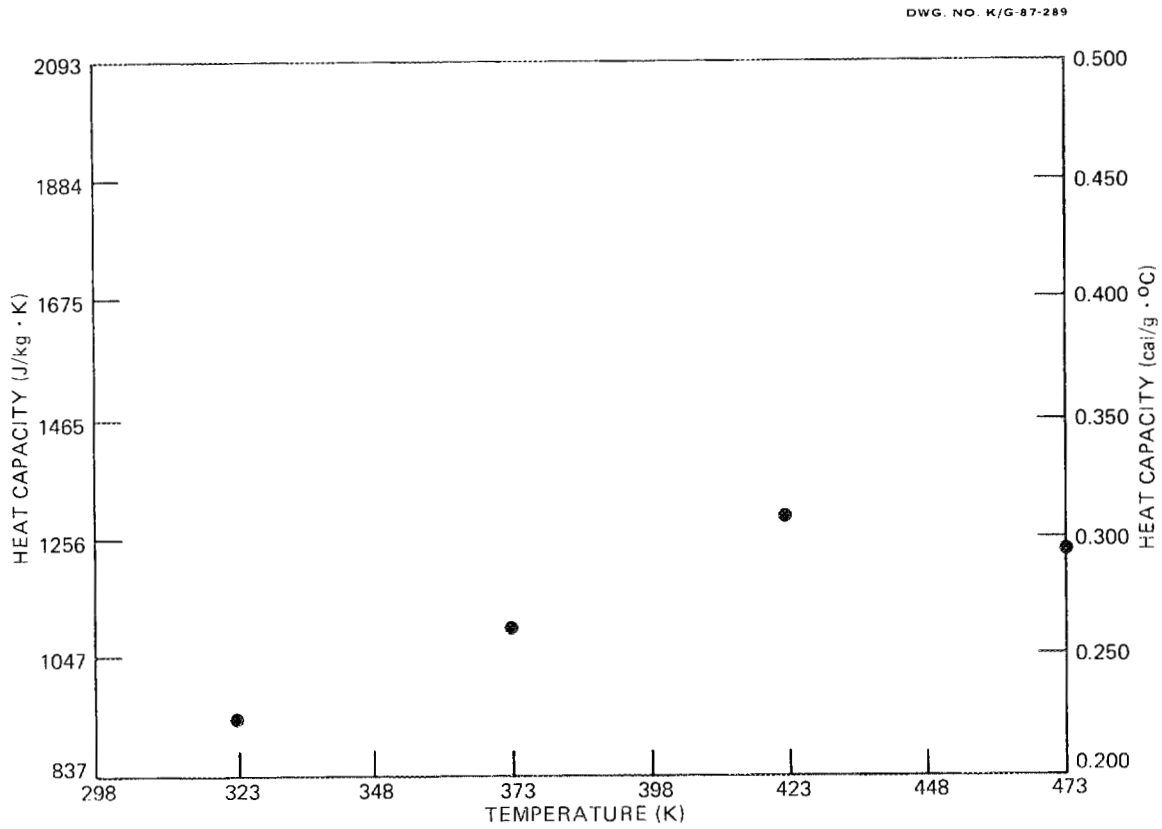


Fig. C.8. Selected heat capacity as a function of temperature for shale from 157.4 m (516.3 ft).

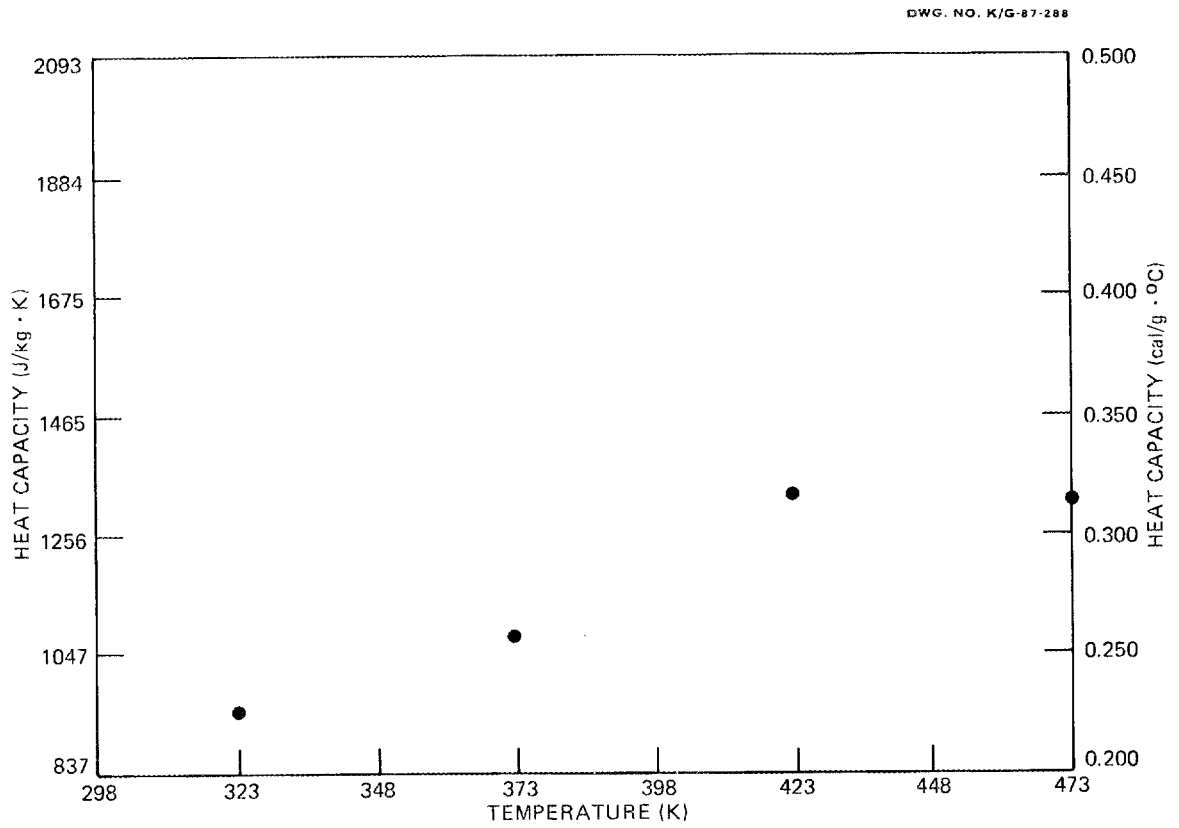


Fig. C.9. Selected heat capacity as a function of temperature for shale from 161.5 m (530 ft).

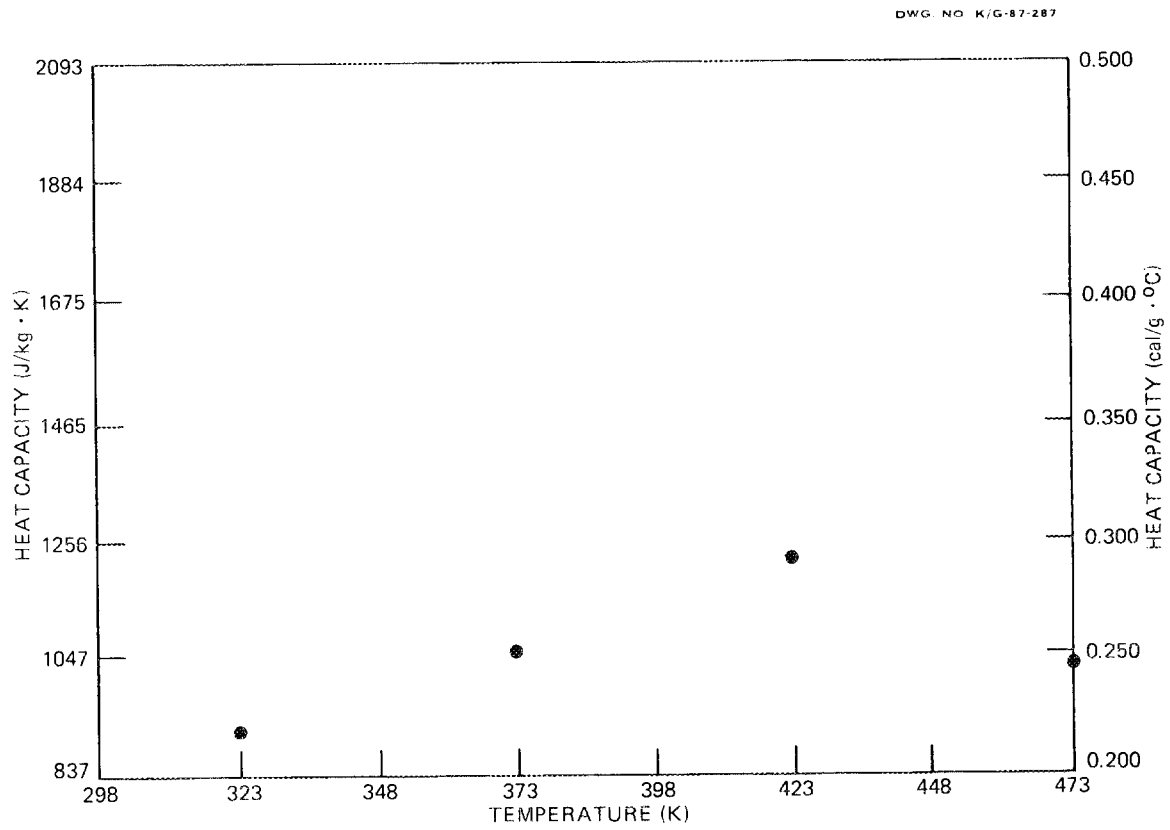


Fig. C.10. Selected heat capacity as a function of temperature for shale from 176.2 m (578.2 ft).

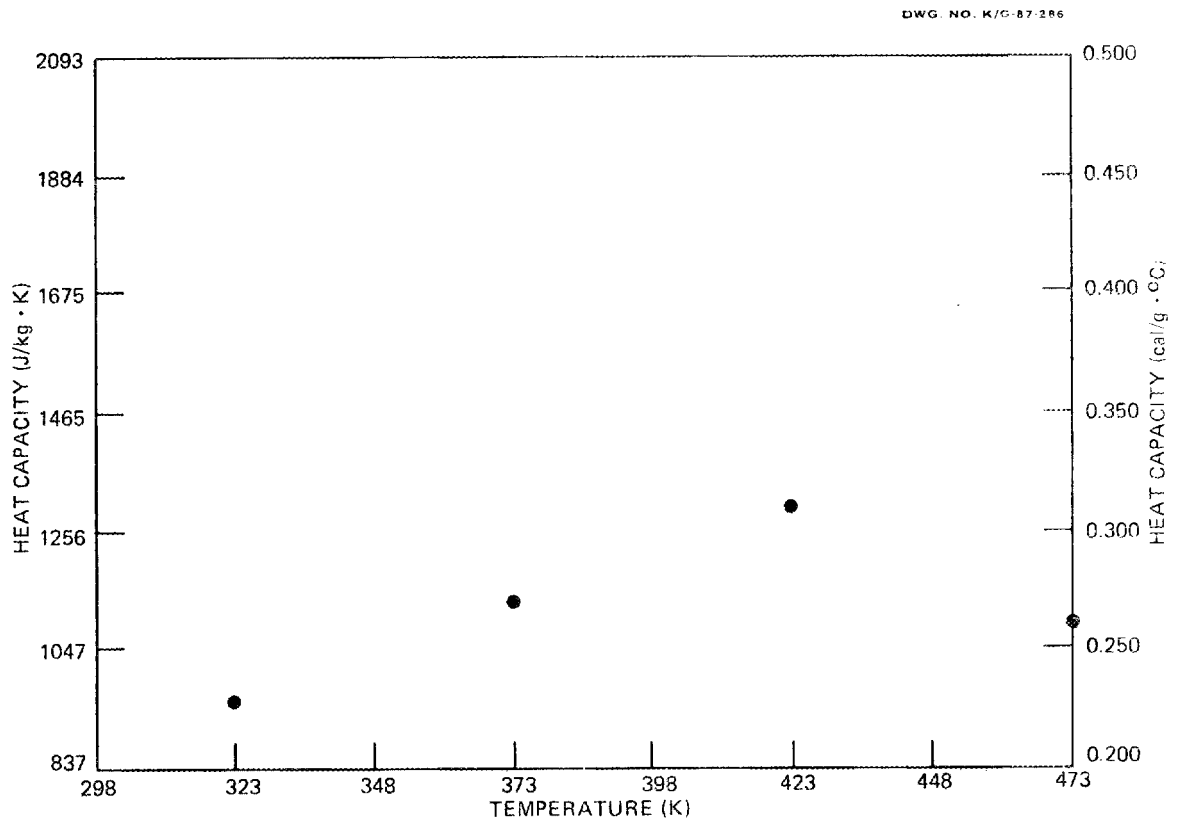


Fig. C.11. Selected heat capacity as a function of temperature for shale from 176.6 m (579.5 ft).

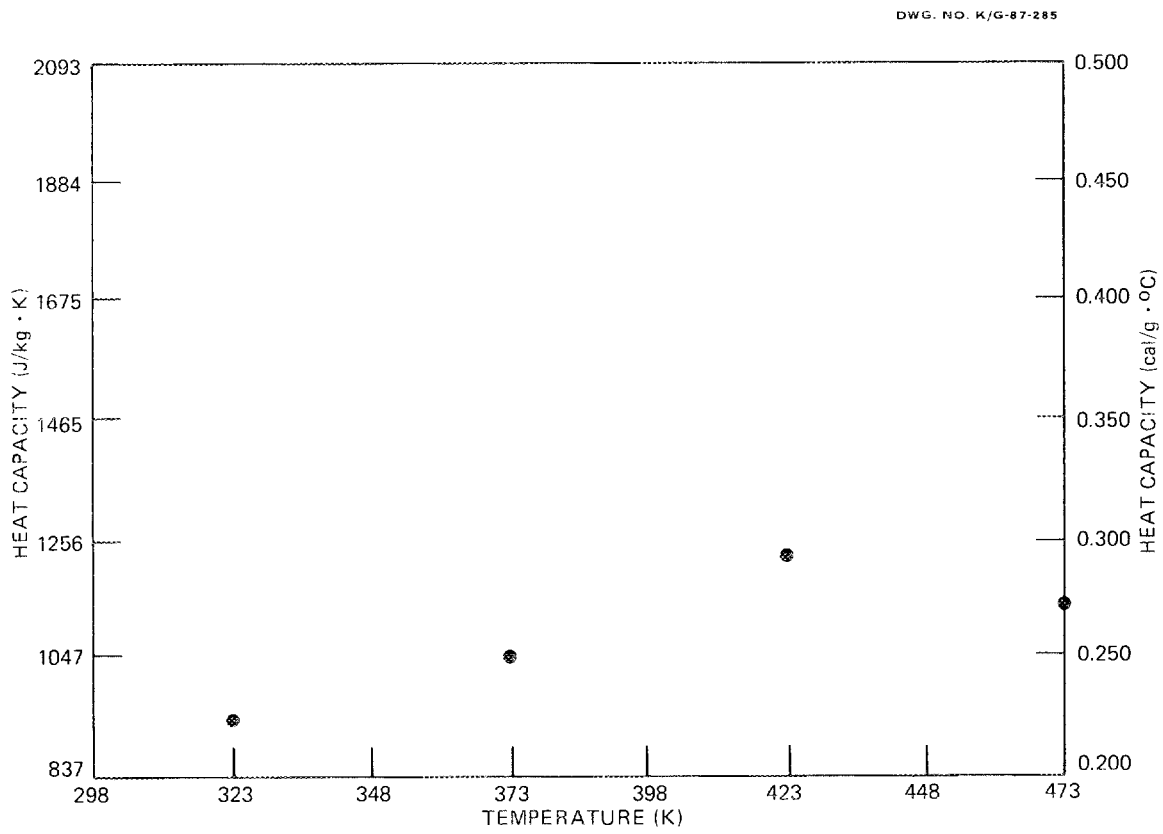


Fig. C.12. Selected heat capacity as a function of temperature for shale from 176.7 m (579.6 ft).

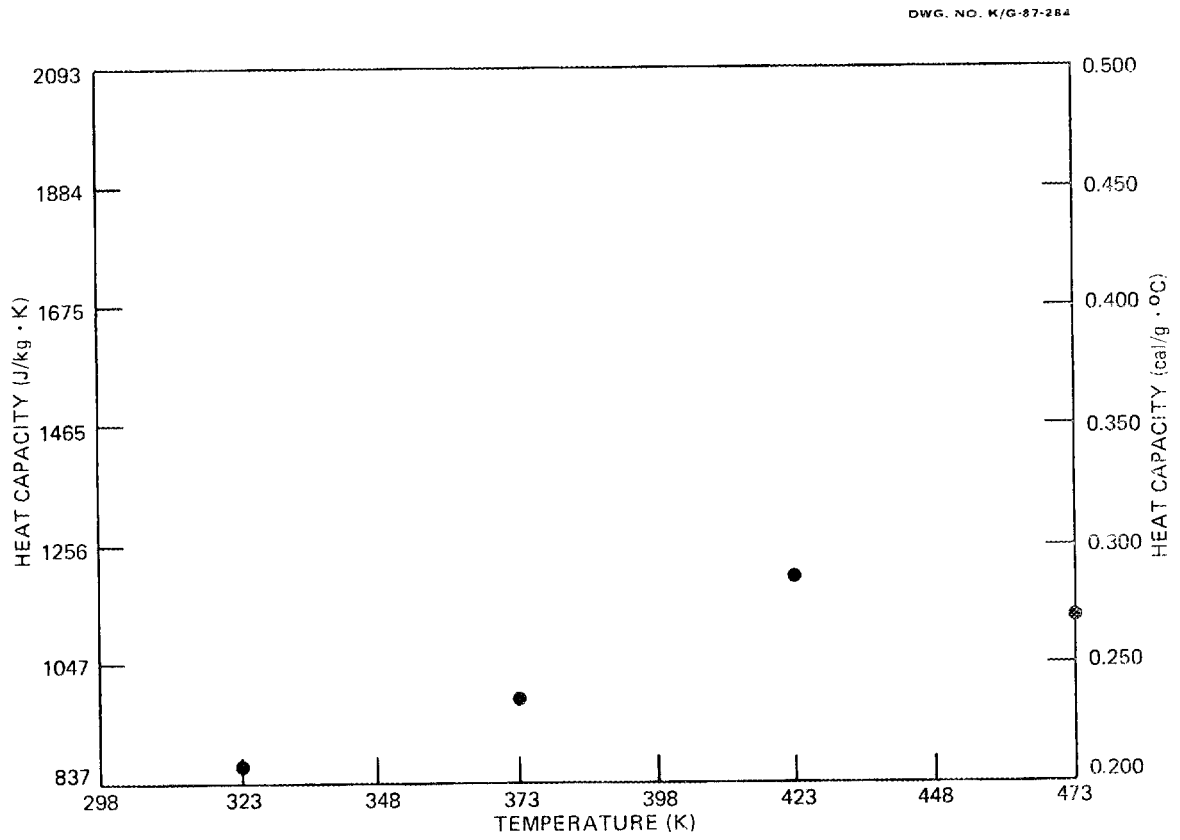


Fig. C.13. Selected heat capacity as a function of temperature for shale from 187.7 m (615.8 ft).

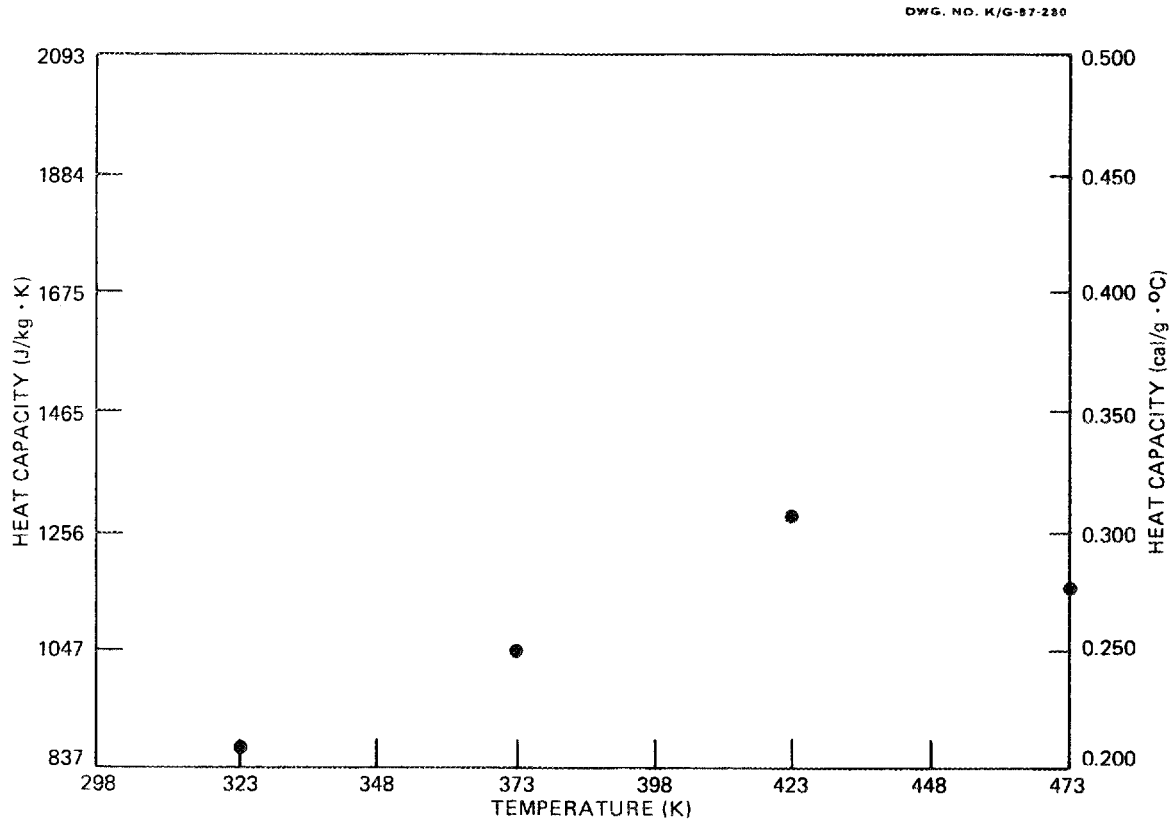


Fig. C.14. Selected heat capacity as a function of temperature for shale from 187.8 m (616 ft).

DWG. NO. K/G-87-301

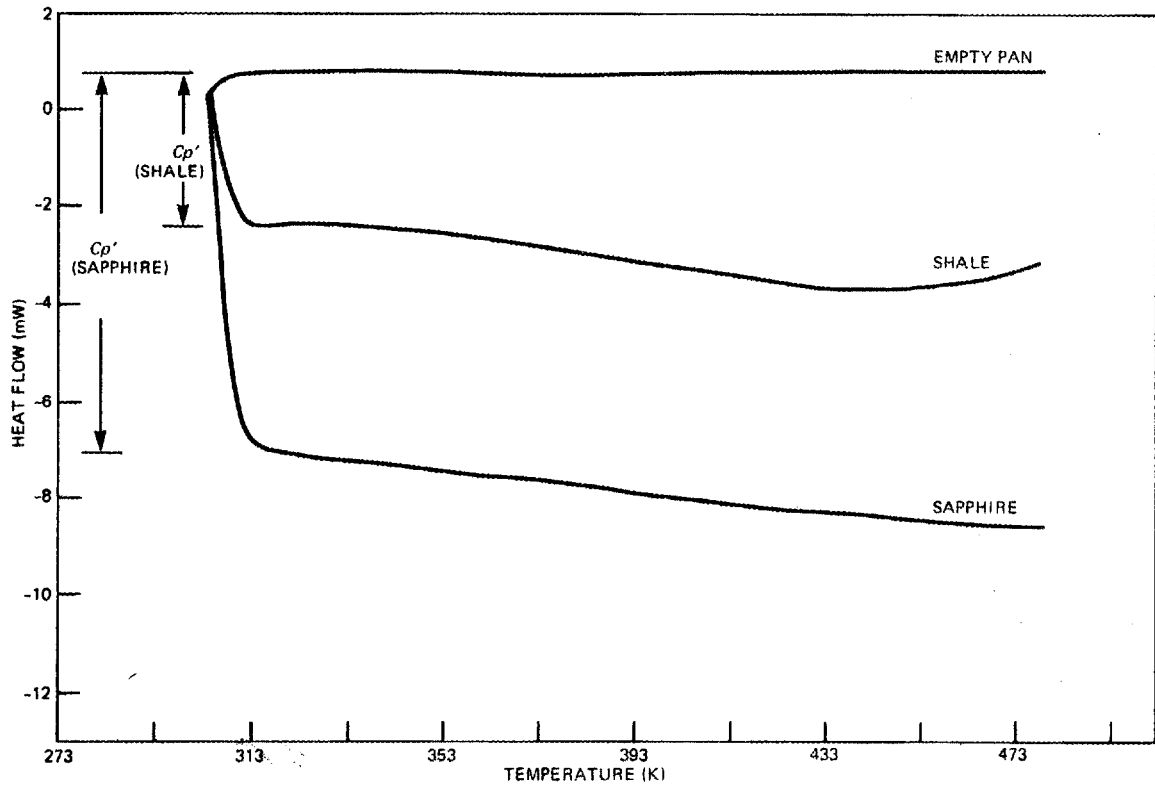


Fig. C.15. DSC curve for shale from 137.2 m (450 ft).

DWG. NO. K/G-87-313

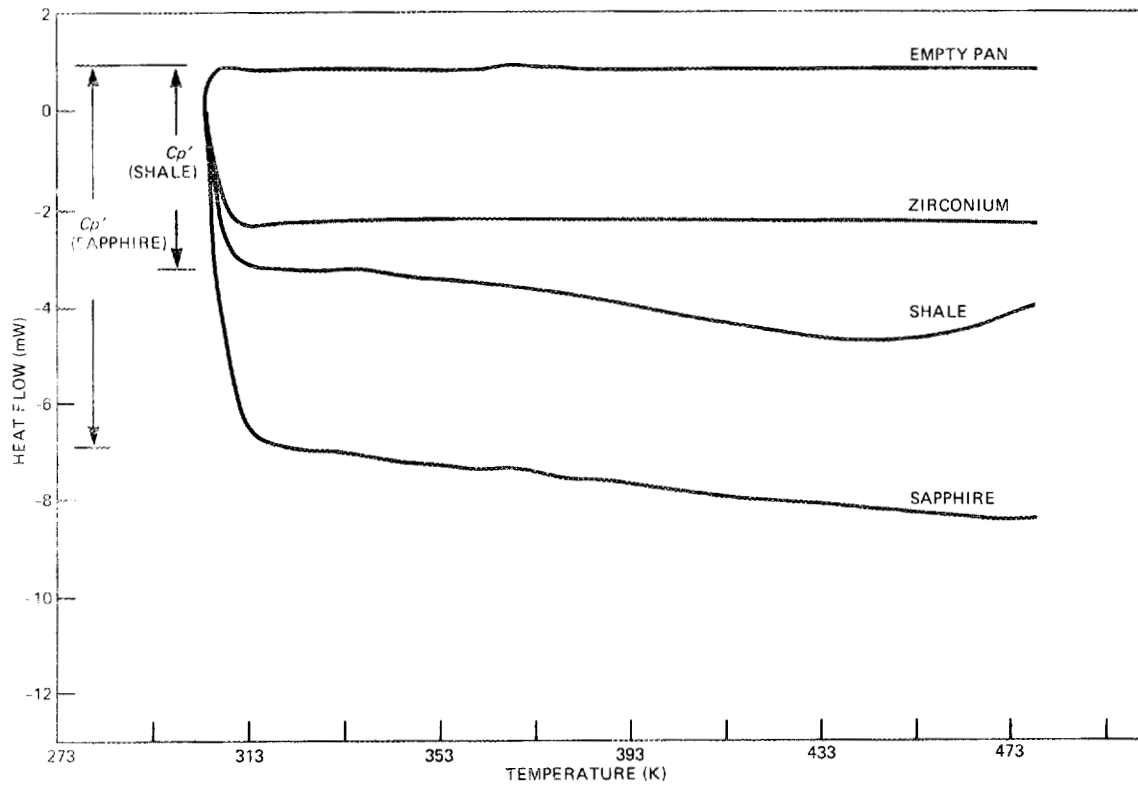


Fig. C.16. DSC curve for shale from 137.2 m (450.1 ft).

DWG. NO. K/G-87-312

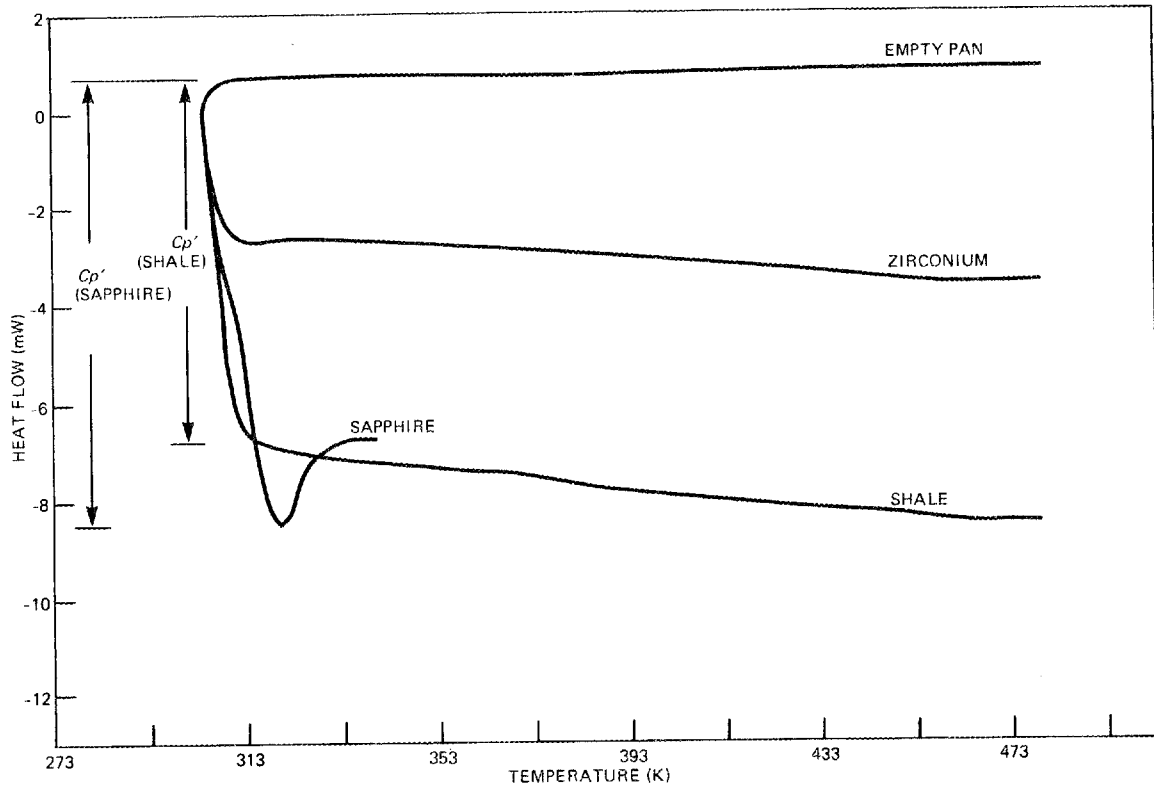


Fig. C.17. DSC curve for shale from 137.3 m (450.4 ft).

DWG. NO. K/G-87-311

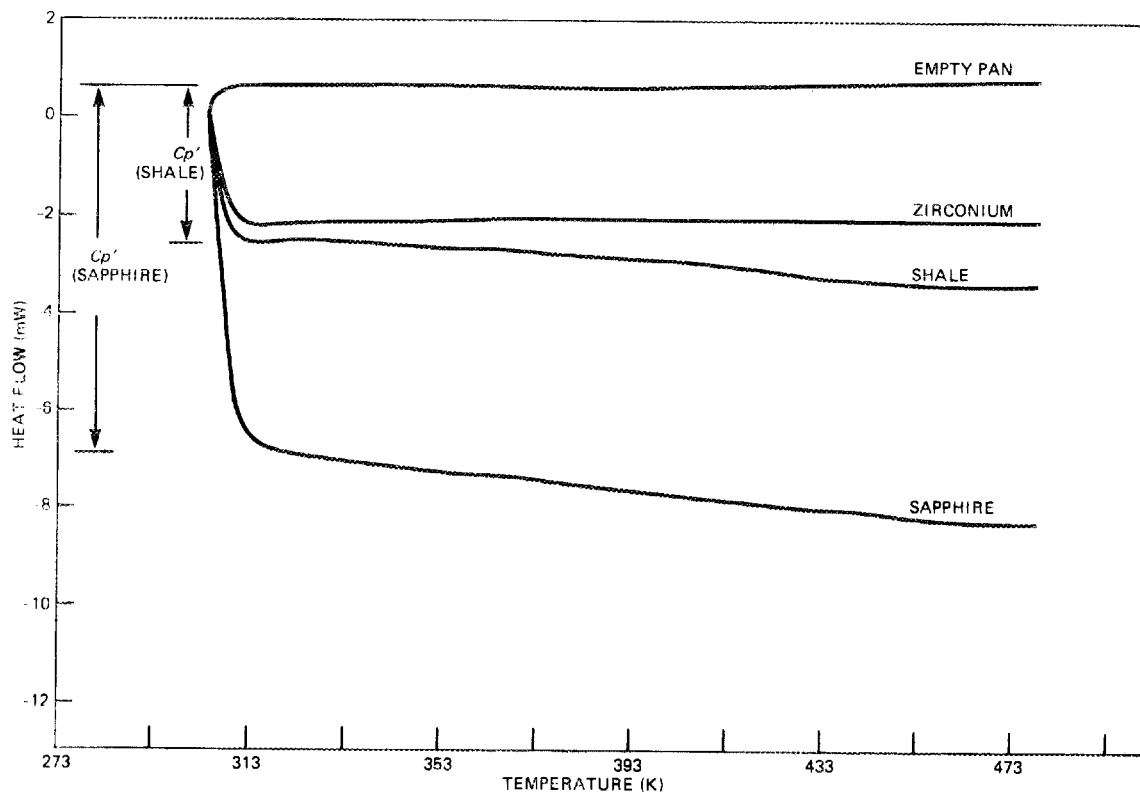


Fig. C.18. DSC curve for shale from 137.4 m (450.7 ft).

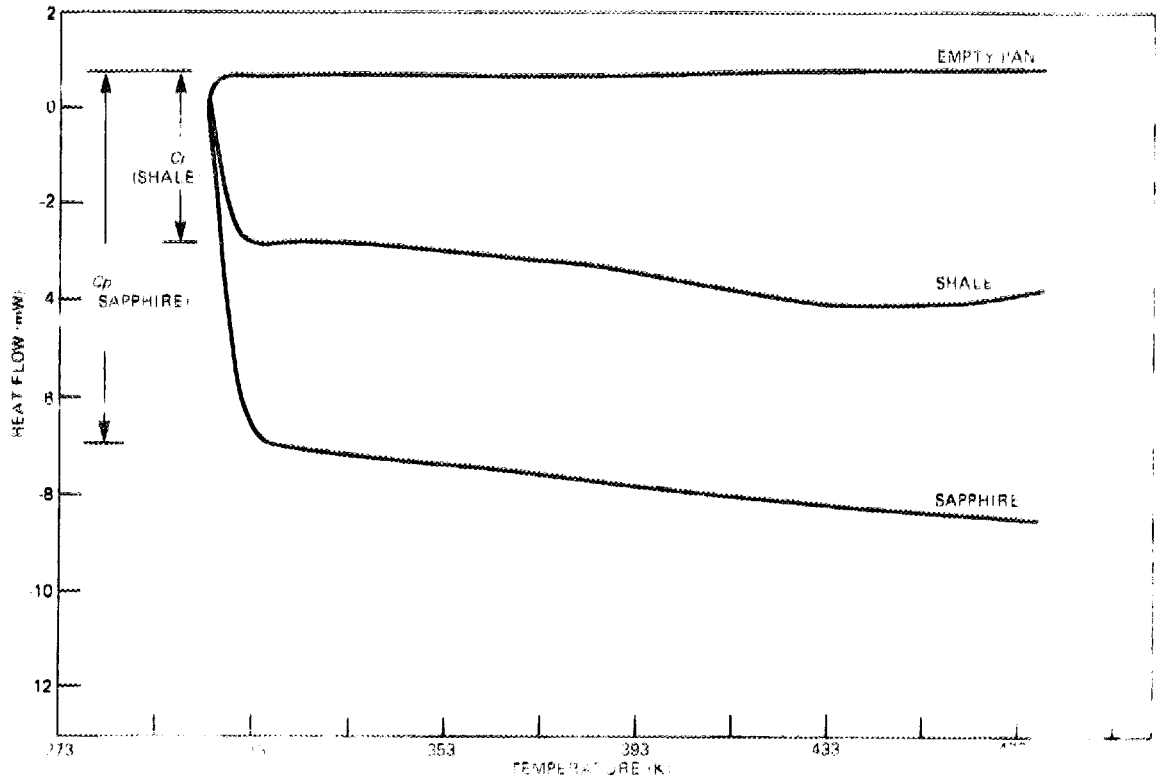


Fig. C.19. DSC curve for shale from 149.4 m (490 ft).

DWG. NO. K/G-87-310

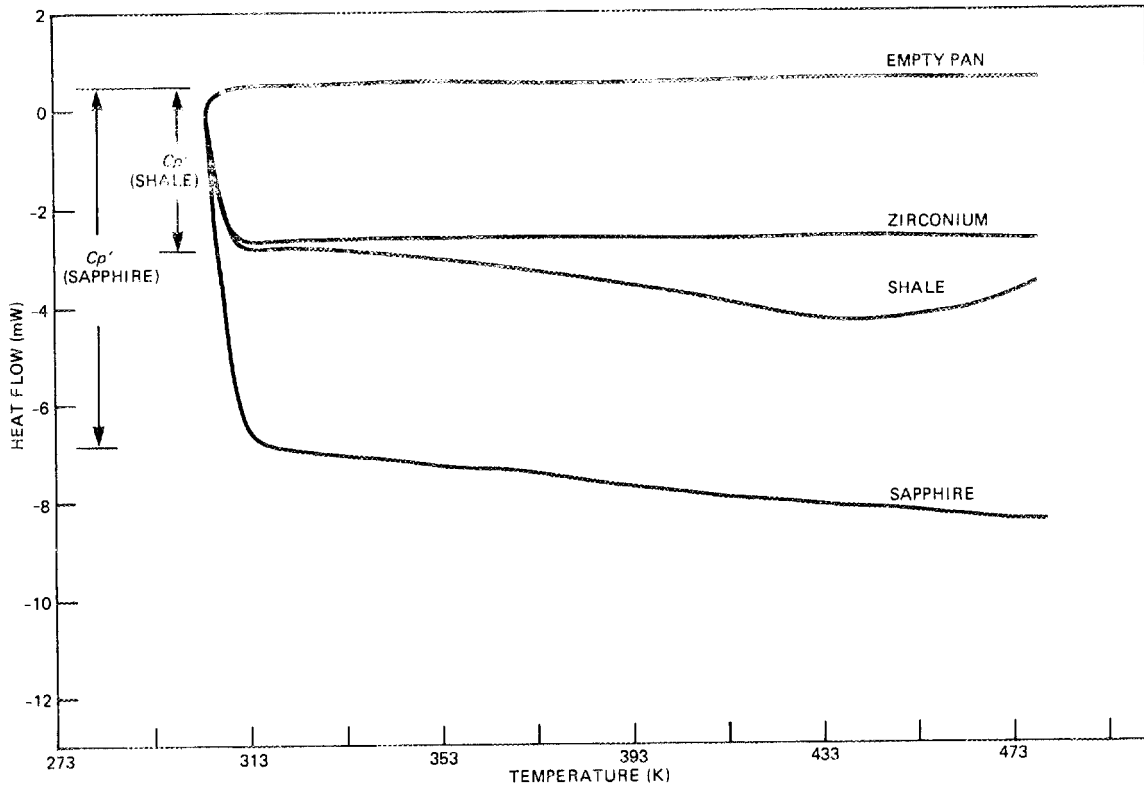


Fig. C.20. DSC curve for shale from 155.4 m (510 ft).

DWG. NO. K/G-87-309

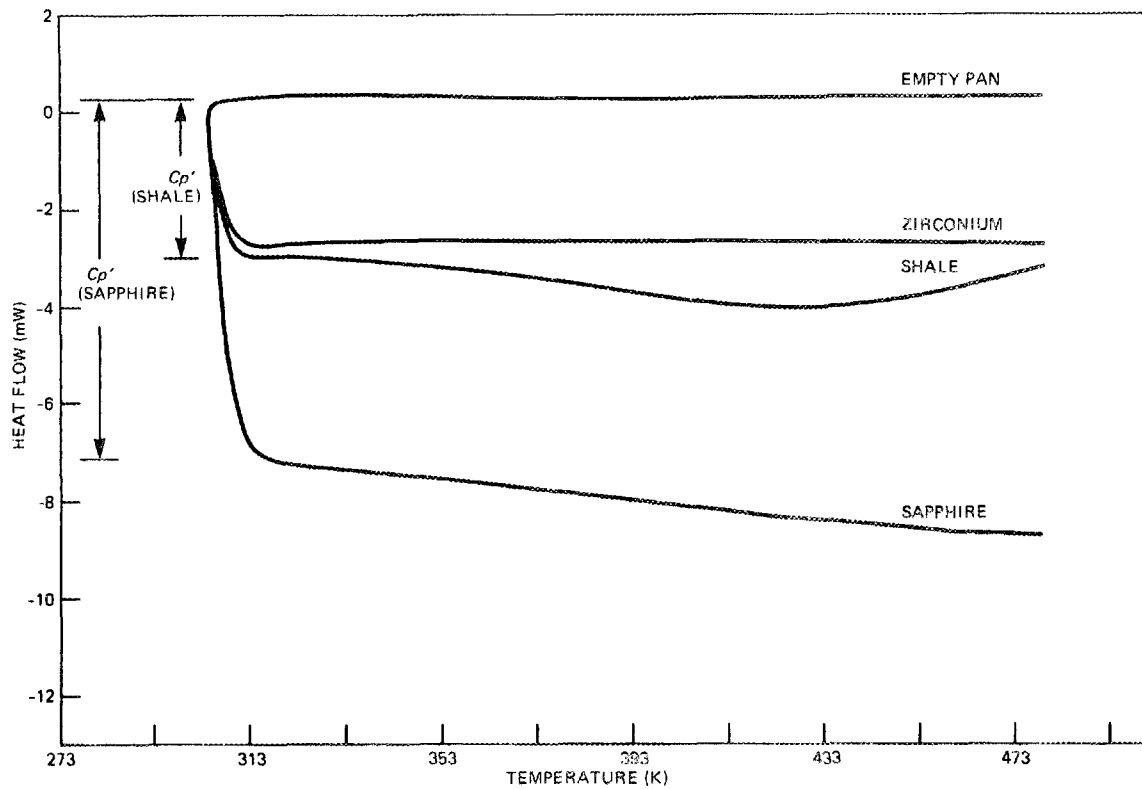


Fig. C.21. DSC curve for shale from 157 m (515 ft).

DWG. NO. K/G-87-298

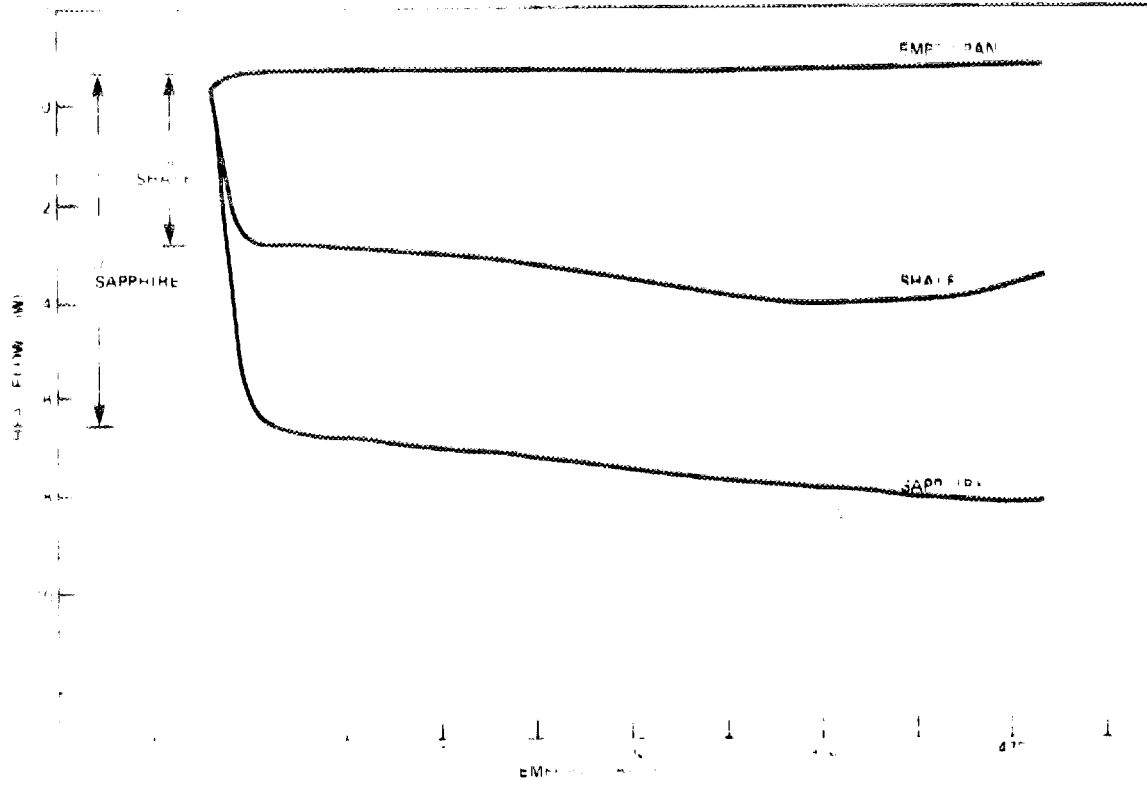


Fig. 1. Wellbore profile for shale from 157.4 m (516.3 ft).

DWG NO K/G-87-300

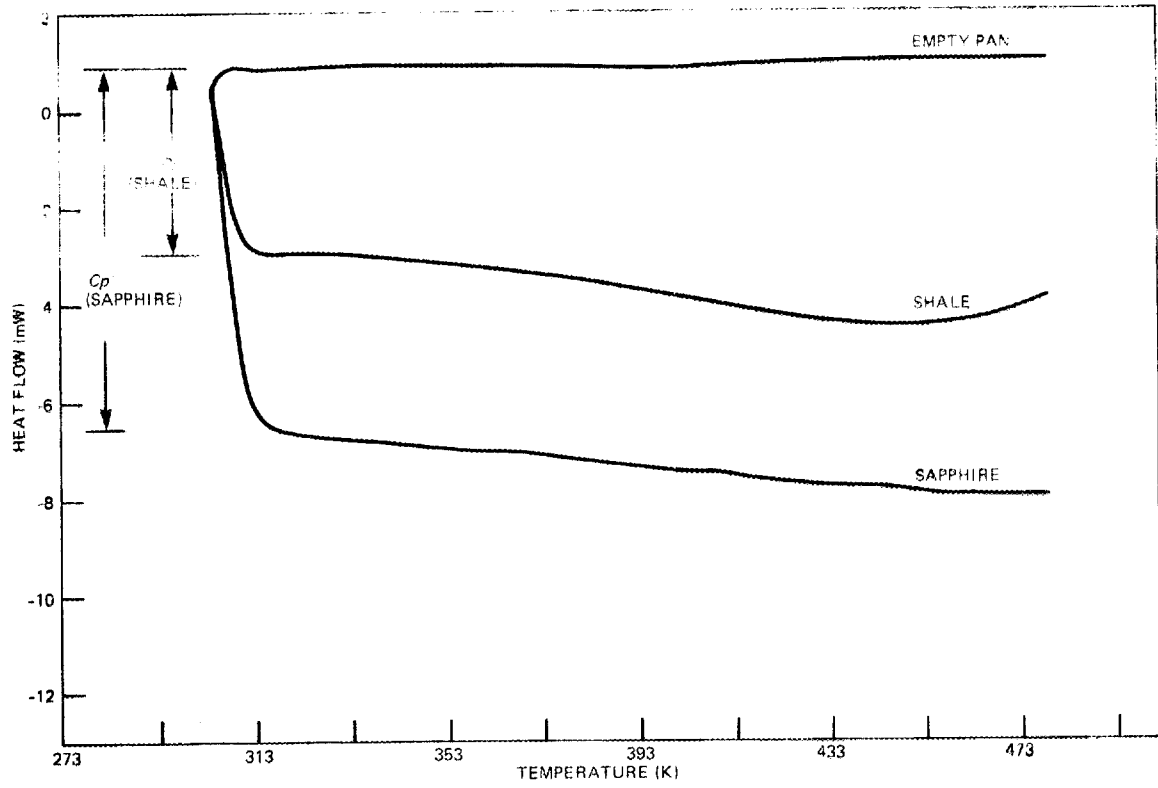


Fig. C.23. DSC curve for shale from 161.5 m (530 ft).

DWG. NO. K/G-87-308

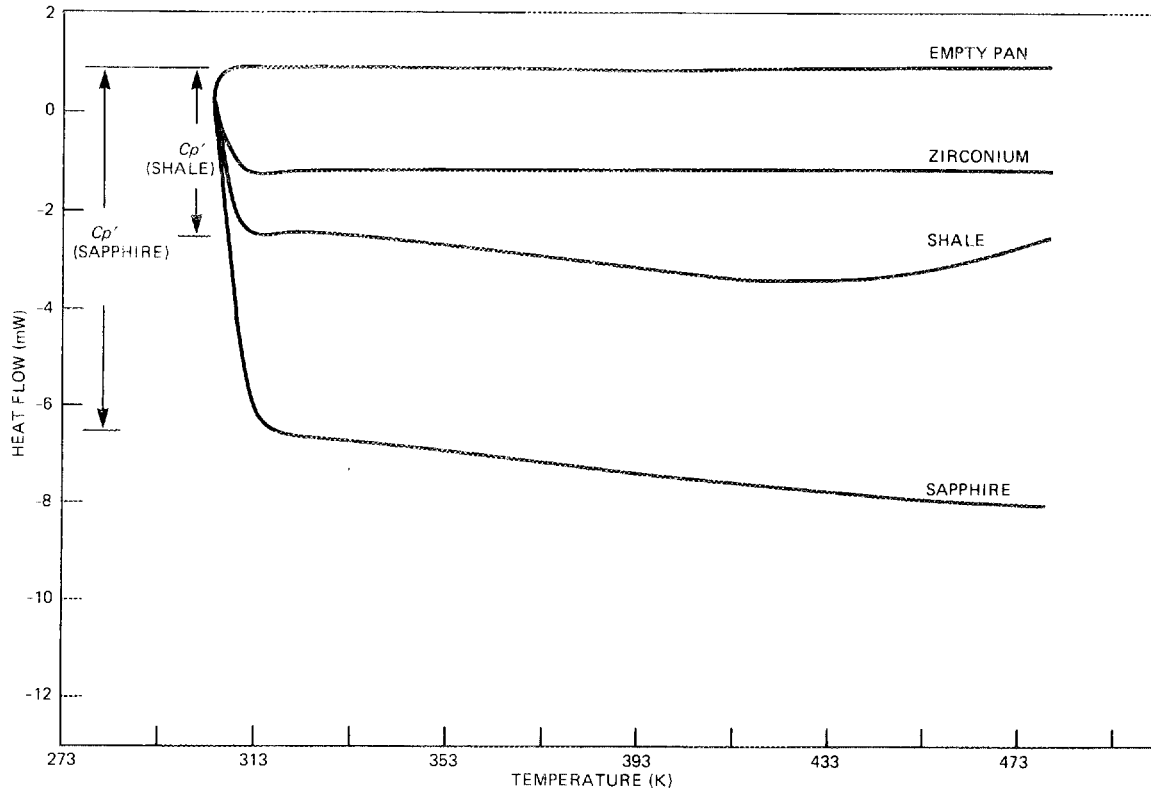


Fig. C.24. DSC curve for shale from 176.2 m (578.2 ft).

DWG. NO. K/G-87-304

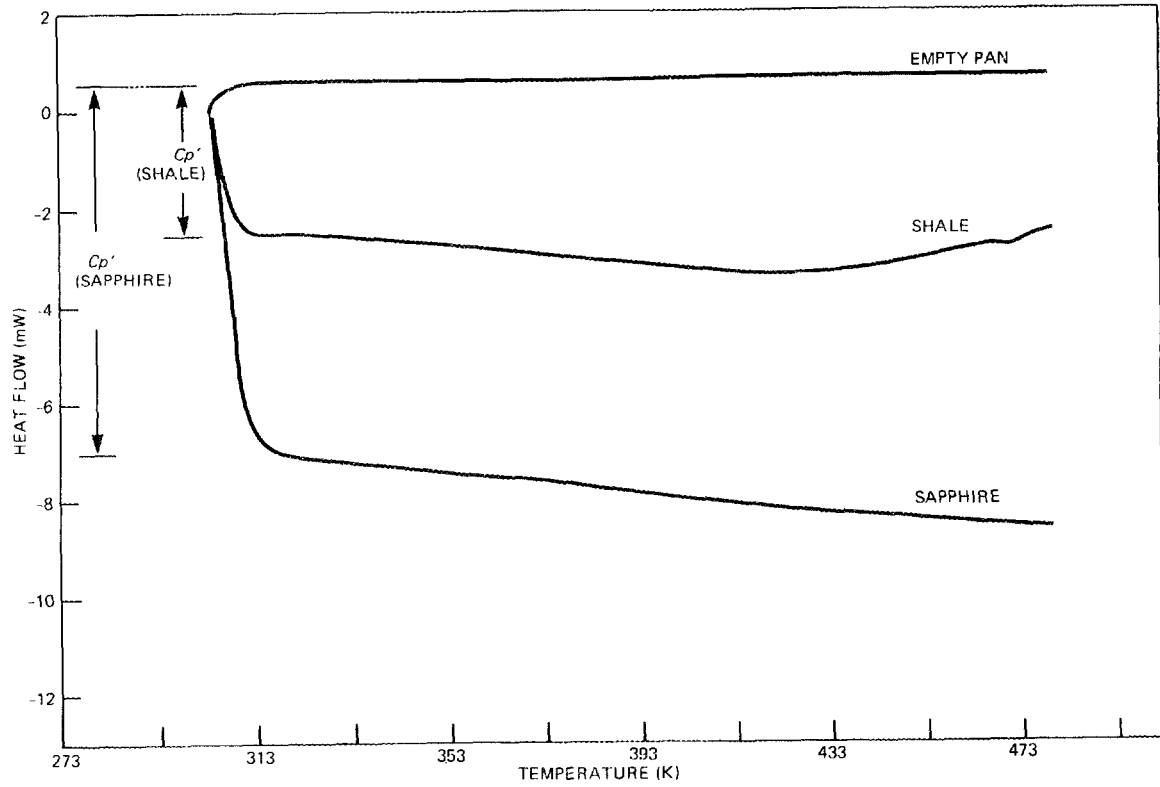


Fig. C.25. DSC curve for shale from 176.6 m (579.5 ft).

DWG. NO K/G-87-315

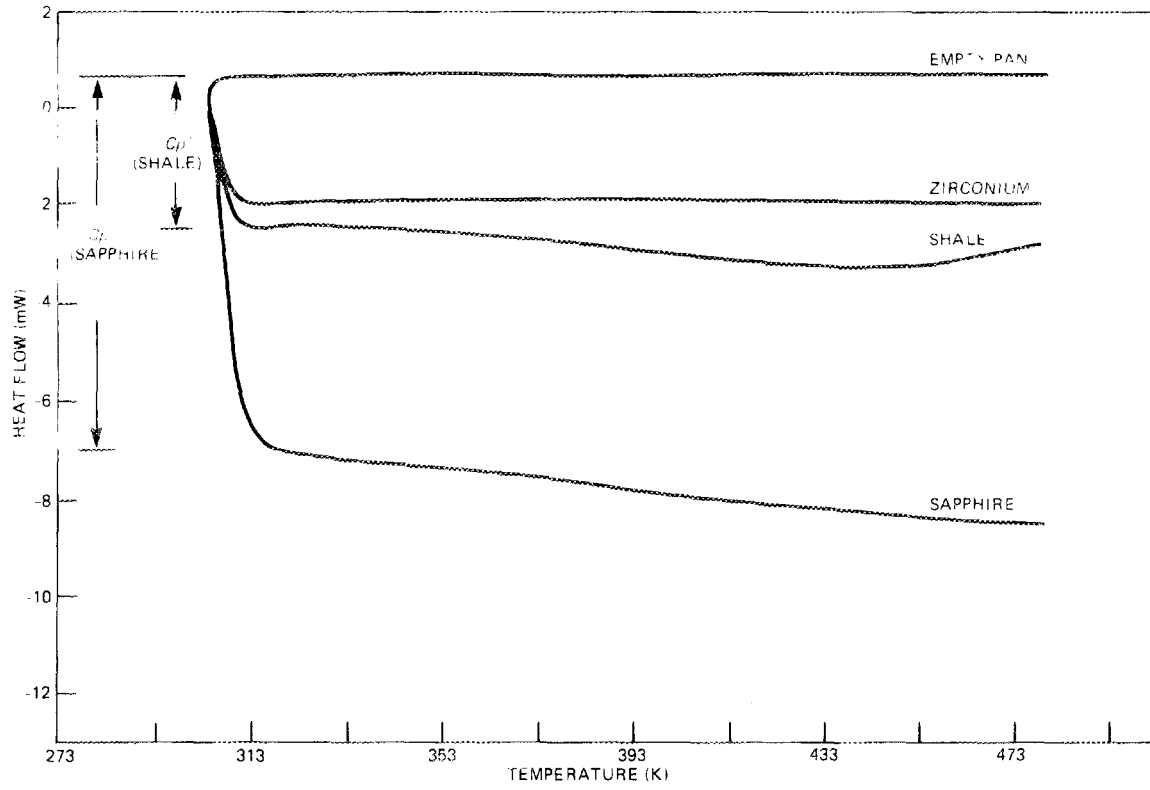


Fig. C.26. DSC curve for shale from 176.7 m (579.6 ft).

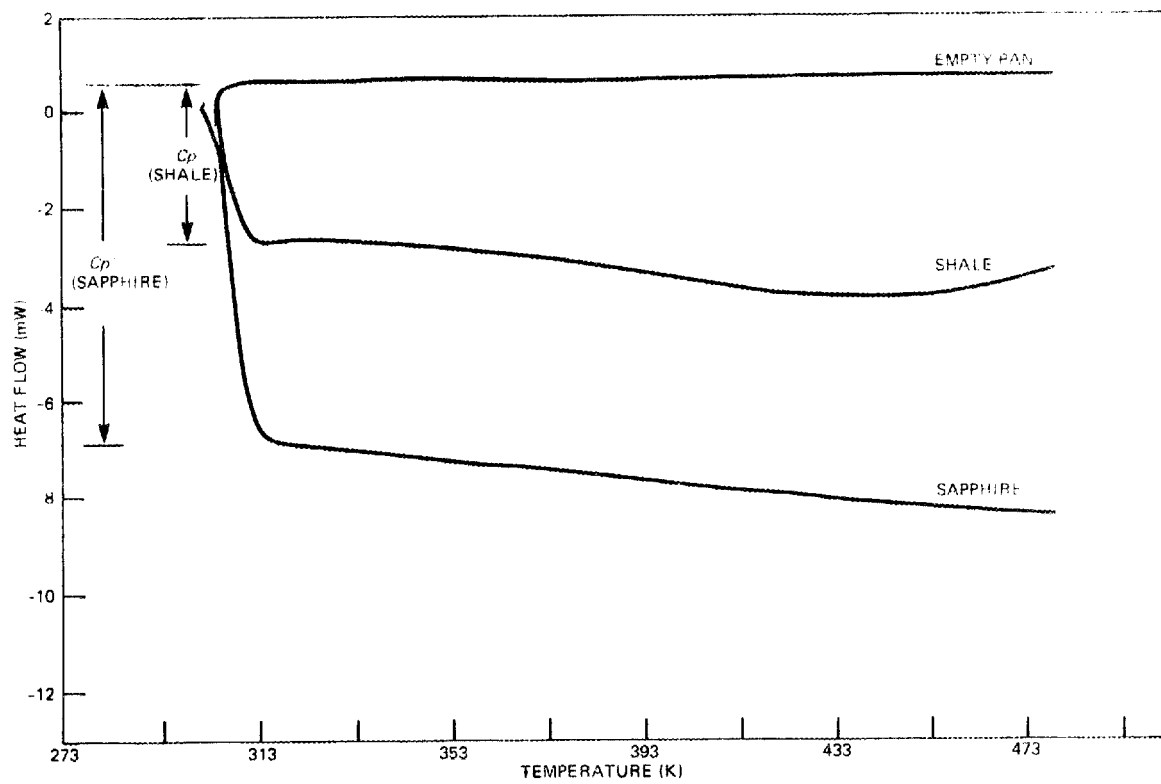


Fig. C.27. DSC curve for shale from 187.7 m (615.8 ft).

DWG. NO. K/G-87-314

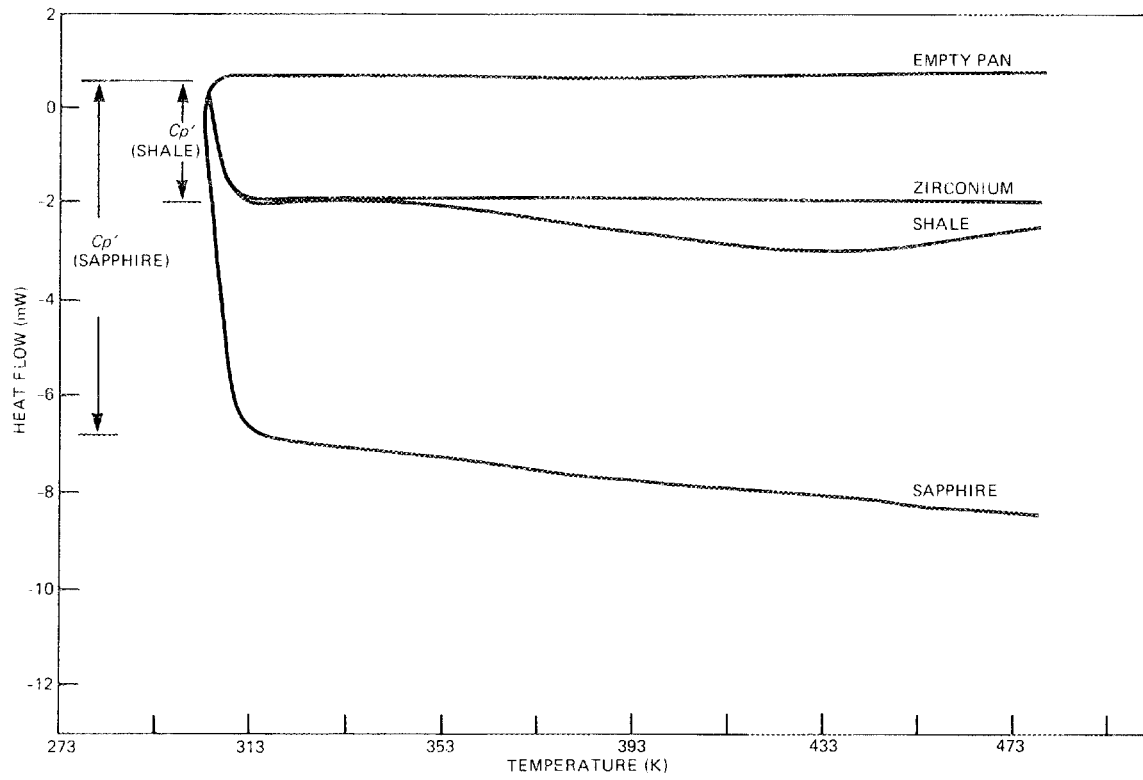


Fig. C.28. DSC curve for shale from 187.8 m (616 ft).

APPENDIX C.2. HEAT CAPACITY DATA FOR PIERRE SHALE SAMPLES

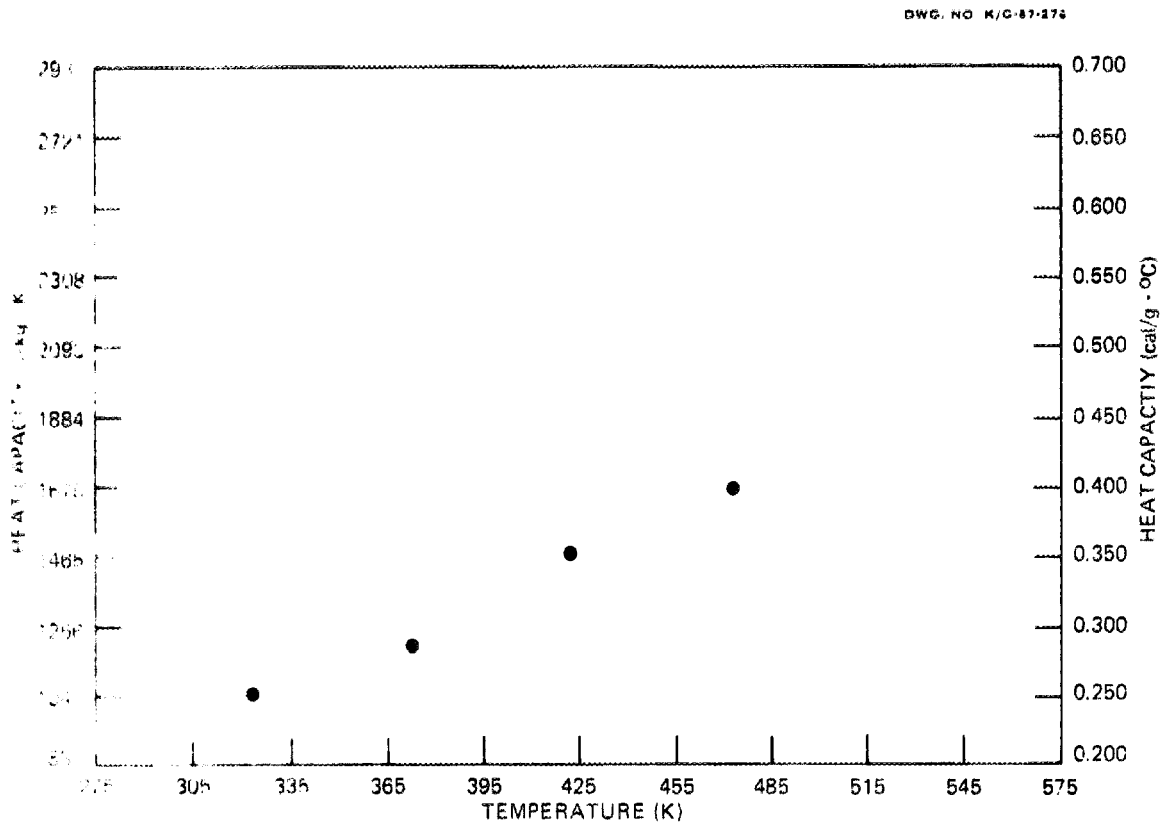


Fig. C.29. Selected heat capacity as a function of temperature for shale from 4+8 m (147 ft).

DWG. NO. K/G-87-277

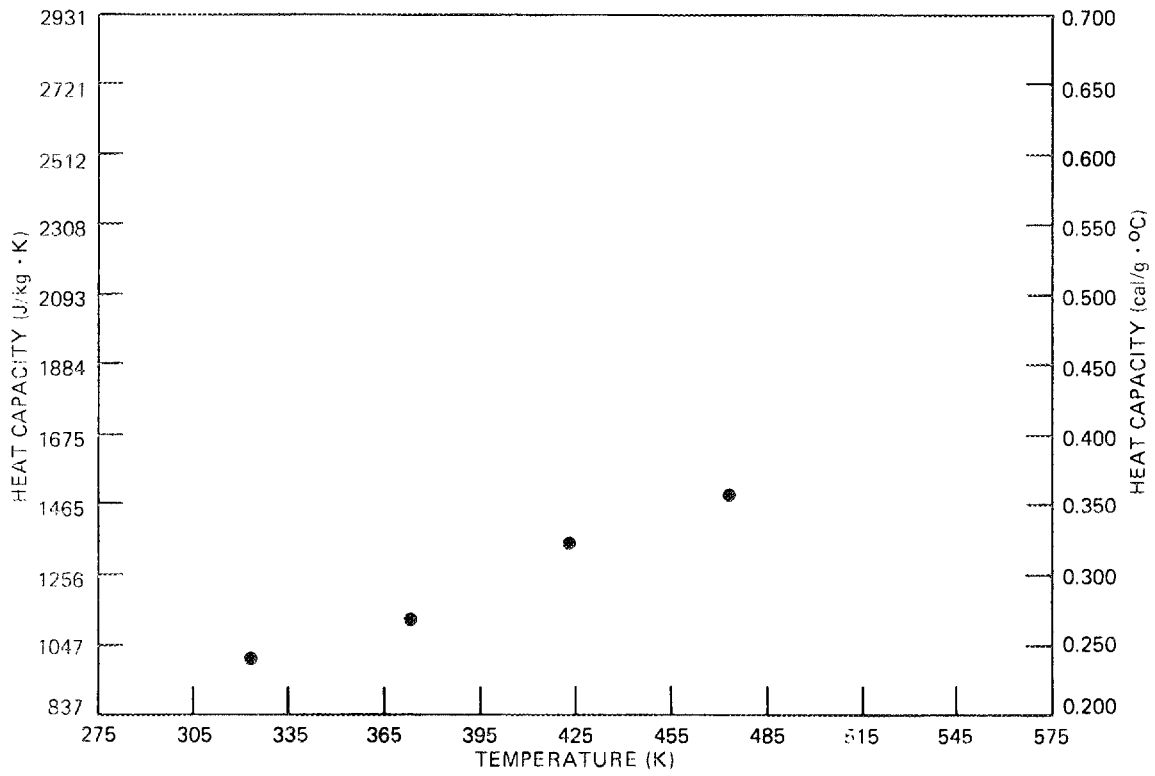


Fig. C.30. Selected heat capacity as a function of temperature for shale from 45.1 m (148 ft).

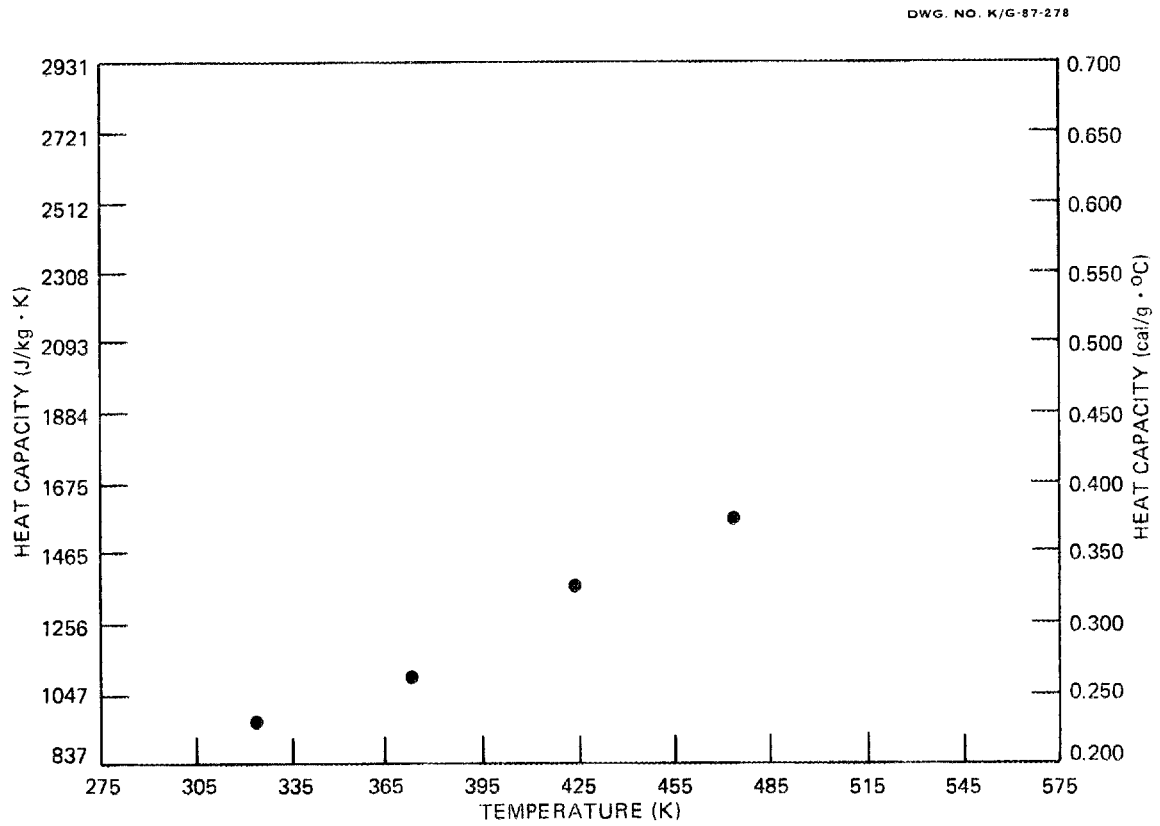


Fig. C.31. Selected heat capacity as a function of temperature for shale from 45.7 m (150 ft).

DWG. NO. K/G-87-299

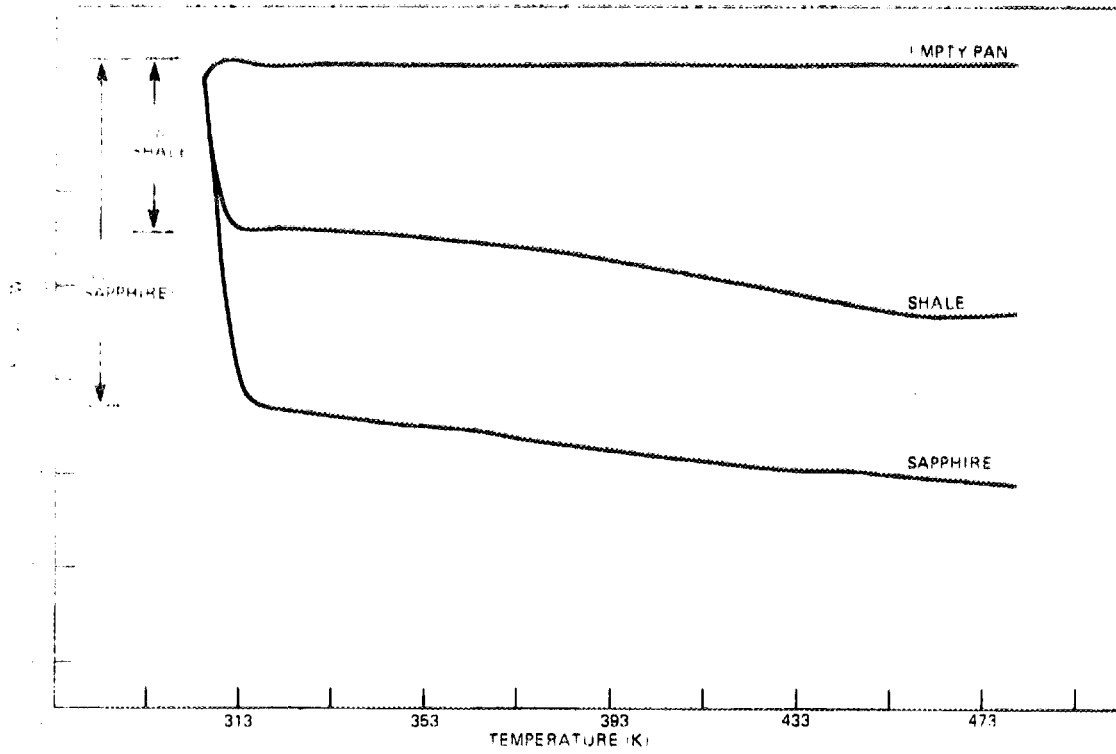


Fig. C.32. DSC curve for shale from 44.8 m (147 ft).

DWG. NO. K/G-87-303

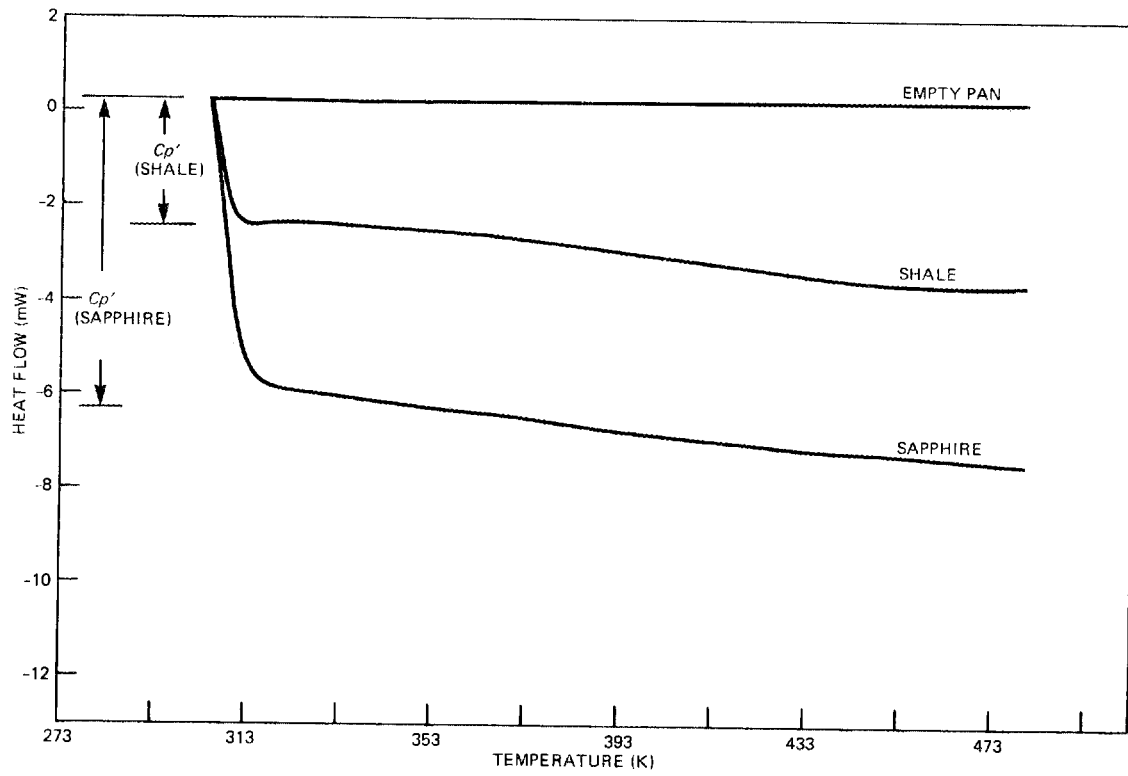


Fig. C.33. DSC curve for shale from 45.1 m (148 ft).

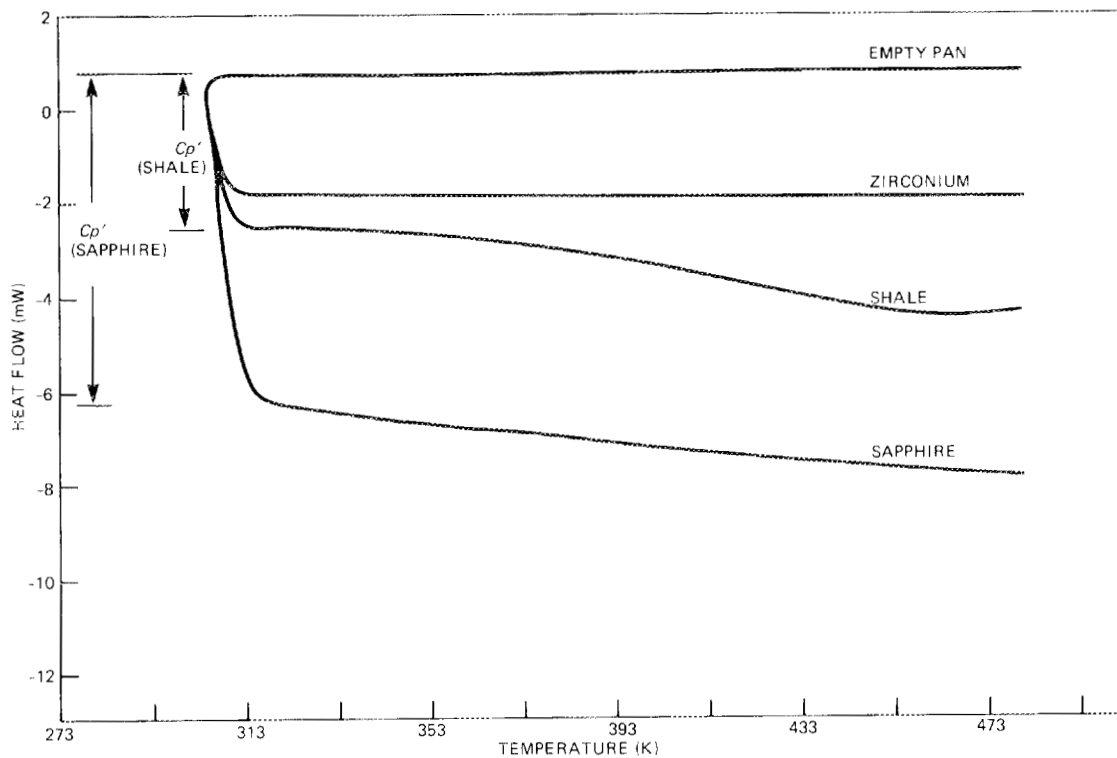


Fig. C.34. DSC curve for shale from 45.7 m (150 ft).

APPENDIX C.3. HEAT CAPACITY DATA FOR GREEN RIVER FORMATION SHALE SAMPLES

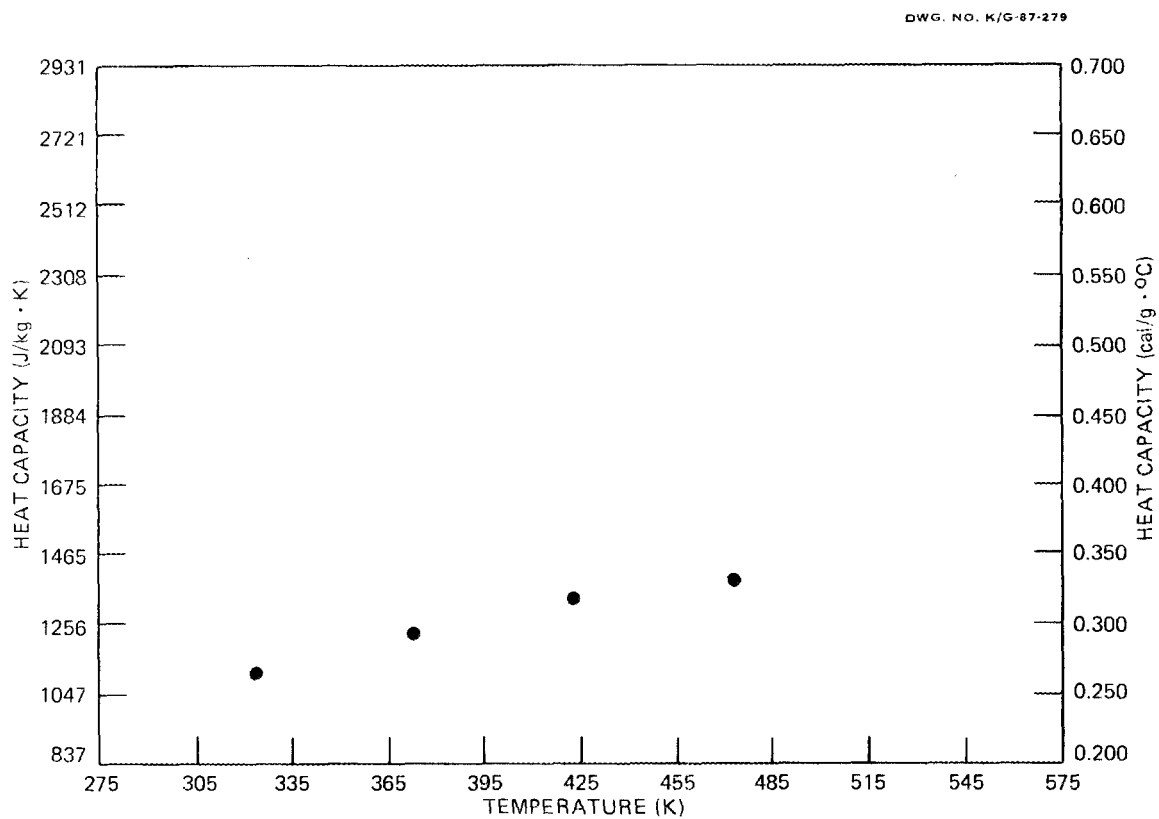


Fig. C.35. Selected heat capacity as a function of temperature.

DWG. NO. K/G-87-307

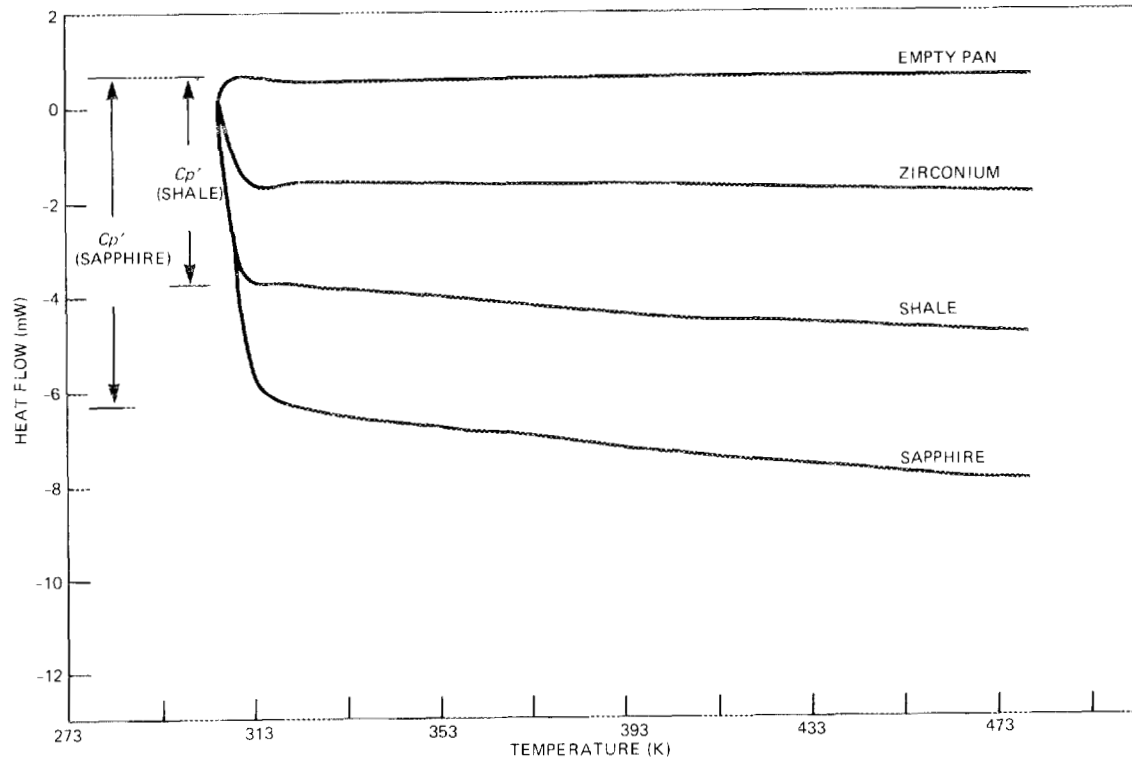


Fig. C.36. DSC curve for Pierre shale sample.

APPENDIX D:
THERMAL EXPANSION DATA FOR SAMPLES OF DEVONIAN SHALE

This appendix presents the thermal expansion data for EGSP Kentucky No. 5 Well Devonian shale samples. Curves and conclusions presented in the text were taken from these data.

Table D.1. Thermal expansion data for shale from 157-m (515-ft) EGSP
Kentucky No. 5 Well

(Corrected values are $\times 10^{-6}\%$.)

NETZSCH DILATOMETER

OPERATOR:	T. R. Oldham	Date:	6 Sep 1985
RUN No.:	1	SAMPLE No.:	Ky #5 (515')
LOT No.:	1	MATERIAL:	Upper Huron
SAMPLE LENGTH, mm:	6.18	STANDARD:	Vacromium
STD LENGTH, mm:	24.96	TUBE MATERIAL:	Quartz
ATMOSPHERE:	Air	FLOW RATE (mL/min):	0
HEAT RATE C/min.:	5	FILE NAME:	IVAN1

UP-CURVE		----CORRECTED----				
TEMPERATURE	TIME	RAW EXP.	CORR. EXP.	REL. EXP.	ALPHA	ALPHA/T
deg. C	min.	micron.	micron.	$\times 10^6$	$\times 10^6$	$\times 10^6$
25	-.01	0	.29	122.9	41.53	35.04
35	4.31	1.78	2.39	462.7	35.56	130.7
45	6.87	3.75	4.54	809.9	30.9	141.8
55	9.07	5.93	6.82	1180	33.34	168.4
65	11.1	8.17	9.14	1554	33.02	180
75	13.01	10.39	11.42	1924	34.92	195.4
85	14.9	12.54	13.61	2278	31.22	165.1
95	16.83	14.49	15.61	2601	32.67	165.1
105	18.72	15.95	17.1	2842	15.22	76.63
115	20.57	16.6	17.79	2954	2.821	16.46
125	22.34	16.81	18.03	2993	5.642	33.01
135	24.13	17.19	18.44	3059	6.205	32.03
145	25.88	17.71	18.99	3149	5.027	31.23
155	27.6	18.37	19.69	3261	11.16	60.69
165	29.38	19.19	20.54	3399	15.93	90.95
175	31.24	20.21	21.59	3570	23.49	119.7
185	33.07	21.39	22.79	3764	23.92	119.5
195	34.9	22.77	24.19	3990	27.32	148.9
205	36.73	24.71	26.16	4308	35.64	215.7
215	38.58	44.81	46.26	7561	-245.1	-1342
225	40.42	35.64	37.11	6080	-72.58	-356.4
235	42.29	41.18	42.67	6979	-46.57	-250.8
245	44.17	38.91	40.42	6616	-32.44	-189.1
255	46	37.47	39.01	6388	-24.52	-129.6
265	47.83	42.08	43.67	7141	-170	-929.5
275	49.68	39.84	41.44	6781	-13.7	-72.74
285	51.79	39.61	41.19	6741	-24.19	-92.9

Table D.2. Thermal expansion data for shale from 157.1-m (515.5-ft) EGSP
Kentucky No. 5 Well
(Corrected values are $\times 10^{-6}\%$.)

NETZSCH DILATOMETER

OPERATOR:	T. R. Oldham	Date:	9 Sep 1985
RUN No.:	1	SAMPLE No.:	Ky #5 (515.5')
LOT No.:	1	MATERIAL:	Cleveland
SAMPLE LENGTH, mm:	15.98	STANDARD:	Vacromium
STD LENGTH, mm:	24.96	TUBE MATERIAL:	Quartz
ATMOSPHERE:	Air	FLOW RATE (mL/min):	0
HEAT RATE C/min.:	5	FILE NAME:	IVAN2

UP-CURVE		-----CORRECTED-----				
TEMPERATURE	TIME	RAW EXP.	CORR. EXP.	REL. EXP.	ALPHA	ALPHA/T
deg. C	min.	micron.	micron.	$\times 10^6$	$\times 10^6$	$\times 10^6$
25	-1.01	0	.76	158.9	-6.729	-11.51
35	4.33	4.97	6.56	521.5	45.45	117.4
45	7.12	11.28	13.32	944.8	32.51	154.5
55	9.48	17.79	20.11	1370	46.86	200.4
65	11.69	24.49	27	1801	44.65	194.6
75	13.7	31.06	33.72	2221	43.07	249.8
85	15.61	37.68	40.47	2644	39.62	218.9
95	17.62	45.48	48.37	3138	62.97	269.2
105	19.55	53.67	56.66	3657	43.95	268.2
115	21.41	61.55	64.62	4155	50.75	228
125	23.23	68.25	71.4	4580	40.5	258.2
135	25.04	74.26	77.49	4960	40.4	202.3
145	26.77	80.12	83.44	5333	41.67	242.8
155	28.54	86.17	89.58	5717	29.21	184.7
165	30.32	92.69	96.18	6130	49.63	229.2
175	32.16	99.78	103.35	6579	46.95	227.8
185	33.98	106.42	110.06	6998	45.3	285.8
195	35.83	118.42	122.11	7753	174.7	953.3
205	37.7	135.71	139.43	8837	42.1	195.4
215	39.52	146.54	150.3	9517	90.73	569.1
225	41.31	143.54	147.33	9331	-29.47	-160.2
235	43.07	144.86	148.69	9416	-78.85	-466.5
245	44.86	138.69	142.59	9034	-15.91	-83.77
255	46.64	136.98	140.97	8933	-19.1	-111.4
265	48.44	134.44	138.53	8780	-5.737	-30.19
275	50.61	130.36	134.51	8529	-43.16	-167.1
285	54.46	118.09	122.17	7757	-139.6	-208.8

Table D.3. Thermal expansion data for shale from 157.4-m (516.3-ft) EGSP
Kentucky No. 5 Well

(Corrected values are $\times 10^{-6}\%$.)

NETZSCH DILATOMETER

OPERATOR:	T. R. Oldham	Date:	9 Sep 1985
RUN No.:	1	SAMPLE No.:	Ky #5 (516.3')
LOT No.:	1	MATERIAL:	Cleveland
SAMPLE LENGTH, mm:	8.28	STANDARD:	Vacromium
STD LENGTH, mm:	24.96	TUBE MATERIAL:	Quartz
ATMOSPHERE:	Air	FLOW RATE (mL/min):	0
HEAT RATE C/min.:	5	FILE NAME:	IVAN3

UP-CURVE		----CORRECTED----				
TEMPERATURE	TIME	RAW EXP.	CORR. EXP.	REL. EXP.	ALPHA	ALPHA/T
deg. C	min.	micron.	micron.	$\times 10^6$	$\times 10^6$	$\times 10^6$
25	-1.01	0	.39	69.62	53.51	53.35
35	4.05	1.69	2.51	325.2	59.28	154.3
45	6.68	4.52	5.58	695.6	35.41	172.7
55	8.9	7.5	8.7	1073	13.45	74.04
65	10.96	10.28	11.58	1421	34.7	203.9
75	12.91	13.41	14.79	1808	47.92	292.1
85	14.84	16.93	18.37	2241	51.82	280.2
95	16.8	20.82	22.32	2717	34.44	156.1
105	18.76	24.32	25.87	3146	51.38	228
115	20.63	26.62	28.21	3429	17.99	112.7
125	22.42	27.38	29.01	3526	2.525	13.94
135	24.27	27.71	29.39	3571	2.023	11.44
145	26	28.34	30.06	3653	13.82	90.51
155	27.76	29.23	31	3766	21.59	101.9
165	29.53	30.24	32.04	3892	9.129	58.59
175	31.42	31.6	33.45	4062	23.68	111.6
185	33.23	33.04	34.93	4240	19.7	111.5
195	35.11	34.79	36.7	4454	24.78	155.4
205	36.92	37.07	39	4732	39.64	176.6
215	38.74	48.33	50.27	6093	91.35	694.6
225	40.61	56.69	58.65	7105	-70.62	-313.5
235	42.47	53.87	55.86	6768	-22.59	-138.7
245	44.32	53.49	55.51	6726	-3.72	-19.48
255	46.19	54.21	56.28	6819	-.9934	-4.975
265	48.03	53.74	55.86	6768	-23.43	-122
275	50.01	62.6	64.75	7842	5.855	25.92

Table D.4. Thermal expansion data for shale from 191.6-m (628.7-ft) EGSP
 Kentucky No. 5 Well
 (Corrected values are $\times 10^{-6}\%$.)

NETZSCH DILATOMETER

OPERATOR:	T. R. Oldham	Date:	9 Sep 1985
RUN No.:	1	SAMPLE No.:	Ky #5 (628.7')
LOT No.:	1	MATERIAL:	Lower Huron
SAMPLE LENGTH, mm:	6.92	STANDARD:	Vacromium
STD LENGTH, mm:	24.96	TUBE MATERIAL:	Quartz
ATMOSPHERE:	Air	FLOW RATE (mL/min):	0
HEAT RATE C/min.:	5	FILE NAME:	IVAN4

UP-CURVE		----CORRECTED----				
TEMPERATURE deg. C	TIME min.	RAW EXP. micron.	CORR. EXP. micron.	REL. EXP. $\times 10^6$	ALPHA $\times 10^6$	ALPHA/T $\times 10^6$
25	0	0	.33	82.51	47.06	49.46
35	3.65	.93	1.62	268.8	39.94	139.5
45	6.19	1.76	2.64	417	28.69	112.2
55	8.4	2.33	3.33	516	24.34	115.5
65	10.44	2.64	3.72	572.9	.6538	4.119
75	12.39	2.86	4.01	614.8	.8766	5.332
85	14.32	3.01	4.22	644.3	3.215	19.77
95	16.28	3.2	4.45	677.9	5.149	31.45
105	18.18	3.42	4.72	716.6	2.843	17.56
115	20.03	3.7	5.03	761.5	5.274	31.05
125	21.86	4	5.36	809.7	5.838	30.01
135	23.7	4.26	5.66	852.4	7.588	31.52
145	25.51	4.36	5.8	872.9	1.02	5.494
155	27.25	4.28	5.75	865.9	-1.483	-10.29
165	29	4.1	5.61	845.5	-1.388	-9.391
175	30.91	3.97	5.51	831.8	.1667	.02301
185	32.77	3.9	5.48	826.3	-1.133	-9.045
195	34.58	3.9	5.5	829	3.265	14.87
205	36.48	4.07	5.68	856	5.162	29.74
215	38.25	4.32	5.94	893.6	4.449	30.26
225	40.09	4.36	6	902	.3215	1.454
235	41.98	4.1	5.76	867.7	-2.003	-12.11
245	43.84	3.83	5.52	832.9	.4553	1.99
255	45.79	3.64	5.37	810.7	.6359	2.752
265	47.64	3.5	5.27	796.6	.5692	3.202
275	49.48	3.38	5.18	783	-2.555	-13.91

INTERNAL DISTRIBUTION

1. W. D. Arnold
2. J. M. Asher
3. T. Baer
4. A. G. Croff
5. N. H. Cutshall
6. L. M. Ferris
- 7-11. T. M. Gilliam
12. P. C. Ho
13. G. K. Jacobs
14. S. Y. Lee
15. T. F. Lomenick
16. R. E. Mesmer
17. R. E. Meyer
18. I. L. Morgan
19. W. W. Pitt
20. T. L. Sawyer
21. R. D. Spence
22. S. H. Stow
23. V. C. A. Vaughen
24. K. L. Von Damm
25. R. G. Wymer
26. Central Research Library
27. Document Reference Section
- 28-29. Laboratory Records Department
30. Laboratory Records, RC
31. ORNL Patent Office

EXTERNAL DISTRIBUTION

32. Office of Assistant Manager for Energy Research and Development,
DOE-ORO, P.O. Box E, Oak Ridge, TN 37831
- 33-34. DOE-Office of Civilian Radioactive Waste Management, 1000 Independence
Avenue, SW, Washington, DC 20585

Donald Alexander
R. Stein

- 35-40. DOE-CHO, 9800 S. Cass Avenue, Chicago, IL 60439

R. Baker
J. Kasprowicz
S. Mann
E. Patera
E. Price
R. Rothman

- 41-42. Battelle Memorial Institute, Office of Nuclear Waste Isolation,
505 King Avenue, Columbus, OH 43201
- P. Cloke
J. Moody
- 43-44. Battelle Memorial Institute, Office of Waste Technology
Development, Battelle Project Management Division, 7000 South
Adams Street, Willowbrook, IL 60521
- W. Newcomb
G. Stirewalt
45. B. Y. Kanehiro, Berkeley Hydrotechnique, Inc., 2150 Shattuck Ave.,
Berkeley, CA 94704
- 46-47. Earth Sciences Division, Lawrence Berkeley Laboratory, One
Cyclotron Road, Berkeley, CA 94720
- L. Meyer
P. A. Witherspoon
- 48-49. RE/SPEC, Inc., P.O. Box 725, Rapid City, SD 57701
- A. Fossum
P. F. Gnirk
- 50-51. Center for Tectonophysics, Texas A&M University, College Station,
TX 77843
- P. A. Domenico
J. E. Russell
52. W. C. McClain, Roy F. Weston, Inc., 2301 Research Boulevard,
Rockville, MD 20850
53. D. G. Brookins, 3410 Groman Ct., N.E., Albuquerque, NM 87110
54. Serge Gonzales, Earth Resource Associates, Inc., 295 E. Dougherty
Street, Suite 105, Athens, GA 30601
55. K. S. Johnson, Earth Resource Associates, 1321 Greenbriar Drive,
Norman, OK 73069
56. T. Pigford, Department of Nuclear Engineering, College of
Engineering, University of California, Berkeley, CA 94720
57. Paul Potter, Department of Geology, University of Cincinnati,
Cincinnati, OH 45221
58. H. W. Smedes, 1126 Buehler Dr., Las Vegas, NV 89102

- 59. Frank J. Wobber, Ecological Research Division, Office of Health and Environmental Research, Office of Energy Research, MS-E201, Department of Energy, Washington, DC 20545
- 60-89. Technical Information Center, Department of Energy, P.O. Box 62, Oak Ridge, TN 37831 (25 copies, NTIS)